

CANADIAN THESES ON MICROFICHE

THÈSES CANADIENNES SUR MICROFICHE



National Library of Canada
Collections Development Branch

Canadian Theses on
Microfiche Service

Ottawa, Canada
K1A 0N4

Bibliothèque nationale du Canada
Direction du développement des collections

Service des thèses canadiennes
sur microfiche

NOTICE

The quality of this microfiche is heavily dependent upon the quality of the original thesis submitted for microfilming. Every effort has been made to ensure the highest quality of reproduction possible.

If pages are missing, contact the university which granted the degree.

Some pages may have indistinct print especially if the original pages were typed with a poor typewriter ribbon or if the university sent us an inferior photocopy.

Previously copyrighted materials (journal articles, published tests, etc.) are not filmed.

Reproduction in full or in part of this film is governed by the Canadian Copyright Act, R.S.C. 1970, c. C-30. Please read the authorization forms which accompany this thesis.

**THIS DISSERTATION
HAS BEEN MICROFILMED
EXACTLY AS RECEIVED**

AVIS

La qualité de cette microfiche dépend grandement de la qualité de la thèse soumise au microfilmage. Nous avons tout fait pour assurer une qualité supérieure de reproduction.

S'il manque des pages, veuillez communiquer avec l'université qui a conféré le grade.

La qualité d'impression de certaines pages peut laisser à désirer, surtout si les pages originales ont été dactylographiées à l'aide d'un ruban usé ou si l'université nous a fait parvenir une photocopie de qualité inférieure.

Les documents qui font déjà l'objet d'un droit d'auteur (articles de revue, examens publiés, etc.) ne sont pas microfilmés.

La reproduction, même partielle, de ce microfilm est soumise à la Loi canadienne sur le droit d'auteur, SRC 1970, c. C-30. Veuillez prendre connaissance des formules d'autorisation qui accompagnent cette thèse.

**LA THÈSE A ÉTÉ
MICROFILMÉE TELLE QUE
NOUS L'AVONS REÇUE**

Canada



National Library
of Canada

Bibliothèque nationale
du Canada

Ottawa, Canada
K1A 0N4

TC -

67506

ISBN

0-315-19598-3

CANADIAN THESES ON MICROFICHE SERVICE - SERVICE DES THÈSES CANADIENNES SUR MICROFICHE

PERMISSION TO MICROFILM - AUTORISATION DE MICROFILMER

• Please print or type - Écrire en lettres moulées ou dactylographier

AUTHOR - AUTEUR

Full Name of Author - Nom complet de l'auteur

FOSSEY, LYNETTE PHILLIS

Date of Birth - Date de naissance

OCT. 14, 1952

Canadian Citizen - Citoyen canadien

☒ Yes / Oui

☐ No / Non

Country of Birth - Lieu de naissance

U.S.A

(Naturalized
Canadian, born
of Canadian
Parents)

Permanent Address - Résidence fixe

2132 Greenwood, Wilmette,
Illinois, 60091

THESIS - THÈSE

Title of Thesis - Titre de la thèse

SOLVENT EXTRACTION / FLOW INJECTION
ANALYSIS FOR THE ASSAY OF DRUGS
AND THE DETERMINATION OF ACIDITY
CONSTANTS

Degree for which thesis was presented
Grade pour lequel cette thèse fut présentée

Ph.D

Year this degree conferred
Année d'obtention de ce grade

1985

University - Université

U. of Alberta

Name of Supervisor - Nom du directeur de thèse

Cantwell

AUTHORIZATION - AUTORISATION

Permission is hereby granted to the NATIONAL LIBRARY OF CANADA to
microfilm this thesis and to lend or sell copies of the film.

The author reserves other publication rights, and neither the thesis nor exten-
sive extracts from it may be printed or otherwise reproduced without the
author's written permission.

L'autorisation est, par la présente, accordée à la BIBLIOTHÈQUE NATIONALE
DU CANADA de microfilmer cette thèse et de prêter ou de vendre des ex-
emplaires du film.

L'auteur se réserve les autres droits de publication; ni la thèse ni de longs ex-
traits de celle-ci ne doivent être imprimés ou autrement reproduits sans
l'autorisation écrite de l'auteur.

ATTACH FORM TO THESIS - VEUILLEZ JOINDRE CE FORMULAIRE À LA THÈSE

Signature

L. Fossey

Date

Jan. 30, 1985

THE UNIVERSITY OF ALBERTA

SOLVENT EXTRACTION/FLOW INJECTION ANALYSIS FOR THE
ASSAY OF DRUGS AND THE DETERMINATION OF ACIDITY CONSTANTS

by



LYNETTE P. FOSSEY

A THESIS

SUBMITTED TO THE FACULTY OF GRADUATE STUDIES AND RESEARCH
IN PARTIAL FULFILMENT OF THE REQUIREMENTS FOR THE DEGREE
DOCTOR OF PHILOSOPHY

DEPARTMENT OF CHEMISTRY

EDMONTON, ALBERTA

SPRING 1985

THE UNIVERSITY OF ALBERTA

RELEASE FORM

NAME OF AUTHOR LYNETTE P. FOSSEY
TITLE OF THESIS SOLVENT EXTRACTION/FLOW INJECTION
 ANALYSIS FOR THE ASSAY OF DRUGS AND THE
 DETERMINATION OF ACIDITY CONSTANTS
DEGREE FOR WHICH THESIS WAS PRESENTED Ph.D.
YEAR THIS DEGREE GRANTED 1985

Permission is hereby granted to THE UNIVERSITY OF ALBERTA LIBRARY to reproduce single copies of this thesis and to lend or sell such copies for private, scholarly or scientific research purposes only.

The author reserves other publication rights, and neither the thesis nor extensive extracts from it may be printed or otherwise reproduced without the author's written permission.

(Signed) *L. Fossey*

PERMANENT ADDRESS:

2132 Greenwood
Wilmette, Illinois
U.S.A. 60091

DATED

January 30 1985

THE UNIVERSITY OF ALBERTA
FACULTY OF GRADUATE STUDIES AND RESEARCH

The undersigned certify that they have read, and
recommend to the Faculty of Graduate Studies and Research,
for acceptance, a thesis entitled SOLVENT EXTRACTION/FLOW
INJECTION ANALYSIS FOR THE ASSAY OF DRUGS AND THE
DETERMINATION OF ACIDITY CONSTANTS
submitted by LYNETTE P. FOSSEY
in partial fulfilment of the requirements for the degree of
DOCTOR OF PHILOSOPHY.

Fredrick J. Cantwell
F.F. Cantwell, Supervisor

Garry Horlick
G. Horlick

B. Kratochvil
B. Kratochvil

P. Kebabian
P. Kebabian

J. A. Rogers
J. A. Rogers

G. Schill
G. Schill, External Examiner

DATE January 30, 1985

This thesis is dedicated to my husband for his support and understanding, and to my parents for their encouragement during my student years.

ABSTRACT

A solvent extraction/flow injection analysis (FIA) apparatus utilizing a porous membrane phase separator and constant pressure pumping is described and characterized in terms of extraction coil length, sample injection volume and flow rates. Equations expressing the quantitative relationship between peak area and various system parameters are derived and verified. Under conditions where the sample component is quantitatively extracted into the organic phase, peak area is directly proportional to the number of moles of sample injected and is inversely proportional to the total flow rate of the organic solvent. A sampling frequency of 4 samples/min is readily achieved with a precision of about 1%.

A rapid assay method for procyclidine hydrochloride in pharmaceutical tablets, based on the ion-pair extraction of the cationic drug with picrate is developed using the extraction/FIA system. Conditions for the assay are optimized by examining the effects of the extraction coil length, reagent pH and picrate concentration on peak areas. Assays are performed at a rate of two per minute with a precision and accuracy of 1%.

Development of a dual-membrane phase separator, which incorporates both a hydrophobic Teflon membrane and a

hydrophilic paper membrane, permits the simultaneous monitoring of the absorbances of both the organic and the aqueous phases. This phase separator is used in the simultaneous assay of diphenhydramine and 8-chlorotheophylline in Dramamine motion sickness tablets by the extraction/FIA technique. At a suitable pH, the former drug is extracted quantitatively into cyclohexane and the latter remains in the aqueous buffer phase. Theoretical equations describing the extraction-pH profiles for diphenhydramine in both phases are presented and verified experimentally. Simultaneous assays of diphenhydramine and 8-chlorotheophylline are performed at a rate of two per minute with a precision and accuracy of 1%.

A method is presented for determination of acidity constants by solvent extraction/FIA using the dual-membrane phase separator. The procedure is especially useful for compounds that have a low solubility in water, and whose conjugate species have the same absorption spectrum. Acidity constants are determined from straight line plots relating the ratio of peak areas in the aqueous and organic phases, A_a/A_o , to the hydrogen ion activity in the aqueous phase. Theoretical equations describing this relationship for both HA and BH^+ charge type acids are derived and verified using 3,5-dimethylphenol ($pK_a = 10.09 \pm 0.01$) and p-toluidinium ion ($pK_a = 5.28 \pm 0.01$). The

distribution coefficient is also obtained during the experiment. Some distinct advantages of using the dual-membrane device over the single-membrane device are discussed.

ACKNOWLEDGEMENTS

My most sincere thanks go to Dr. F.F. Cantwell for his guidance during the course of this work and for his helpful suggestions in the preparation of this manuscript.

Thanks are also extended to Miss A. Wiseman for the speed and accuracy exhibited in typing this thesis.

The author would like to acknowledge Burroughs Wellcome Ltd., La Salle, Quebec, and G.D. Searle and Co., Skokie, Illinois, for their gracious supply of sample drugs and information.

Thanks go to the Chemistry Department Machine Shop for making the aluminum pressure cylinders and membrane phase separators, and to the Chemistry Department Electronics Shop for building the timer and power supply for the automatic injection valve.

Financial support from the University of Alberta and the Alberta Heritage Foundation for Medical Research is gratefully acknowledged.

TABLE OF CONTENTS

CHAPER	PAGE
1. INTRODUCTION.....	1
2. OPTIMIZATION AND CHARACTERIZATION OF AN EXTRACTION/FIA SYSTEM.....	10
2.1 Introduction.....	10
2.2 Experimental.....	11
2.2.1 Chemicals and Solvents.....	11
2.2.2 Apparatus.....	12
2.2.3 Calibration of the Sample In- jection Loops.....	17
2.3 Results and Discussion.....	17
2.3.1 Extraction Coil Length.....	18
2.3.2 Sample Injection Volume.....	22
2.3.3 Flow Rates.....	26
2.3.4 Sampling Frequency.....	35
3. ANALYSIS OF PROCYCLIDINE HYDROCHLORIDE IN TABLETS BY ION-PAIR EXTRACTION WITH PICRATE.....	38
3.1 Introduction.....	38
3.2 Experimental.....	42
3.2.1 Chemicals and Solvents.....	42
3.2.2 Reagents.....	43
3.2.3 Standards and Samples.....	44
3.2.4 Apparatus.....	45
3.2.5 Tablet Assay Procedure.....	45

CHAPTER	PAGE
3.3 Results and Discussion.....	46
3.3.1 Extraction Coil Length.....	46
3.3.2 Reagent pH.....	47
3.3.3 Picrate Concentration.....	50
3.3.4 Calibration.....	50
3.3.5 Tablet Assay.....	52
4. ASSAY OF DRAMAMINE TABLETS BY SIMULTANEOUS MONITORING OF AQUEOUS AND ORGANIC PHASES.....	54
4.1 Introduction.....	54
4.2 Experimental.....	55
4.2.1 Chemicals and Solvents.....	55
4.2.2 Standards and Samples.....	56
4.2.3 Reagents.....	58
4.2.4 Apparatus.....	59
4.2.5 Calibration Curves.....	64
4.2.6 Tablet Assay.....	65
4.3 Results and Discussion.....	66
4.3.1 Instrument Parameters.....	67
4.3.2 Reagent pH.....	69
4.3.3 Calibration Curves.....	75
4.3.4 Tablet Assay.....	78
4.3.5 Comments.....	80

CHAPTER	PAGE
5. ACIDITY CONSTANT DETERMINATION BY SOLVENT	
EXTRACTION/FIA.....	81
5.1 Introduction.....	81
5.2 Theory.....	86
5.2.1 HA Charge Type Acid.....	86
5.2.2 BH ⁺ Charge Type Acid.....	93
5.3 Experimental.....	97
5.3.1 Chemicals.....	97
5.3.2 Solvents and Reagents.....	98
5.3.3 Sample Solutions.....	100
5.3.4 Apparatus.....	101
5.3.5 Calibration Curves.....	104
5.3.6 Molar Absorptivity Ratios.....	107
5.3.7 Acidity Constant Determination.....	108
5.4 Results and Discussion.....	110
5.4.1 Choice of Experimental Conditions.....	110
5.4.2 Refractive Index Peaks.....	113
5.4.3 Ultraviolet Absorption Spectra.....	120
5.4.4 Dimerization and Ion-Pair Extraction..	120
5.4.5 Calibration Curves.....	126
5.4.6 Molar Absorptivity Ratios.....	126
5.4.7 Acidity Constants.....	128
5.4.8 Distribution Coefficients.....	133
5.4.9 Comments.....	141

BIBLIOGRAPHY.....	144
APPENDIX I.....	153
APPENDIX II.....	162

LIST OF TABLES

TABLE	PAGE
1. Data for Peak Area and Height Dependence on Flow Rates.....	31
2. Calibration Curve Data for 3,5-Dimethylphenol and p-Toluidine.....	127
3. Acidity Constant Determination by Solvent Extraction/FIA.....	132
4. Distribution Coefficient Determination by Solvent Extraction/FIA.....	142
A1. Data for Trial #1 of the Determination of the Acidity Constant and Distribution Coefficient for 3,5-Dimethylphenol.....	154
A2. Data for Trial #2 of the Determination of the Acidity Constant and Distribution Coefficient for 3,5-Dimethylphenol.....	155
A3. Data for Trial #3 for the Determination of the Distribution Coefficient for 3,5-Dimethylphenol.....	157
A4. Data for Trial #1 of the Determination of the Acidity Constant and Distribution Coefficient for p-Toluidine.....	158
A5. Data for Trial #2 of the Determination of the Acidity Constant and Distribution Coefficient for p-Toluidine.....	160

TABLE

PAGE

A6. Data for the Acidity Constant Determination of 8-Chlorotheophylline.....	174
---	-----

LIST OF FIGURES

FIGURE		PAGE
1.	Block diagram of a simple solvent extraction/FIA system showing an expanded section of the segmented flow.	4
2.	Solvent extraction/FIA apparatus used for system characterization.	13
3.	Cross section of the single-membrane phase separator (A).....	16
4.	Peak area (A) and peak width at half-height (B) for 90 ppm caffeine versus extraction coil length.....	20
5.	Plot of peak height for 90 ppm caffeine versus extraction coil length.....	21
6.	Peak area (A) and height (B) for 90 ppm caffeine versus sample volume injected.....	23
7.	Peak width at half-height for 90 ppm caffeine versus sample volume injected.....	24
8.	Calibration curve for caffeine.....	29
9.	Plot of $1/A$ versus $F_T + F_O(D-1)$ for caffeine...32	
10.	Plot of peak area versus $1/F_O$ for caffeine.....	33
11.	Plot of peak area versus flow rate through the membrane with total flow rate of organic phase held constant.....	36

FIGURE

PAGE

12. Replicate injections of a 90 ppm caffeine solution at a frequency of four per minute.....	37
13. Peak area versus extraction coil length for procyclidine hydrochloride extracted as a picrate ion pair.....	48
14. Peak area of extracted procyclidinium picrate as a function of reagent/sample concentration ratio.....	51
15. Calibration curve for procyclidine hydrochloride extracted as a picrate ion pair.....	53
16. Solvent extraction/FIA system used with the dual-membrane phase separator for the Dramamine assay.....	60
17. Cross section of the dual-membrane phase separator.....	62
18. Peak area versus extraction coil length for diphenhydramine.....	68
19. Peak area for the aqueous phase (A) and the organic phase (B) versus reagent pH for diphenhydramine.....	71
20. Calibration curve for diphenhydramine in the organic phase.....	76

21. Calibration curve for 8-chlorotheophylline in the aqueous phase..... 77
22. Solvent extraction/FIA system used to determine acidity constants..... 102
23. Apparatus used to measure molar absorptivity ratios..... 105
24. Recorder tracings for the aqueous phase injecting H_2O (A) and 0.1 M NaCl (B) into ionic strength 0.1 , $\text{pH} = 9.8 \text{ NH}_3/\text{NH}_4\text{Cl}$ buffer..... 115
25. Recorder tracings for the aqueous phase injecting $2 \times 10^{-4} \text{ M}$ 3,5-dimethylphenol (A) and ionic strength 0.1 , $2 \times 10^{-4} \text{ M}$ 3,5-dimethylphenol (B) into ionic strength 0.1 , $\text{pH} = 9.8 \text{ NH}_3/\text{NH}_4\text{Cl}$ buffer..... 119
26. U.V. absorption spectra of: (A) $8.0 \times 10^{-4} \text{ M}$ 3,5-dimethylphenol in cyclohexane; (B) $\text{pH} = 2.0$, $6.0 \times 10^{-4} \text{ M}$ aqueous 3,5-dimethylphenol; (C) $\text{pH} = 12.5$, $6.0 \times 10^{-4} \text{ M}$ aqueous 3,5-dimethylphenol..... 121
27. U.V. absorption spectra of: (A) $6.0 \times 10^{-4} \text{ M}$ p-toluidine in cyclohexane; (B) $\text{pH} = 2.0$, $5.0 \times 10^{-4} \text{ M}$ aqueous p-toluidine; (C) $\text{pH} = 12.0$, $5.0 \times 10^{-4} \text{ M}$ aqueous p-toluidine..... 122

28. Beer's law plot for 3,5-dimethylphenol in cyclohexane at 281 nm..... 123
29. Beer's law plot for p-toluidine in cyclohexane at 287 nm..... 125
30. Plot of A_a/A_o versus $1/a_H$ for trial #1 of the K_a determination of 3,5-dimethylphenol at 25.0°C with ionic strength = 0.10..... 129
31. Plot of A_a/A_o versus $1/a_H$ for trial #2 of the K_a determination of 3,5-dimethylphenol at 25.0°C with ionic strength = 0.10..... 130
32. Plot of A_a/A_o versus a_H for trial #1 of the K_a determination of p-toluidinium at 20.0°C with ionic strength = 0.10..... 134
33. Plot of A_a/A_o versus a_H for trial #2 of the K_a determination of p-toluidinium at 20.0°C with ionic strength = 0.10..... 135
34. Plot of $1/A_o$ versus $1/a_H$ for trial #1 of the K_{HA} determination of 3,5-dimethylphenol between cyclohexane and ionic strength 0.10 ammonia buffer at 25.0°C..... 136
35. Plot of $1/A_o$ versus $1/a_H$ for trial #2 of the K_{HA} determination of 3,5-dimethylphenol between cyclohexane and ionic strength 0.10 ammonia buffer at 25.0°C..... 137

36. Plot of $1/A_0$ versus $1/a_H$ for trial #3 of the K_{HA} determination of 3,5-dimethylphenol between cyclohexane and ionic strength 0.10 ammonia buffer at 25.0°C..... 138
37. Plot of $1/A_0$ versus a_H for trial #1 of the K_B determination of p-toluidine between cyclohexane and ionic strength 0.10 acetate buffer at 20.0°C..... 139
38. Plot of $1/A_0$ versus a_H for trial #2 of the K_B determination of p-toluidine between cyclohexane and ionic strength 0.10 acetate buffer at 20.0°C..... 140
- A1. Apparatus used to determine the acidity constant of 8-chlorotheophylline..... 166
- A2. Apparatus used to measure the system constant for 8-chlorotheophylline..... 168
- A3. Plot of $1/A_0$ versus $1/a_H$ for the acidity constant determination of 8-chlorotheophylline..... 173

LIST OF SYMBOLS

SYMBOL	DESCRIPTION
A	peak area
A _a	peak area for the aqueous phase
A _o	peak area for the organic phase
a _H	hydrogen ion activity
α _{A⁻}	fraction of the sample in the aqueous phase which is present in the A ⁻ form
α _B	fraction of the sample in the aqueous phase which is present in the B form
α _{BH⁺}	fraction of the sample in the aqueous phase which is present in the BH ⁺ form
α _{HA}	fraction of the sample in the aqueous phase which is present in the HA form
b	pathlength of the organic phase detector flowcell
b'	pathlength of the aqueous phase detector flowcell
D	distribution ratio
D _B	distribution ratio for component B
D _{HA}	distribution ratio for component HA
ε	molar absorptivity
ε _{A⁻,a}	molar absorptivity of A ⁻ in the aqueous phase
ε _{B,a}	molar absorptivity of B in the aqueous phase
ε _{B,o}	molar absorptivity of B in the organic phase
ε _{BH⁺,a}	molar absorptivity of BH ⁺ in the aqueous phase
ε _{HA,a}	molar absorptivity of HA in the aqueous phase

SYMBOL	DESCRIPTION
$\epsilon_{HA,O}$	molar absorptivity of HA in the organic phase
F	volumetric flow rate
F_a	total volumetric flow rate of aqueous phase
F_m	volumetric flow rate through the membrane
$F_{m,a}$	volumetric flow rate of aqueous phase through the paper membrane
$F_{m,o}$	volumetric flow rate of organic phase through the Teflon membrane
F_o	total volumetric flow rate of organic phase
F_T	total volumetric flow rate ($F_o + F_a$)
f	response factor for organic phase detector and integrator
f'	response factor for aqueous phase detector and integrator
I_1	y-intercept of a plot of A_a/A_o vs $1/a_H$
I_2	y-intercept of a plot of $1/A_o$ vs $1/a_H$
I_3	y-intercept of a plot of A_a/A_o vs a_H
I_4	y-intercept of a plot of $1/A_o$ vs a_H
K	system (proportionality) constant for the organic phase
K'	system (proportionality) constant for the aqueous phase
K_a	acidity constant
K_B	distribution coefficient for species B

SYMBOL	DESCRIPTION
K_{HA}	distribution coefficient for species HA
$K_{I,BHX}$	$[BHX]_O/[BH]$
$K_{I,MA}$	$[MA]_O/[A]$
K_S	$[BHA]_O/([BH][A])$
k'	capacity factor
n	number of moles of sample injected
S_1	slope of a plot of A_a/A_O <u>vs</u> $1/a_H$
S_2	slope of a plot of $1/A_O$ <u>vs</u> $1/a_H$
S_3	slope of a plot of A_a/A_O <u>vs</u> a_H
S_4	slope of a plot of $1/A_O$ <u>vs</u> a_H

CHAPTER 1

INTRODUCTION

Flow injection analysis (FIA) has been defined as a type of continuous flow analysis that utilizes an analytical stream, unsegmented by air bubbles, into which highly reproducible volumes of sample are injected [1]. The technique was introduced in the early 1970's, and has developed very rapidly since then. Numerous reviews of FIA have been published [1-7], and a textbook devoted to the subject has been written by Ruzicka and Hansen [8].

Flow injection analysis is based on a combination of three principles: sample injection, controlled dispersion and exact timing. In the simplest FIA manifold, a sample is introduced into a reagent stream, by means of an injection valve, in the form of a discrete "slug" of well defined volume and length. A constant, steady flow of the reagent stream is normally achieved by use of a peristaltic, constant pressure, long stroke piston or reciprocating pump. The sample zone disperses and reacts with the components of the reagent stream as the sample and reagent move through a reaction tube or coil. The species produced is monitored by a flow-through detector linked to a recorder. The reaction product is normally analyzed before equilibrium is reached (before the

response curve reaches the steady-state plateau), and the output is in the form of sharp peaks. However, because the time between sample injection and detection is highly reproducible, as is the dispersion of the sample zone, very accurate and precise analyses can be performed.

Dispersion of the sample zone occurs primarily by laminar flow. Radial diffusion tends to relax the parabolic velocity profile somewhat, as does coiling the tube which induces a secondary flow in the radial direction [9]. Dispersion is controlled in FIA by the choice of sample injection volume, flow rate, tube radius and tube length [8]. These parameters are adjusted to give the required sample dispersion as well as allow sufficient time for the reaction to take place.

A review by Rocks and Riley [5] summarizes the differences between air-segmented continuous flow analysis and flow injection analysis. Air-segmented instruments (such as the Technicon Autoanalyzer) are more complex than FIA apparatus because of the need for the introduction of air and its removal before sample detection. Because of the compressibility of air, the streams tend to pulsate rather than flow regularly. This causes irregularities in sampling times and flow rates, which are usually minimized by allowing 95% or better achievement of the steady-state plateau to be reached [10]. This requires relatively long

sampling times and larger sample volumes which results in lower sampling frequencies. Start-up times are significantly longer for air-segmented systems compared to those for FIA, the latter allowing detection within seconds of introducing the sample.

Automation of solvent extraction by flow injection analysis was introduced independently by Karlberg and Thelander [11] and Bergamin et al. [12] in 1978. A schematic diagram of a simple solvent extraction/FIA system is shown in Figure 1. Sample, S, is injected into a flowing aqueous phase, A, by injection valve I. The organic phase, O, is merged with the aqueous phase, at a "tee" or other shaped junction to produce alternating small segments of organic and aqueous phase which flow through the extraction coil, C. The sample, occupying many aqueous segments, will extract into the adjoining organic segments as it moves along the extraction coil. The two-phase flow will then enter a phase separator, P, which allows a portion of the phase of interest to enter a flow-through detector, D. Some property of the sample (absorbance, fluorescence, etc.) is monitored, and the output is displayed on a recorder, R, in the form of peaks, one for each sample injected.

In the enlarged section of the extraction coil shown in Figure 1 the coil is assumed to be made of Teflon. The

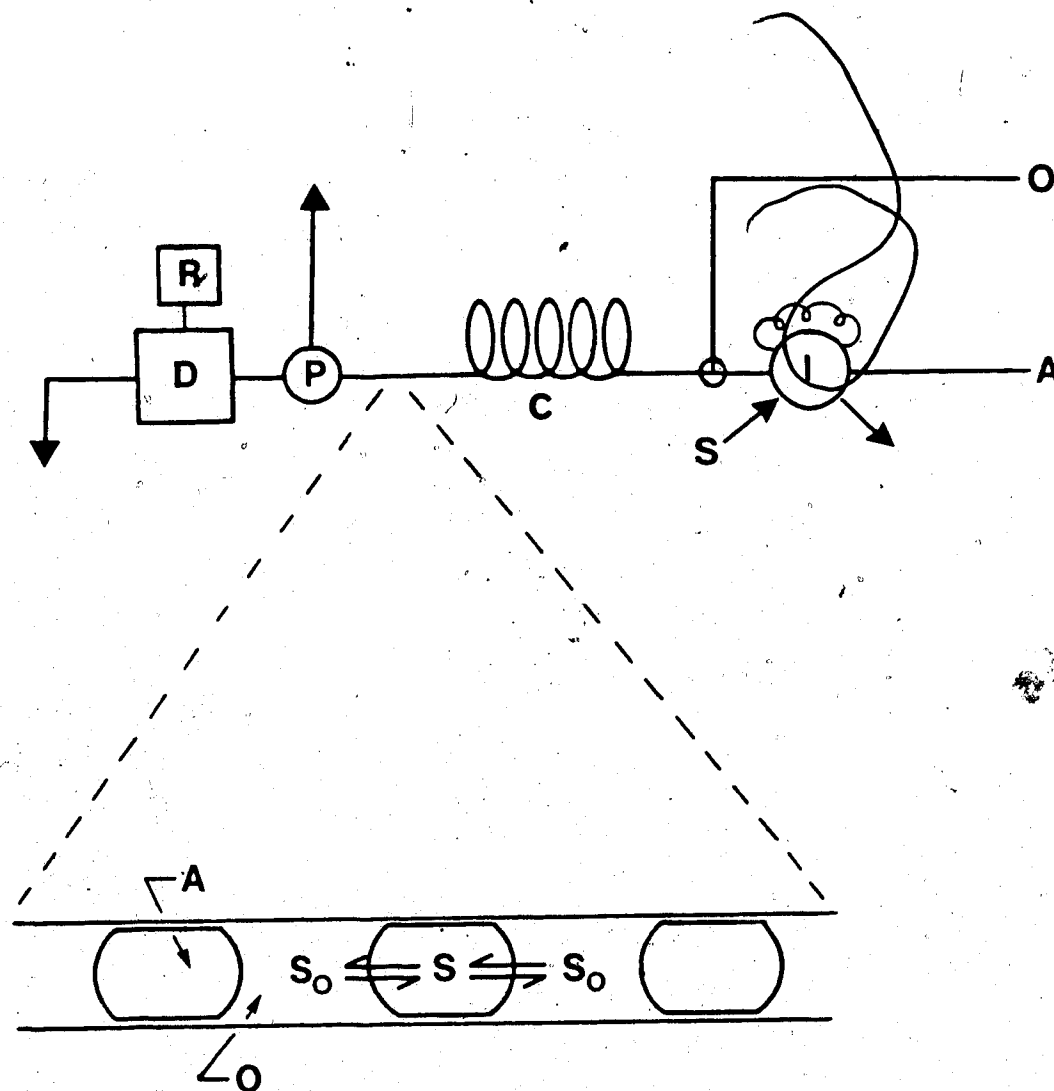


Figure 1. Block diagram of a simple solvent extraction/FIA system showing an expanded section of the segmented flow. O is the organic phase, A is the aqueous phase, S is the sample, I is the injection valve, C is the extraction coil, P is the phase separator, D is the detector and R is the recorder. See text for details.

organic phase will preferentially wet the coil walls, and it is believed that the aqueous segments will be separated from the coil walls by a thin layer of the organic phase [13-16]. The sample will extract from the aqueous segments to the organic segments by diffusion across the interfaces. Wall-drag causes bolus flow within the segments, analogous to air-segmented systems [10,17], promoting rapid longitudinal mixing of fluid within each segment. If the tube is coiled, secondary flow may develop [9], as previously discussed for FIA, producing convective radial mixing [10]. The net result is rapid transport of the sample from within the segments to the aqueous-organic interface, which creates conditions for rapid extraction. Equilibrium is therefore often achieved much faster in a solvent extraction/FIA system as opposed to manual extraction in a separatory funnel [18,19].

Sample dispersion is limited in the extraction coil by the two-phase flow. Some inter-segment mixing may occur in the extraction coil as a result of the wetting phenomenon [20,21]. Several authors have however observed that dispersion within the extraction coil is negligible [22,23]. Dispersion also occurs in the unsegmented regions of the solvent extraction/FIA system, as well as in the injection valve, phase separator and detector flow cell. By proper design of these components, the

dispersion can be kept low allowing high sampling frequencies. As discussed for unsegmented FIA, the constancy of flow rates and sample injection volume leads to good reproducibility and accurate analyses.

Air-segmented continuous flow analyzers incorporating a solvent extraction step have been in use for quite some time [24]. The disadvantages of the air-segmented approach compared to flow injection analysis have already been mentioned. In addition, the efficiency of solvent extraction in air-segmented systems is lowered as a result of a decrease in the effective transfer surfaces [8].

Several types of phase separators have been used in solvent extraction/FIA systems. The earliest phase separators utilized were Technicon T-piece connectors modified with a phase guide material [11]. Phase separation was achieved by gravity and preferential wetting. Chamber devices relying solely on gravity for phase separation have been employed [12], as have phase splitters which are based on dissimilar phase wetting of hydrophobic and hydrophilic surfaces [13]. Some work has been done on monitoring concentration via fluorescence in a two-phase flowing stream without employing a phase separating device [20,25]. A major development in extraction/FIA has been the use of porous membrane phase separators. Such devices are compatible with high flow

velocities, and their small internal volumes reduce bandbroadening [16,20,26-30]. A dual-membrane phase separator has been described by Fossey and Cantwell which incorporates both a hydrophobic porous Teflon membrane and a hydrophilic porous paper membrane, thus permitting simultaneous monitoring of both the organic and aqueous phases [31].

Solvent extraction/FIA has been applied to metal analysis with extraction of neutral complexes or ion pairs followed by visible-absorbance or fluorescence detection [12,20,25,32]. It has also proven useful as a separation and/or concentration technique prior to flame and graphite furnace atomic absorption spectrometry [16,19,33-36].

Frei and his coworkers have been instrumental in developing post-column ion pair extraction detectors for liquid chromatography, based on the extraction/FIA approach [21,37-41]. Contributions to bandbroadening have been evaluated for both liquid segmented and non-segmented flow in postcolumn reactors for liquid chromatography [23,42]. Solvent extraction/FIA has also found application in post-column, on-stream derivitization techniques [43,44], and has been used as an interface between a reversed-phase liquid chromatograph and a mass spectrometer for on-line detection of ion pairs [45].

Ion pair extraction/FIA has been applied to analysis

of surfactants [26,28], and to assay procedures for pharmaceutical tablets [18,29]. A multiple solvent extraction procedure with flow injection technology has been reported for isolation of polynuclear aromatics from a complex organic matrix [14,15]. Solvent extraction/FIA methods have been developed for the determination of extraction constants, distribution ratios and acidity constants [13,22,46].

In Chapter 2 of this work, a solvent extraction/FIA apparatus utilizing a porous membrane phase separator and constant pressure pumping is described and characterized. Under optimum conditions, a sampling frequency of 4 samples/min is readily achieved. Equations relating peak area of the extracted sample to flow rates are derived and experimentally verified.

Chapter 3 describes the application of the extraction/FIA system to a rapid assay method for procyclidine hydrochloride in pharmaceutical tablets, based on the ion pair extraction of the drug with picrate.

In Chapter 4, a dual-membrane phase separator is developed which allows simultaneous monitoring of both the organic and aqueous phases. This phase separator is used to analyze Dramamine motion sickness tablets for both diphenhydramine and 8-chlorotheophylline by the extraction/FIA technique.

A method for determining acidity constants by solvent

extraction/FIA is presented in Chapter 5. The procedure is especially useful for compounds that have a low solubility in water, and whose conjugate species have the same absorption spectrum. Acidity constants are determined from straight line plots relating the ratio of peak areas in the aqueous and organic phases, A_a/A_o , to the hydrogen ion activity in the aqueous phase. Equations describing this relationship are derived and verified for both HA and BH^+ charge type acids.

CHAPTER 2

OPTIMIZATION AND CHARACTERIZATION OF AN EXTRACTION/FIA SYSTEM

2.1 Introduction

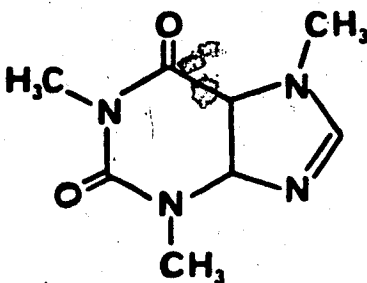
In this chapter, a solvent extraction/flow injection analysis apparatus is described. Its distinctive features include aluminum pressure cylinders to provide constant pressure pumping of the aqueous and organic phases, and a specially designed porous membrane phase separator.

The instrument is characterized by examining the dependence of peak area on extraction coil length, sample injection volume and flow rates. Equations expressing the quantitative relationship between peak area and various system parameters are derived and verified. These equations facilitate system optimization by providing a more fundamental understanding of the conditions which lead to an increase or decrease in peak areas. Recently Cantwell and Sweileh have developed equations for quantification based on peak height [47].

2.2 Experimental

2.2.1 Chemicals and Solvents

Caffeine, supplied by L. Chatten (Faculty of Pharmacy, University of Alberta), was U.S.P. grade and was used without further purification. Its structure is:



Methylene Blue (U.S.P. equivalent) was used as received from Fisher Scientific Co., Fair Lawn, New Jersey.

Double Distilled Water was prepared by distilling the laboratory distilled water from alkaline permanganate in an all-glass still. The first 20% of the distillate was discarded and the middle fraction was collected. This water was used to prepare all aqueous solutions referred to in this work.

Chloroform was analytical grade (B.D.H. Chemicals) and was distilled before use to remove uv-absorbing impurities.

Methanol was analytical grade (Terochem Labs Ltd.) and was used as received.

2.2.2 Apparatus

A schematic diagram of the solvent extraction/FIA system used is shown in Figure 2. The chloroform to be pumped is held in a 1700 mL glass bottle while the water, the aqueous reagent and the methanol to be pumped are held in 2 litre polyethylene bottles. These bottles are placed inside aluminum cylinders which are pressurized with nitrogen.

All tubing is Teflon, with 0.3 mm i.d. tubing used whenever it is desirable to minimize sample bandbroadening or to provide increased resistance to flow and 0.8 mm tubing used in the rest of the system. Two-way Teflon valves, V_1 (part no. CAV2031, Laboratory Data Control, Riviera Beach, FL), placed in the solvent delivery lines from the cylinders allow shut-off of each individual flow. A three-way valve, V_2 (part no. CAV3031, LDC), allows selection of either chloroform or methanol. The latter is used to wash out the system at the beginning and end of the day.

The water flows first through an automatic sample injection valve, V_3 (part no. SVA-8031, LDC), before joining the aqueous reagent stream at tee-fitting, T_1

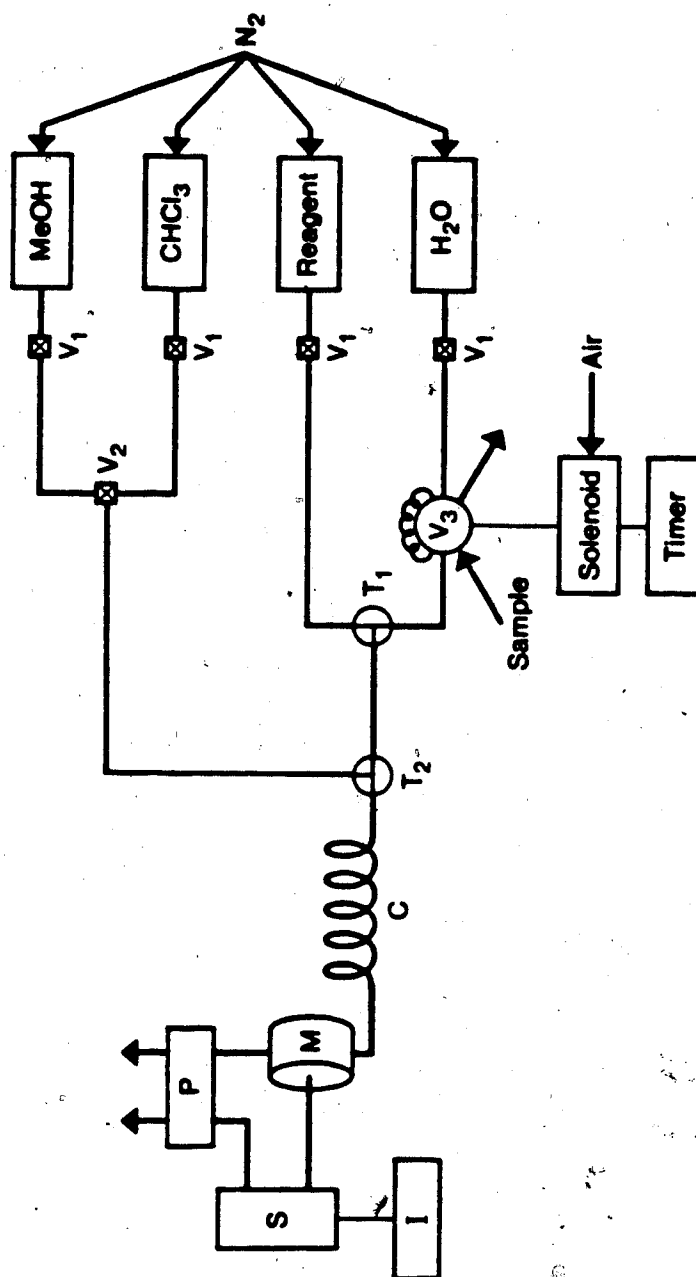


Figure 2. Solvent extraction/FIA apparatus used for system characterization. H_2O , reagent, chloroform and methanol are in pressure cylinders; V_1 and V_2 are two-way and three-way valves; V_3 is an injection valve; T_1 and T_2 are tees; C is the extraction coil; M is the membrane phase separator; S is the spectrophotometer; I is the integrator and P is a peristaltic pump. See text for details.

(part no. CJ-3031, LDC). In this chapter, the aqueous reagent stream used is water, but in general it could be a buffer, ion-pairing reagent, etc. Valve V_3 is actuated by an air solenoid valve (part no. SOL-3-24-VDC, LDC) controlled by an electrical timer which allows variation of fill time and injection time. The injection valve contains a "dummy" loop of equal size to the injection loop, so that the flow rate of aqueous phase is the same in both the load and inject positions. The sample is loaded onto the injection valve either by gravity flow or by use of a peristaltic pump (not shown).

The combined aqueous stream then joins the chloroform stream at tee-fitting, T_2 , and the resulting segmented flow stream passes through the extraction coil, C, in which solvent extraction occurs between the aqueous and chloroform phases. The lengths of 0.3 mm i.d. tubing connecting T_1 to both V_3 and T_2 are made as short as possible to minimize dispersion of the sample zone in these unsegmented flow regions.

A specified length of 0.8 mm i.d. Teflon extraction tube, C, connects T_2 with the membrane phase separator, M. In M, a fraction of the chloroform phase is separated from the segmented aqueous/chloroform flow stream and passes through a 10 μ L flow cell of the spectrophotometer, S (UV-50 photometric detector, Varian Instruments, Walnut

Creek, CA). The length of 0.3 mm i.d. tubing connecting M to S is made as short as possible for the reasons given above.

The chloroform flow stream exiting the spectrophotometer and the aqueous/chloroform flow stream exiting the membrane phase separator pass through Acidflex pump tubes (Technicon Corp., Tarrytown, NY) in a variable speed peristaltic pump, P (Minipuls 2, Gilson Instruments, Ville-le-Belle, France). Flow rates in both streams are measured by collecting the effluents in burets or graduated cylinders and timing with a stopwatch. The speed of pump P is set so that the total flow rate of both phases is somewhat less than the flow rate observed when the tension is released from the pump rollers. This ensures a slight back pressure and prevents out-gassing from the solvents. The signal from S is fed to a Model 3390A digital recording integrator, I, (Hewlett-Packard Co.) which allows measurement of both peak areas and heights. The signal is also monitored on a Fisher Series 5000 recorder (not shown).

Figure 3 shows a cross section of the membrane phase separator, M. Two layers of 4 mil, 10-20 μ pore size Teflon membrane (Zitex, No. E249-122, Chemplast Inc., Wayne, NJ) backed by a perforated Teflon support are sandwiched between two main body pieces which are made of

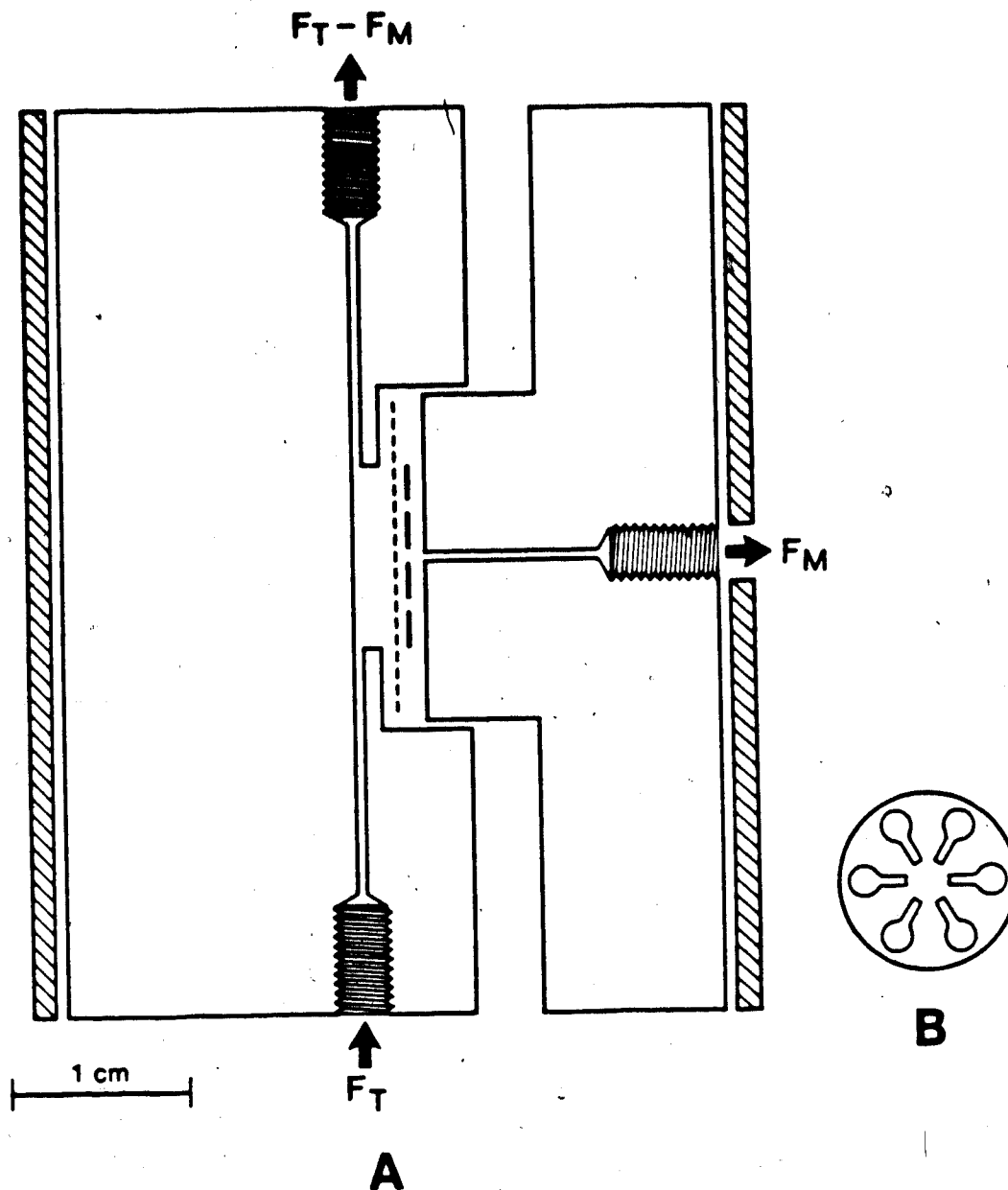


Figure 3. Cross section of the single-membrane phase separator (A). Teflon membrane shown as short dashes. Stainless steel end-plates shown as hashing. Perforated Teflon membrane-support shown as long dashes in A and in front view in B. F_M is flow rate of organic phase through the membrane and F_T is total flow rate of both aqueous and organic phases.

Kel-F. The main body pieces are pressed together with four screws and two stainless steel end plates. The volume of the membrane chamber is about 0.06 mL. The three threaded holes accept the standard polypropylene end pieces (part no. TEF 107, LDC) and flaired Teflon tubing.

2.2.3 Calibration of the Sample Injection Loops

Different lengths of sample loops used in the automatic injection valve were calibrated in terms of volume injected by filling them with a 1×10^{-3} M aqueous solution of methylene blue while the valve was in the load position. The valve was then switched to the inject position and the contents of the sample loop were washed into 100 mL volumetric flasks. The flasks were brought up to volume with water and the absorbance of each solution was measured at a wavelength of 668 nm using a Cary 118 spectrophotometer. The volume of each sample loop was determined from a standard curve.

2.3 Results and Discussion

The characteristics of the extraction/FIA system were studied by using caffeine as a sample component. Each injection of sample resulted in a peak on the recording device. The variations of sample peak area, width and height were investigated as a function of extraction coil

length, sample injection volume and flow rates. The following symbols are used for flow rates: F_O is the total flow rate of the organic phase, F_a is the total flow rate of the aqueous phase, F_m is the flow rate of organic phase through the membrane and F_T is the sum of F_O and F_a . Each data point plotted on every figure in this chapter is an average resulting from six replicate injections of sample.

2.3.1 Extraction Coil Length

The influence of the length of the extraction coil on peak area, height and width at half-height was studied by changing the length of the coil while keeping constant both the concentration and volume of the caffeine solution injected. Flow rates F_O , F_a and F_m , measured after each run, were found to vary slightly with increasing length of the extraction coil. Peak areas were therefore corrected to $F_O = 4.60$ mL/min via equation 2.6 discussed later in Section 2.3.3. Important instrument parameters for the study were as follows: wavelength, 273 nm; injection volume, 44 μ L; sampling frequency, two injections per min; N_2 pressure, 40 psig; caffeine concentration, 90 ppm; $F_O \sim 4.6$ mL/min; $F_a \sim 3$ mL/min; $F_m \sim 2$ mL/min.

The plots of peak area, peak width at half-height and peak height versus extraction coil length are given in

Figures 4A, 4B, and 5 respectively. Figure 4A shows peak area increasing with extraction coil length prior to attainment of distribution equilibria at about 75 cm, beyond which it becomes constant.

Peak width at half-height exhibits an initial increase of about 20% with increasing coil length up to the region where distribution equilibrium is attained, and thereafter it increases at only a very slow rate (Figure 4B). The most significant aspect of peak width behavior revealed in Figure 4B is the fact that for coil lengths in the equilibrium region, peak widths become nearly independent of coil length. Consequently, the extraction coil contributes only very slightly to sample zone dispersion. This is in marked contrast to the extensive laminar flow zone broadening observed in unsegmented flow through small-bore tubing.

The plot of peak height versus extraction coil length (Figure 5) is of a similar shape to the corresponding plot for peak area, although the plateau region is obtained at somewhat shorter coil lengths. The plot is also similar to that obtained by Karlberg and Thelander for the extraction of caffeine into chloroform [11]. To ensure extraction equilibrium, an extraction coil length of 200 cm was used in subsequent studies to characterize the system.

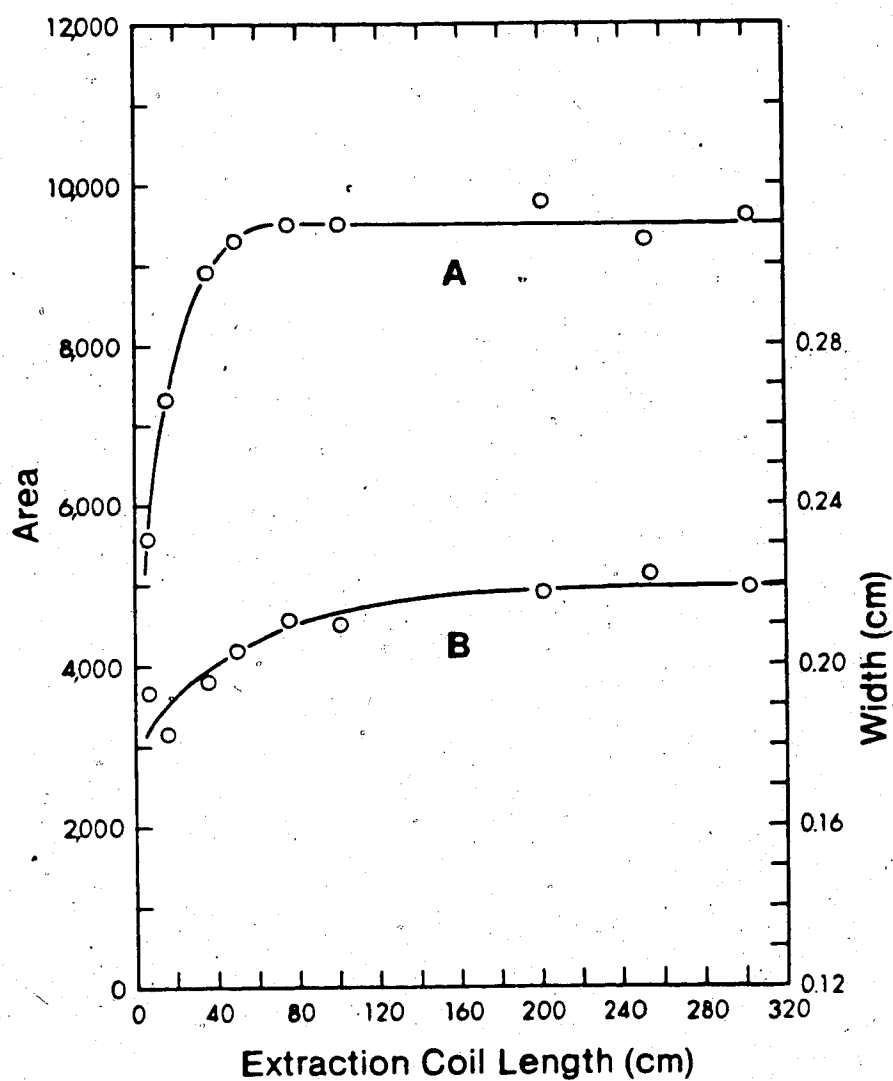


Figure 4. Peak area (A) and peak width at half-height (B) for 90 ppm caffeine versus extraction coil length. The relative standard deviation in peak area and peak width at half-height, for each plotted point, falls within the range of 0.35% to 1.8% and 0.51% to 1.7% respectively.

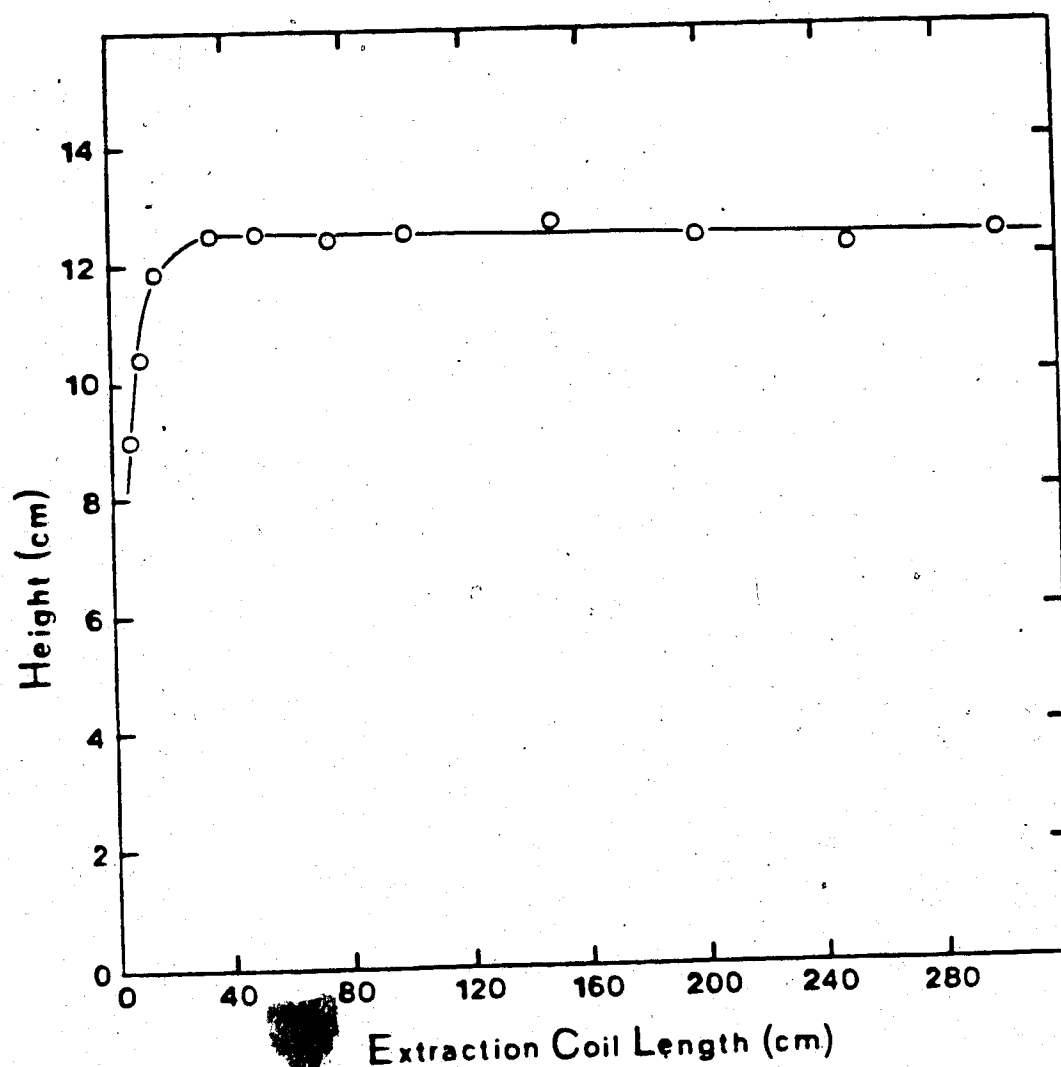


Figure 5. Plot of peak height for .90 ppm caffeine versus extraction coil length. The relative standard deviation in peak height, for each plotted point, falls within the range of 0.53% to 1.2%.

2.3.2 Sample Injection Volume

The volume of sample injected was varied by changing the volume of the sample loop in the automatic injection valve while the extraction coil length, caffeine concentration and flow rates F_o , F_a and F_m were held constant. The volume injected by each loop was determined in a separate experiment using spectrophotometry, as described in Section 2.2.3. The volume of the "dummy" loop was kept equal to that of the injection loop to insure that the flow rate of the aqueous stream was the same in both the load and inject positions. A plot of peak area versus injection volume, shown in Figure 6A was linear with a relative standard deviation of 1.4% for the slope. The intercept, in arbitrary integration units, and its 95% confidence limits were $-1.7 \times 10^3 \pm 4.0 \times 10^3$, showing that the intercept was zero. The linear relationship is as expected since, as shown later in equation 2.4, peak area is directly proportional to the number of moles of sample injected.

A plot of peak width at half-height versus sample volume injected is presented in Figure 7. The general shape of the curve is understood as follows: when injection volumes are sufficiently small ($< 50 \mu\text{L}$), laminar flow of the caffeine zone in the unsegmented flow regions and the mixing chamber effect in the phase

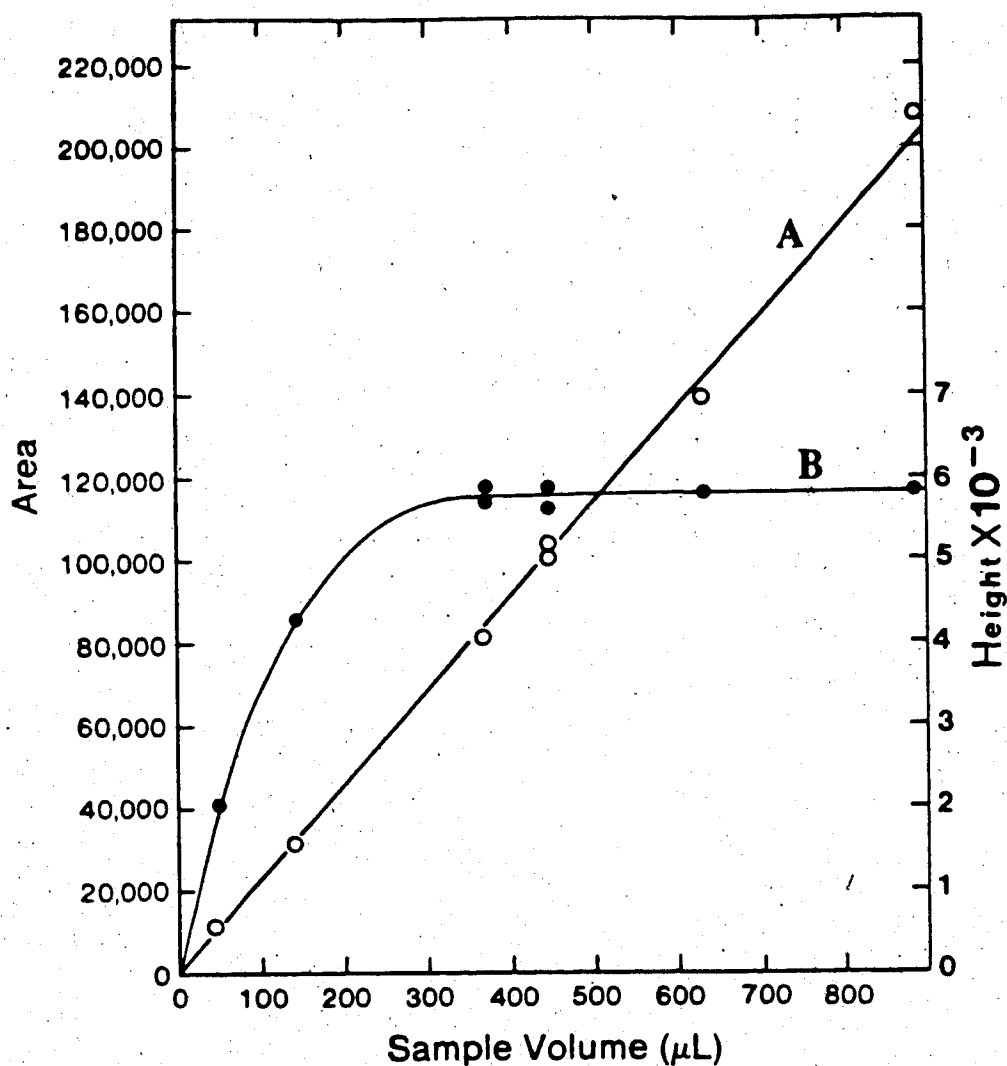


Figure 6. Peak area (A) and height (B) for 90 ppm caffeine versus sample volume injected. Instrument parameters: wavelength, 273 nm; extraction coil length, 200 cm; N₂ pressure, 40 psig; F_O = 4.35 mL/min; F_a = 3.07 mL/min; F_m = 1.68 mL/min. The relative standard deviation in peak height, for each plotted point, falls within the range of 0.23% to 0.70%.

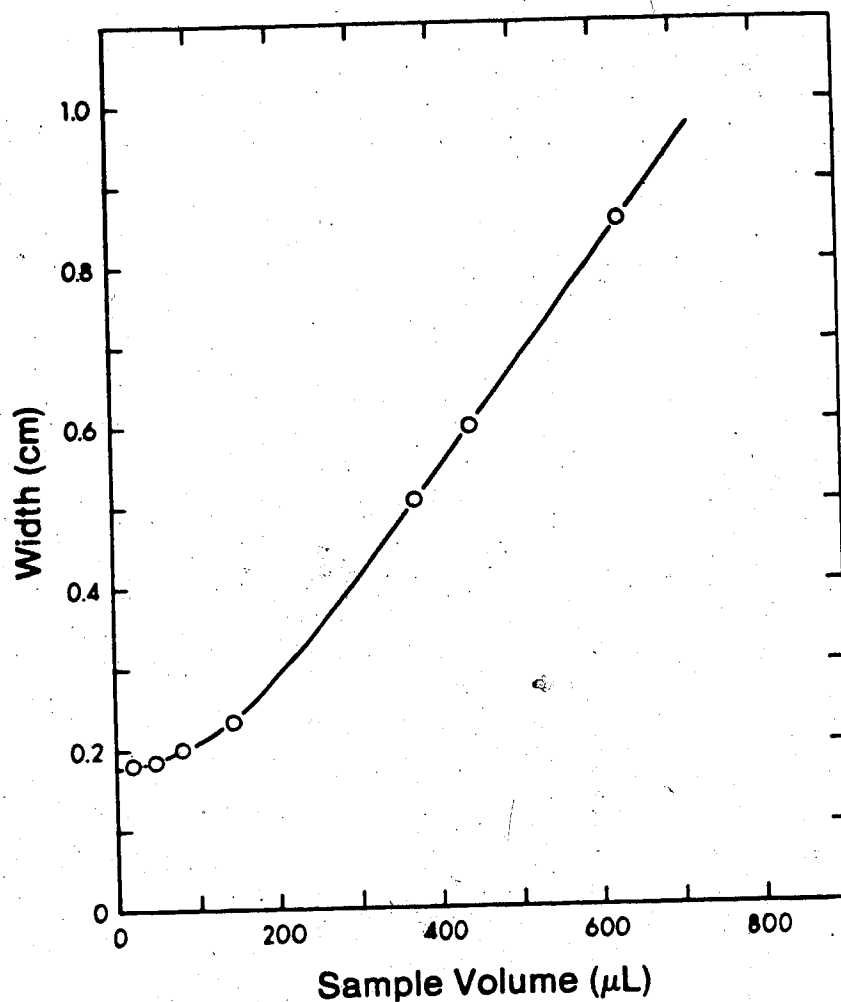


Figure 7. Peak width at half-height for 90 ppm caffeine versus sample volume injected. Instrument parameters: wavelength, 273 nm; extraction coil length, 200 cm; N_2 pressure, 40 psig; $F_O = 3.1$ mL/min; $F_a = 4.0$ mL/min; $F_m = 1.9$ mL/min. The relative standard deviation in peak width at half-height, for each plotted point, falls within the range of 0.10% to 1.7%.

separator are sufficient to affect the concentration profile along the whole length of the caffeine zone, giving it a more or less skewed Gaussian shape [48,49]. Thus, for small injection volumes the peak width will remain more or less constant. When the injected volume is large enough ($> 250 \mu\text{L}$) so that laminar flow and mixing chamber effects influence only the leading and trailing edges of the caffeine zone, but not the central portion, then the concentration profile of caffeine along the zone exhibits a flat "peak" whose height is independent of injection volume and whose width is directly proportional to injection volume. For injection volumes between $50 \mu\text{L}$ and $250 \mu\text{L}$ intermediate behavior is observed. This interpretation of peak width behavior is borne out by a plot of peak height, in arbitrary integration units, versus volume injected (Figure 6B). Peak height increases more or less linearly for injection volume $< 50 \mu\text{L}$, is constant for injection volumes $> 250 \mu\text{L}$, and is increasing nonlinearly at intermediate injection volumes.

A sample volume of $44 \mu\text{L}$ was used in all other experiments since this volume is in the region where peak widths are nearly independent of volume injected and, thus, it allows a maximum sampling frequency without unnecessary sacrifice of sensitivity (i.e., peak area per unit caffeine concentration in the injected solution).

2.3.3 Flow Rates

The dependence of peak area in the organic phase, A_O , on flow rates F_O , F_a and F_m can be predicted as follows. In a concentration-type detector, such as a spectrophotometer, the area of the peak is inversely proportional to the flow rate through the detector F_m . In an extraction process involving a fixed number of moles of sample component injected, the peak area is also proportional to the fraction of sample in the organic phase. At equilibrium this fraction is $(k'/(1+k'))$ where k' is the so-called capacity factor of the sample component [50] and is equal to the ratio of moles of sample component in the organic phase to the moles in the aqueous phase. Peak area is also proportional to the fraction of the organic phase that goes through the membrane and thus goes through the detector (F_m/F_O), and it is proportional to the number of moles of sample injected, n . Combining these relationships and adding the proportionality constant K gives an equation for peak area for a single uv-absorbing sample in the organic phase:

$$A_O = K \frac{n}{F_m} \frac{F_m}{F_O} \frac{k'}{(1+k')} \quad (2.1)$$

Constant K includes the molar absorptivity of the sample in the phase being analyzed, ϵ , the pathlength of the spectrophotometer flowcell, b , and a response factor which relates the absorbance from the detector to a count rate on the integrator, f . It is therefore defined as:

$$K = \epsilon b f \quad (2.2)$$

and has units of $\text{mL min}^{-1} \text{mole}^{-1}$.

The capacity factor may be expressed in terms of the distribution ratio, D (the ratio of concentrations of sample component in the two phases), and the ratio of phase volumes [50]. Since the phase volume ratio is equal to the flow rate ratio for the phases, k' may be expressed as

$$k' = D F_O / F_a \quad (2.3)$$

Combining equations 2.1 and 2.3 and simplifying gives the following general equation for peak area in the organic phase:

$$A_O = \frac{nDK}{F_a + DF_O} \quad (2.4)$$

This expression shows that peak area is independent of flow rate through the detector, F_m . Qualitatively, this is understood by the fact that as F_m is, for example, doubled with F_o and F_a held constant, the sample component will spend only half as much time in the flow cell but twice as many moles of sample will pass through the cell. Hence the area will not change.

Equation 2.4 can be rearranged to give

$$\frac{1}{A_o} = \frac{1}{nDK} [F_T + F_o(D-1)] \quad (2.5)$$

which indicates that a plot of $1/A_o$ versus $[F_T + F_o(D-1)]$ should be linear with a zero intercept.

Equation 2.5, of course, assumes a linear relationship between integrator signal and concentration. This was checked first for caffeine concentrations in the range of 1-90 ppm. The calibration curve obtained, shown in Figure 8, was a straight line with a relative standard deviation for the slope of 0.7%. The y-intercept and its 95% confidence limits were 81 ± 162 integration units.

The validity of equation 2.5 was then examined in a study where peak areas were measured for F_o varying between 2.7 and 8.2 mL/min, with $D = 20$ for caffeine

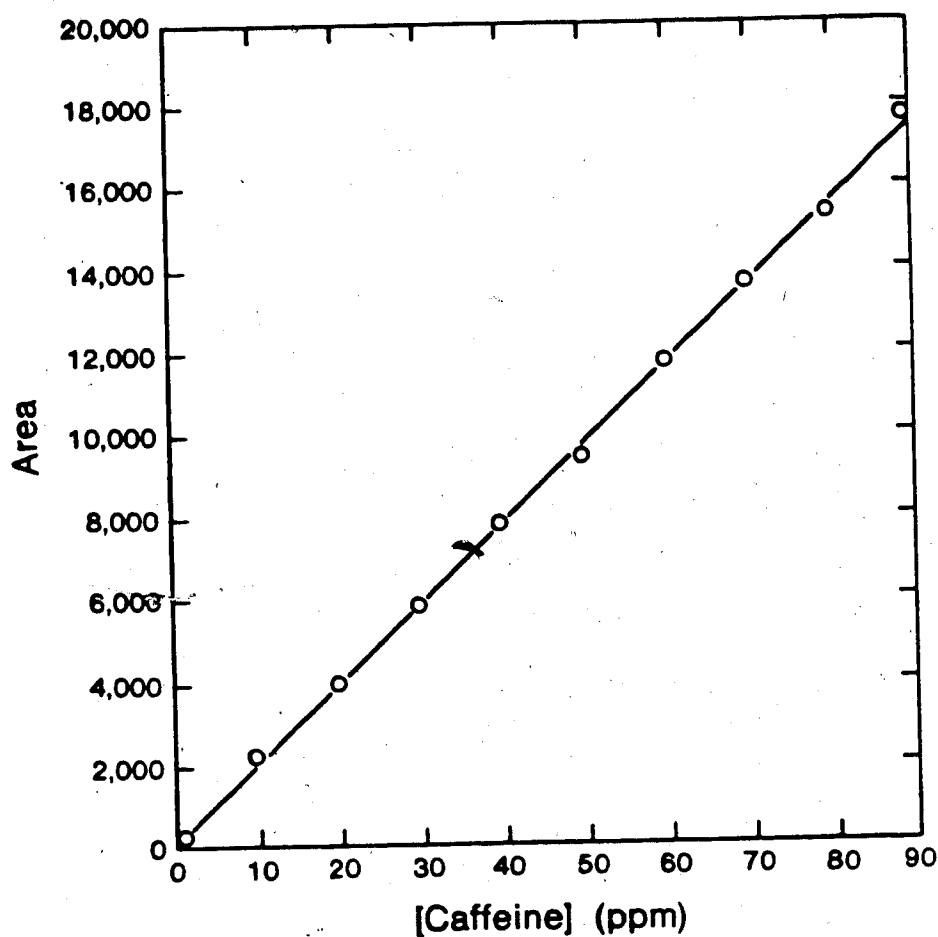


Figure 8. Calibration curve for caffeine. Instrument parameters: wavelength, 273 nm; extraction coil length, 200 cm; injection volume, 44 μL ; sampling frequency, two injections per min; N_2 pressure, 40 psig; $F_o = 5.01$ mL/min; $F_a = 3.02$ mL/min; $F_m = 2.30$ mL/min.

[51]. Important instrument parameters were: caffeine concentration, 90 ppm; wavelength, 273 nm; extraction coil length, 200 cm; injection volume, 44 μ L; sampling frequency, two injections per minute; N_2 pressure, 40 psig. Data for peak area and height dependence on flow rates is given in Table 1. Figure 9 shows a plot of $1/A_O$ versus $[F_T + F_O(D-1)]$. It is linear with a relative standard deviation (RSD) of 1.3% for the slope. The y-intercept and its 95% confidence limits, in arbitrary integration units are $(1.9 \pm 3.6) \times 10^{-6}$, showing that the intercept is zero.

Under conditions of sufficiently large D, such that $DF_O \gg F_a$, the denominator in equation 2.4 can be approximated by DF_O . Substituting and rearranging yields:

$$A_O = \frac{K \cdot n}{F_O} \quad (2.6)$$

This equation shows that when the sample component is quantitatively extracted into the organic phase, the peak area in the organic phase depends only on the number of moles of sample injected and the total flow rate of organic solvent. A plot of A_O versus $1/F_O$ should be linear with a zero intercept. Such a plot is presented in Figure 10 using the caffeine data from the case discussed

Table 1. Data for Peak Area and Height Dependence on Flow Rates (Figures 9 and 10).

F_o (mL/min)	F_a (mL/min)	F_m (mL/min)	Area ^a	Height ^a
2.73	3.99	1.73	15,144 ± 133	3,583 ± 22
3.42	3.59	1.81	12,384 ± 153	2,943 ± 21
4.09	3.11	1.95	10,700 ± 108	2,430 ± 15
4.31	3.03	1.97	9,853 ± 58	2,210 ± 11
4.38	3.00	2.01	10,059 ± 91	2,228 ± 16
5.01	2.67	2.11	8,740 ± 72	1,890 ± 12
5.06	2.94	2.12	8,799 ± 62	1,937 ± 11
5.78	1.30	1.82	7,764 ± 264	1,180 ± 8
6.60	1.79	2.31	6,686 ± 36	1,322 ± 15
8.06	2.08	2.94	5,619 ± 127	1,281 ± 49
8.20	2.41	3.08	5,401 ± 39	1,328 ± 8

a) Average from six replicate injections, in arbitrary integration units, with uncertainties expressed as one standard deviation.

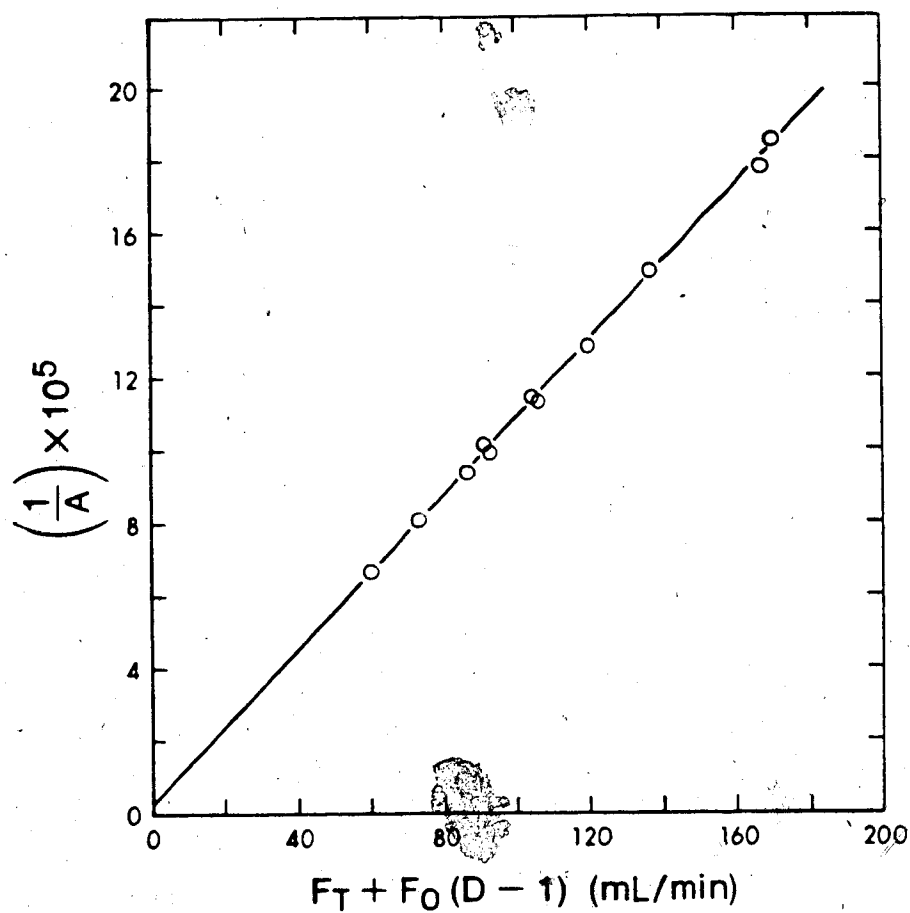


Figure 9. Plot of $1/A$ versus $F_T + F_O(D-1)$ for caffeine.
Line is a linear least-squares fit to the data points.

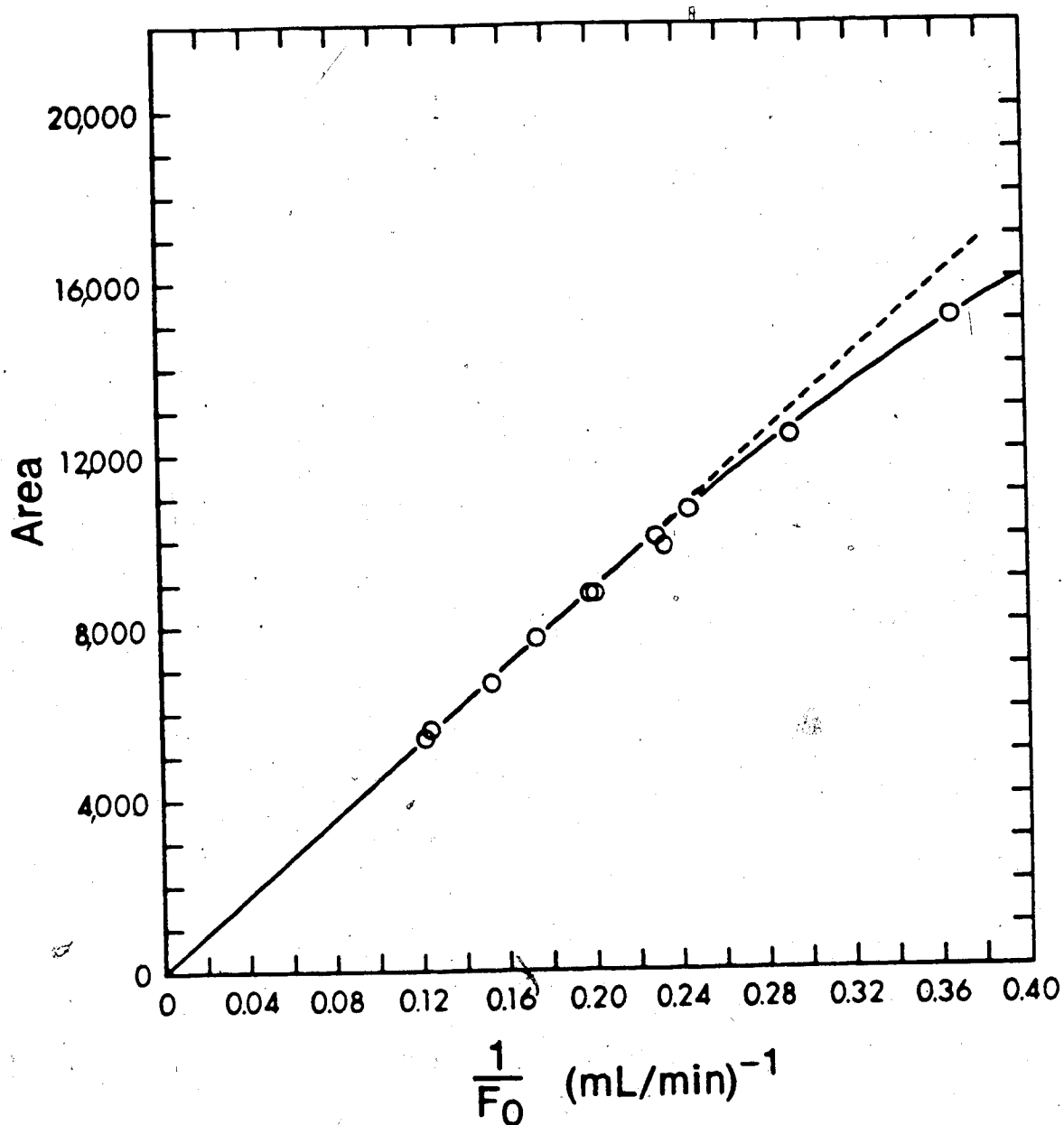


Figure 10. Plot of peak area versus $1/F_0$ for caffeine. Deviation from linearity occurs for low values of F_0 where the assumption $DF_0 \gg F_a$ is no longer valid.

above and reported in Table 1. Deviation from linearity occurs for low values of F_O , where the assumption $DF_O \gg F_a$ is no longer valid. Equation 2.4 or 2.6 can be used where necessary to compensate for the effects of changing flow rates on peak areas.

The increase in peak area with decreasing F_O predicted from equation 2.6 might suggest that a very small ratio of F_O/F_a should be used to achieve increased sensitivity. The more rigorous equation 2.4 shows, however, that there is a theoretically calculable limit to the advantage resulting from this practice. As well, there is a practical limit. As F_O/F_a is decreased, there comes a point where water will "break through" the Teflon membrane and enter the detector flow cell causing an erratic signal. In the present system the "break through" occurred at a value of $F_O/F_a \leq 0.7$ (though the value depends on F_m). In our analyses we have found that low rate ratios $F_O/F_a \approx 1$ and $F_m/F_O \approx 0.5$ are always reliable.

For more direct proof of the lack of dependence of peak area on F_m , a study was performed in which F_O was held constant while F_m was varied. Two separate peristaltic pumps were used in place of pump P in Figure 2. Experimental conditions were the same as those given for the previous study with F_O held constant at 5.6 mL/min by means of a Teflon/glass needle valve placed in the

chloroform stream between V_2 and T_2 . The resulting plot of A_0 versus F_m , shown in Figure 11, was horizontal with a slope and 95% confidence limits of 31 ± 280 integration units indicating that the slope is zero and A_0 is indeed independent of F_m .

2.3.4 Sampling Frequency

A study was performed under optimum conditions to determine the sampling frequency that can be routinely achieved with moderate N_2 pressure applied to the aluminum pump cylinders. Figure 12 presents a series of replicate injections of a caffeine solution made at the frequency of four per minute. (Nitrogen pressure was 60 psig.) Base line separation is achieved between each peak and the relative standard deviation for the replicate injections is 1.2%. This sampling rate can be achieved routinely with no special care or precautions. For safety reasons with the present cylinder design, pressures above 100 psig are not recommended.

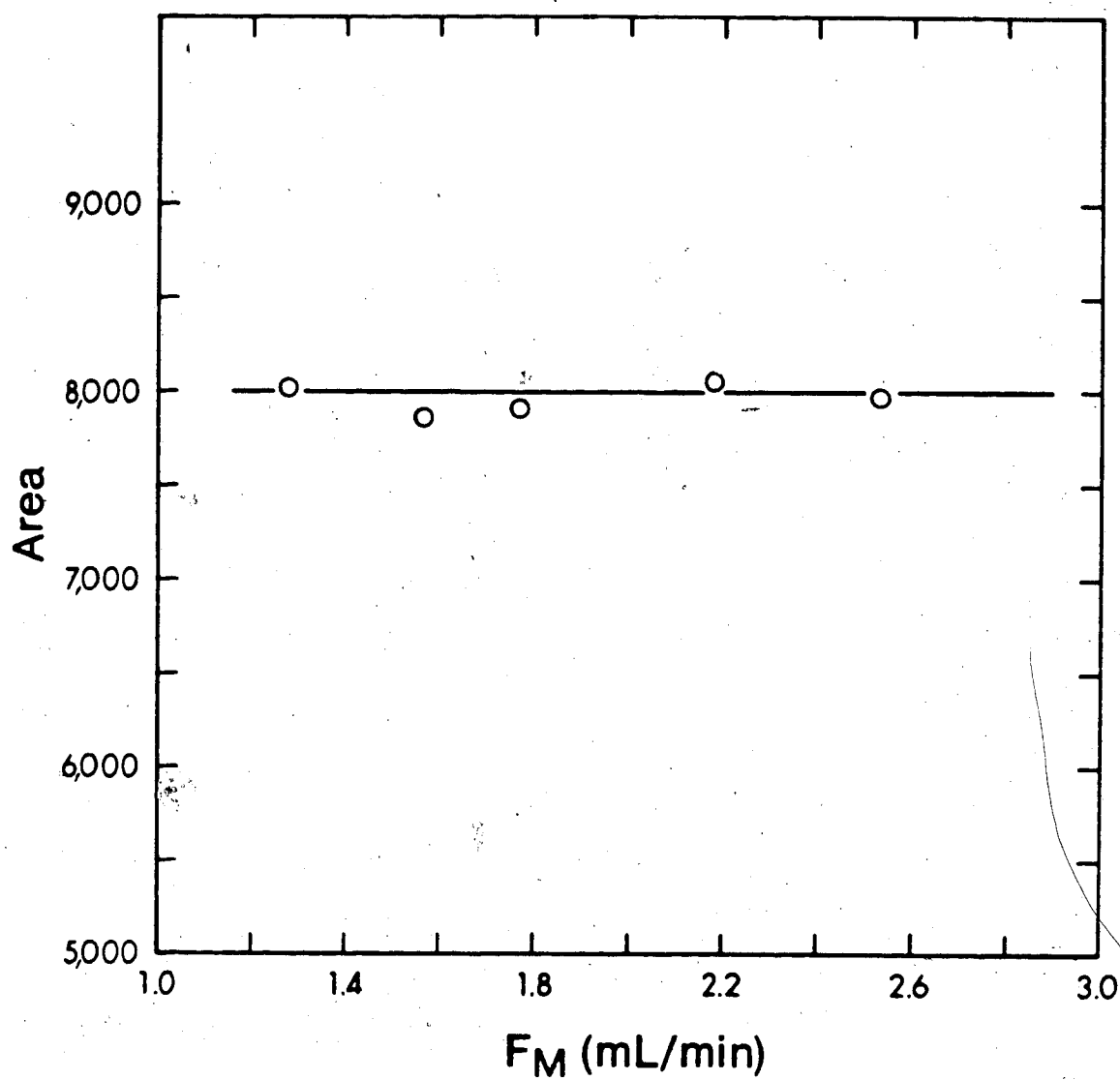


Figure 11. Plot of peak area versus flow rate through the membrane with total flow rate of organic phase held constant.

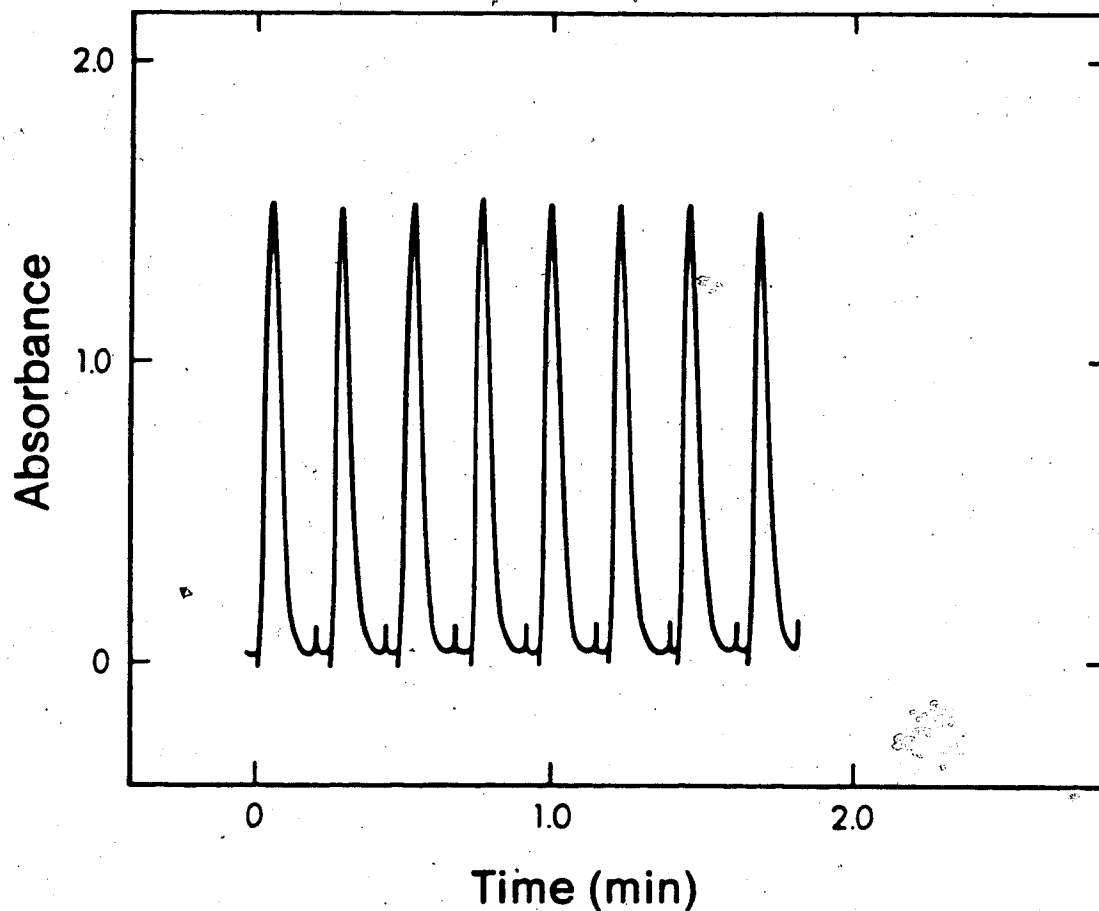


Figure 12. Replicate injections of a 90 ppm caffeine solution at a frequency of four per minute. Instrument parameters: wavelength, 273 nm; extraction coil length, 200 cm; injection volume, 44 μ L; sampling frequency, two injections per min; N_2 pressure, 60 psig; $F_O = 4.4$ mL/min; $F_a = 4.6$ mL/min; $F_m = 3.2$ mL/min.

CHAPTER 3

ANALYSIS OF PROCYCLIDINE HYDROCHLORIDE IN TABLETS BY ION-PAIR EXTRACTION WITH PICRATE

3.1 Introduction

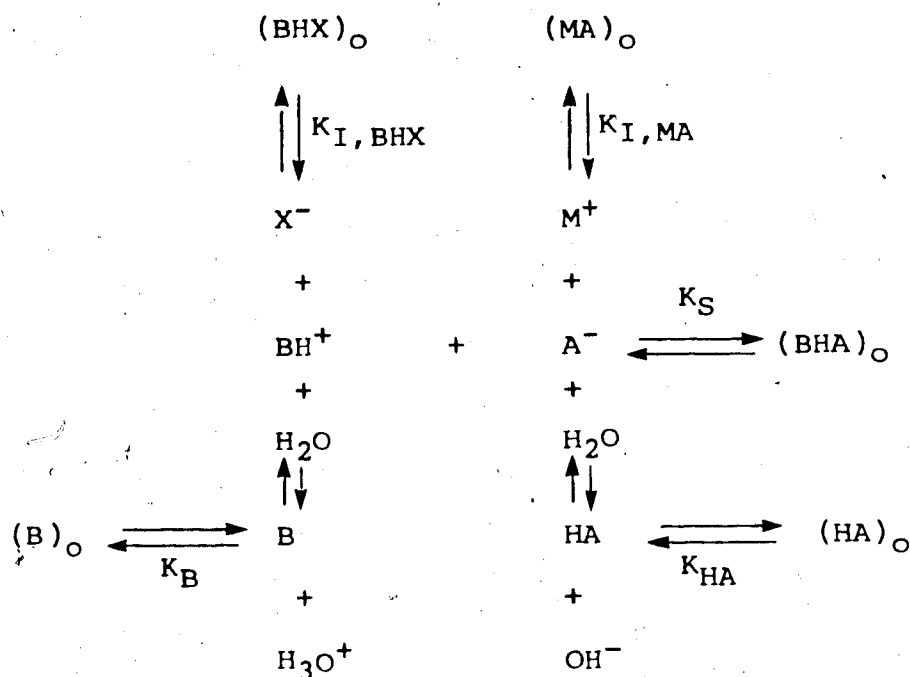
Procyclidine hydrochloride is an antispasmodic drug used in the treatment of Parkinsonism. Official methods of assay for procyclidine hydrochloride in tablets include ion-pair extraction of the procyclidinium bromocresol purple ion pair [52]. Ion-pair extraction is, in fact, a sensitive and precise technique for the determination of basic drugs [53-61] which is amenable to use in an extraction/FIA system. It involves extraction of ionic species into organic solvents as ion aggregates (the simplest being ion pairs) which have zero net charge.

Extraction is favored when the ions are large and the charge is low [62]. If one of the ions is sufficiently large, and hydrophobic, however, it can form extractable ion pairs with relatively small ions such as Na^+ and Cl^- . The extraction and stability of the ion pairs will depend on the solvating ability of the organic phase (through hydrogen bonding, dipole-induced dipole attraction, etc.). In general, the extraction constant

increases with increasing polarity of the organic phase [55]. Alcoholic phases have high extraction capacities but, at the same time, low selectivity for hydrophilic compounds. Solvents, such as chloroform and methylene chloride, which are weak hydrogen donors have a high selectivity, evidenced by large differences in extraction constants of closely related ion pairs.

In addition to the choice of the organic phase, the degree of ion-pair extraction can be regulated by the kind and concentration of the counter ion [53]. Picrate is often used as an ion-pairing reagent for amines and quaternary ammonium ions [53-61]. Its high acidity constant ($K_a = 0.47$ and $pK_a = 0.33$ at ionic strength 0.1) makes it useful as a counter ion over a broad pH range, and its large molar absorptivity provides high sensitivity for photometric determinations [56]. An additional advantage is the negligible extraction of sodium picrate between chloroform or methylene chloride and aqueous solution [56,59-61].

The ion-pair extraction of a cation, BH^+ , with an anion, A^- , may be influenced by a variety of side reactions. Some of these side reactions are represented by the following chemical and phase distribution equilibria [59]:



Species without subscripts are in the aqueous phase and those with the subscript "o" are in the organic phase. In the present study, K_{S} represents the ion-pair extraction constant for procyclidinium picrate with chloroform as the organic phase. M^{+} and X^{-} are the sodium and chloride ions present in the aqueous reagent phase.

The procyclidinium cation and the picrate anion are involved in pH-dependent equilibria with their conjugate forms, base B and acid HA respectively. These species distribute between chloroform and aqueous phases. A value for $K_{\text{HA}} = 29.5$ has been reported for the partitioning of picric acid between chloroform and aqueous solution [58]. Optimal adjustment of the pH insures that

negligible amounts of the neutral forms B and HA exist [59].

Extractable ion pairs may also be formed between the procyclidinium cation and chloride anion, $(\text{BHX})_O$, and the picrate anion and sodium cation, $(\text{MA})_O$. As mentioned earlier, the extraction of sodium picrate into chloroform is negligible. The ion-pair extraction constant for procyclidinium chloride is not known but it is expected to be small as compared to the ion-pair extraction constant for procyclidinium picrate. Cantwell and Carmichael [61] report $K_S = 4 \times 10^6$ for promethazinium picrate and $K_{I,\text{BHX}} = 10.8$ for promethazinium chloride, with chloroform as the organic phase. A constant value for $K_{I,\text{BHX}}$ can be insured by keeping the chloride concentration in the aqueous phase constant and high compared to the procyclidinium ion concentration.

Side reactions in the aqueous phase, such as ion pair formation and self-association of anions and cations, are not expected to occur to a significant extent [55,57,59]. Additional side reactions that may occur in the organic phase include dissociation and further association of the ion pairs. These effects serve to enhance extraction into the organic phase, but cause non-linear distribution isotherms [63]. The tendency towards

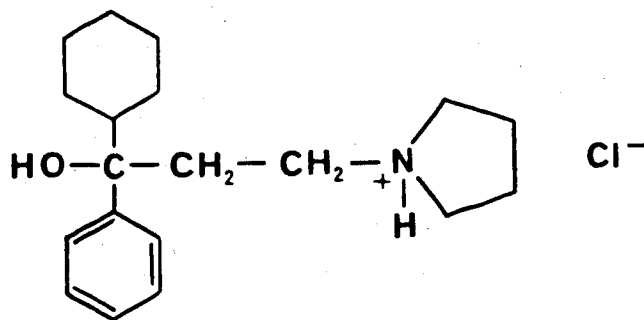
dissociation of ion pairs is greater when sample concentrations are low and when the organic solvent is more polar [53,55]. Dimerization of ion pairs or formation of larger aggregates in the organic phase may occur at high sample concentrations and with low polarity organic solvents [55]. Neither dissociation nor association of the procyclidinium picrate ion pairs is expected to occur to any significant extent at the concentrations used in the present study.

This chapter will deal with the assay of procyclidine hydrochloride in commercial tablets by ion-pair extraction with picrate, as a practical application of the solvent extraction/FIA system.

3.2 Experimental

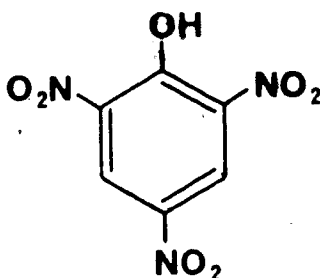
3.2.1 Chemicals and Solvents

Procyclidine Hydrochloride was B.P. grade and was used as received from Burroughs Wellcome Ltd., La Salle, Quebec. Its structure is:



Procyclidine Hydrochloride Tablets (Kemedrin tablets, 5 mg) were supplied by Burroughs Wellcome Ltd., and were B.P. grade.

Picric Acid (reagent grade) was used as received from Matheson, Coleman and Bell, Norwood, Ohio. Its structure is:



Other Chemicals including sodium chloride, sodium hydroxide and perchloric acid were all reagent grade.

Double Distilled Water, Chloroform and Methanol were described in Chapter 2.

3.2.2 Reagents

4.9×10^{-2} M Picric Acid Stock Solution was prepared in water and standardized with sodium hydroxide.

Picrate solutions, 0.1 M in NaCl, were prepared at the following pH values and picrate concentrations by combining the appropriate weight of NaCl and aliquot of stock solution with enough HCl or NaOH to yield the desired concentrations and pH upon dilution to the final

volume:

1. pH = 1.65, 5.0×10^{-4} M picrate
2. pH = 2.04, 5.0×10^{-4} M picrate
3. pH = 2.12, 5.0×10^{-4} M picrate
4. pH = 2.60, 5.0×10^{-4} M picrate
5. pH = 2.91, 5.0×10^{-4} M picrate
6. pH = 2.0, 5.0×10^{-5} M picrate
7. pH = 2.0, 2.5×10^{-3} M picrate
8. pH = 2.0, 4.9×10^{-3} M picrate
9. pH = 2.0, 2.5×10^{-2} M picrate

3.2.3 Standards and Samples

Procyclidine Hydrochloride Standards, for the tablet assay, of concentrations 1.23×10^{-4} M and 1.72×10^{-4} M were prepared by pipetting the appropriate volumes of a 2.46×10^{-3} M stock solution into 200 mL volumetric flasks, followed by dilution to volume with water.

Procyclidine Hydrochloride Sample Solutions were prepared by first weighing, then grinding, 20 tablets to a fine powder with a mortar and pestle. One equivalent tablet weight of powder was then transferred in duplicate into 100 mL volumetric flasks, diluted to volume with water, and shaken vigorously for 5 min. The solutions were centrifuged and the clear supernatant liquids constituted the sample solutions.

3.2.4 Apparatus

The solvent extraction/FIA system used for the analysis of procyclidine hydrochloride is shown in Figure 2. It is exactly the same as the apparatus discussed in Chapter 2 for the caffeine determination except that the reagent phase is a picrate solution, 0.10 M in NaCl and of optimum pH. The configuration used, in which the sample is injected into an inert carrier stream which is then merged with the reagent stream, promotes better mixing than if the sample is injected directly into the reagent stream.

3.2.5 Tablet Assay Procedure

Standards and samples for the tablet assay were injected alternately into the extraction/FIA system and peak areas were measured for six injections of each solution. A pH = 2.01, 2.46×10^{-2} M picrate solution that was 0.10 M in NaCl was used as the reagent phase. The procyclidine hydrochloride sample solutions were centrifuged rather than filtered before injection since it was found that filtration yielded low results, likely due to adsorption of some procyclidine hydrochloride onto the filter paper.

Important instrument parameters for the tablet assay were: wavelength, 400 nm; injection volume, 44 μ L;

sampling frequency, two injections per min; N_2 pressure, 40 psig; extraction coil length, 200 cm; F_o , 3.21 mL/min; F_a , 3.25 mL/min; F_m , 1.72 mL/min.

3.3 Results and Discussion

The conditions for the assay of procyclidine hydrochloride in tablets were optimized by examining the effects of the extraction coil length, reagent pH and picrate concentration in the reagent on peak areas. Each data point plotted on every figure in this chapter is an average resulting from six replicate injections of sample.

3.3.1 Extraction Coil Length

A study was done to determine the length of the extraction coil needed to achieve equilibrium for the extraction of the procyclidinium picrate ion pair into chloroform. Peak areas were measured for replicate injections of a 6.2×10^{-5} M aqueous procyclidine hydrochloride solution using a pH = 2.04, 0.10 M NaCl, 5.0×10^{-4} M picrate solution as the reagent phase.

Extraction coils varied in length from 25 cm to 302 cm. All other variables were fixed. Since flow rates, F_o , F_a and F_m varied somewhat with extraction coil length, peak areas were corrected to $F_o = 3.55$ mL/min via equation 2.6, as discussed for caffeine in Chapter 2.

Instrument parameters for the study were as follows: wavelength, 400 nm; injection volume, 44 μ L; sampling frequency, two injections per min; N_2 pressure, 40 psig; $F_o \sim 3.6$ mL/min; $F_a \sim 3.8$ mL/min; $F_m \sim 2.0$ mL/min.

The plot of peak area versus extraction coil length is shown in Figure 13. The shape is very similar to that shown in Figure 4A for caffeine. In order to insure extraction equilibrium, an extraction coil length of 200 cm was used in subsequent studies.

3.3.2 Reagent pH

The pH dependency of the ion-pair extraction of several tertiary amine drugs with picrate has been previously studied by Cantwell and Carmichael using chloroform as the organic phase [61]. Plots of the conditional ion-pair extraction constant versus aqueous phase pH were found to attain a maximum plateau in the pH range of about 2-5. The conditional extraction constants decreased for pH values ≤ 2 due to protonation of the picrate anion. The pH at which this decrease occurs will depend primarily on both the acidity constant for picric acid and the distribution coefficient for picric acid between chloroform and the aqueous phase. The conditional extraction constant for the ion pair of interest will fall

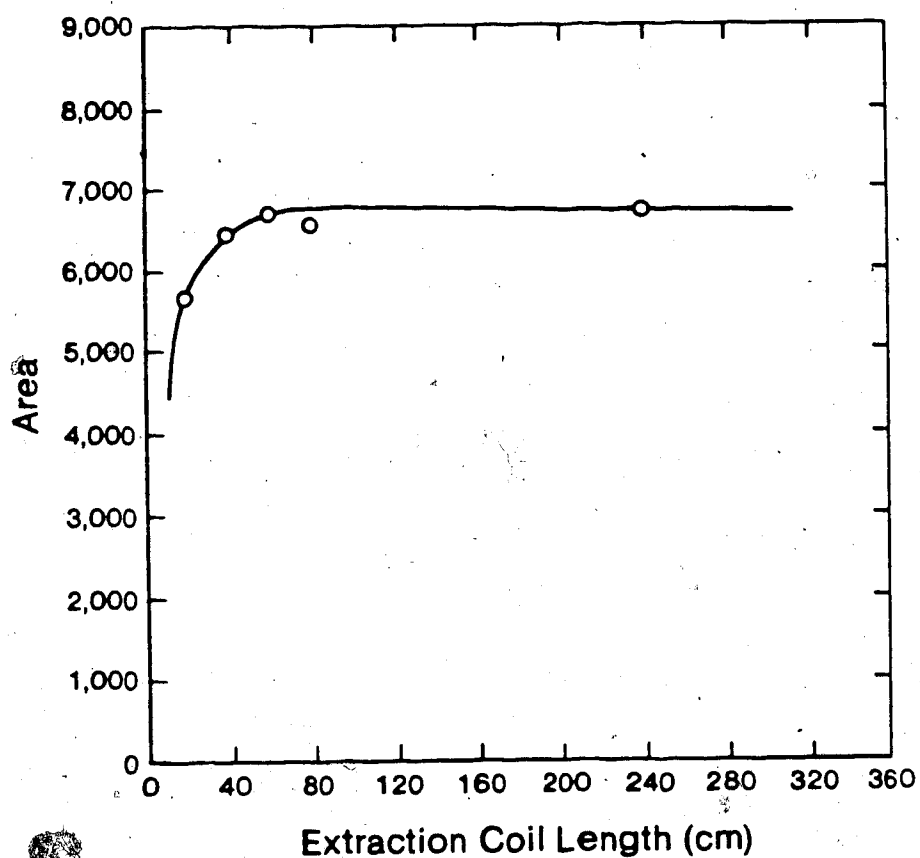


Figure 13. Peak area versus extraction coil length for procyclidine hydrochloride extracted as a picrate ion pair. The relative standard deviation in peak area, for each plotted point, falls within the range of 0.57% to 1.3%.

off at higher pH values due to deprotonation of the cationic conjugate species of the amine drug, BH^+ . The pH at which this decrease occurs will depend on both the acidity constant for BH^+ and the distribution coefficient for the corresponding conjugate base species, B, between chloroform and the aqueous phase.

For the ion-pair extraction of diphenhydramine with picrate into chloroform, Cantwell and Carmichael observed, a maximum extraction plateau in the pH range of about 2.5 to 3.5 [61]. We expect the extraction maximum for the procyclidinium picrate ion pair to also occur in approximately this pH range (based on the structural similarity of diphenhydramine and procyclidine).

This was checked by measurement of peak areas for replicate injections of a 4.9×10^{-5} M procyclidine hydrochloride solution into picrate reagents of pH values 1.65, 2.12, 2.60 and 2.91. The NaCl concentration and picrate concentration of the reagents were fixed at 0.10 M and 5.0×10^{-4} M respectively. Instrument parameters were the same as those used in the extraction coil study with $F_o = 3.4$ mL/min, $F_a = 3.4$ mL/min, $F_m = 1.8$ mL/min and extraction coil length = 200 cm.

Peak areas were found to be constant over the pH range studied indicating that the pH maximum plateau had indeed been achieved. Consequently, a reagent pH of 2.0 was chosen for subsequent experiments.

3.3.3 Picrate Concentration

The optimum picrate concentration was determined in a study where a 4.9×10^{-5} M procyclidine hydrochloride sample solution was injected into pH = 2.0 reagents, 0.10 M in NaCl, ranging in picrate concentration from 5.0×10^{-5} M to 2.5×10^{-2} M. Instrument parameters were the same as those used in the extraction coil length study with $F_o = 3.46$ mL/min, $F_a = 3.5$ mL/min, $F_m = 1.86$ mL/min and extraction coil length = 200 cm.

A plot of peak area versus the ratio of picrate in the reagent to procyclidine hydrochloride in the sample is shown in Figure 14. Peak area increases until a ratio of about 100:1, above which the peak area increases only slightly with increasing ratio. In subsequent studies, a picrate reagent concentration of 2.46×10^{-2} M was used which represents a picrate/procyclidine hydrochloride ratio of about 500:1 for the procyclidine hydrochloride concentration used in the study reported in Figure 14.

3.3.4 Calibration

A calibration curve was prepared with procyclidine hydrochloride sample concentrations ranging from 2.5×10^{-6} M to 2.0×10^{-4} M. A pH = 2.0, 0.10 M NaCl, 2.46×10^{-2} M picrate solution was used as the reagent phase. Instrument parameters were the same as those used in the

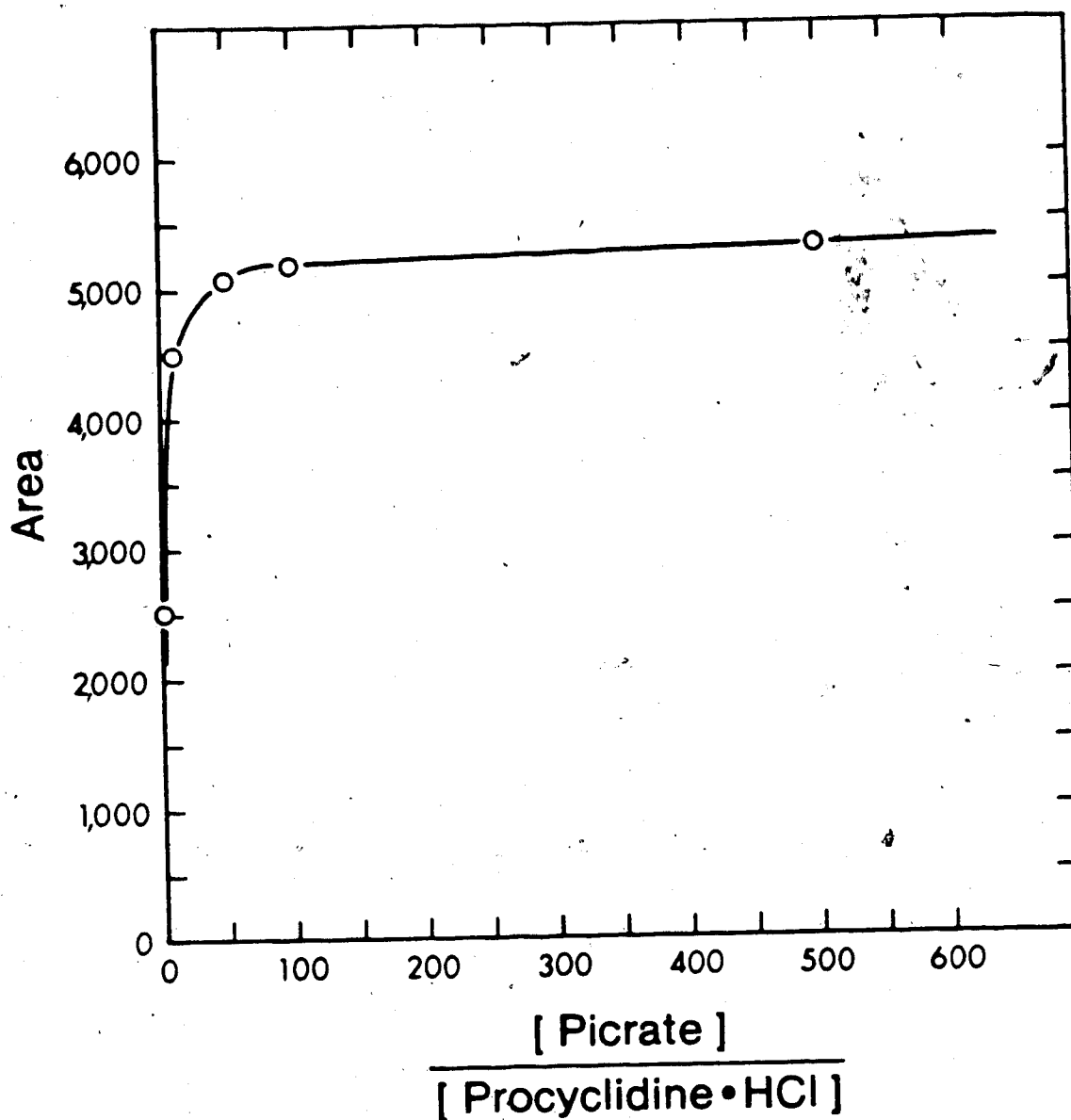


Figure 14. Peak area of extracted procyclidinium picrate as a function of reagent/sample concentration ratio. The relative standard deviation in peak area, for each plotted point, falls within the range of 0.81% to 2.4%.

extraction coil length study with $F_o = 3.27$ mL/min, $F_a = 3.20$ mL/min, $F_m = 1.71$ mL/min and extraction coil length = 200 cm.

Figure 15 shows the resulting plot of peak area versus procyclidine hydrochloride concentration. It is a straight line with a relative standard deviation for the slope of 1.3%. The y-intercept and its 95% confidence limits were -58 ± 216 integration units. The linearity of the calibration curve, in the concentration range studied, suggests the absence of concentration-dependent side reactions such as dimerization and dissociation of ion pairs in the organic phase.

3.3.5 Tablet Assay

When the procyclidine hydrochloride content of tablets having a label claim of 5 mg/tablet was assayed by the procedure given in Section 3.2.5, an assay value of 4.88 mg/tablet was obtained with a standard deviation of 0.06 mg/tablet based on six replicate injections of each standard and each sample solution. This assay value, which corresponds to 97.6% of label claim, is well within the $\pm 10\%$ tolerance limits allowed by the British Pharmacopeia, and is in excellent agreement with the value of 98.2% reported by the manufacturer [64].

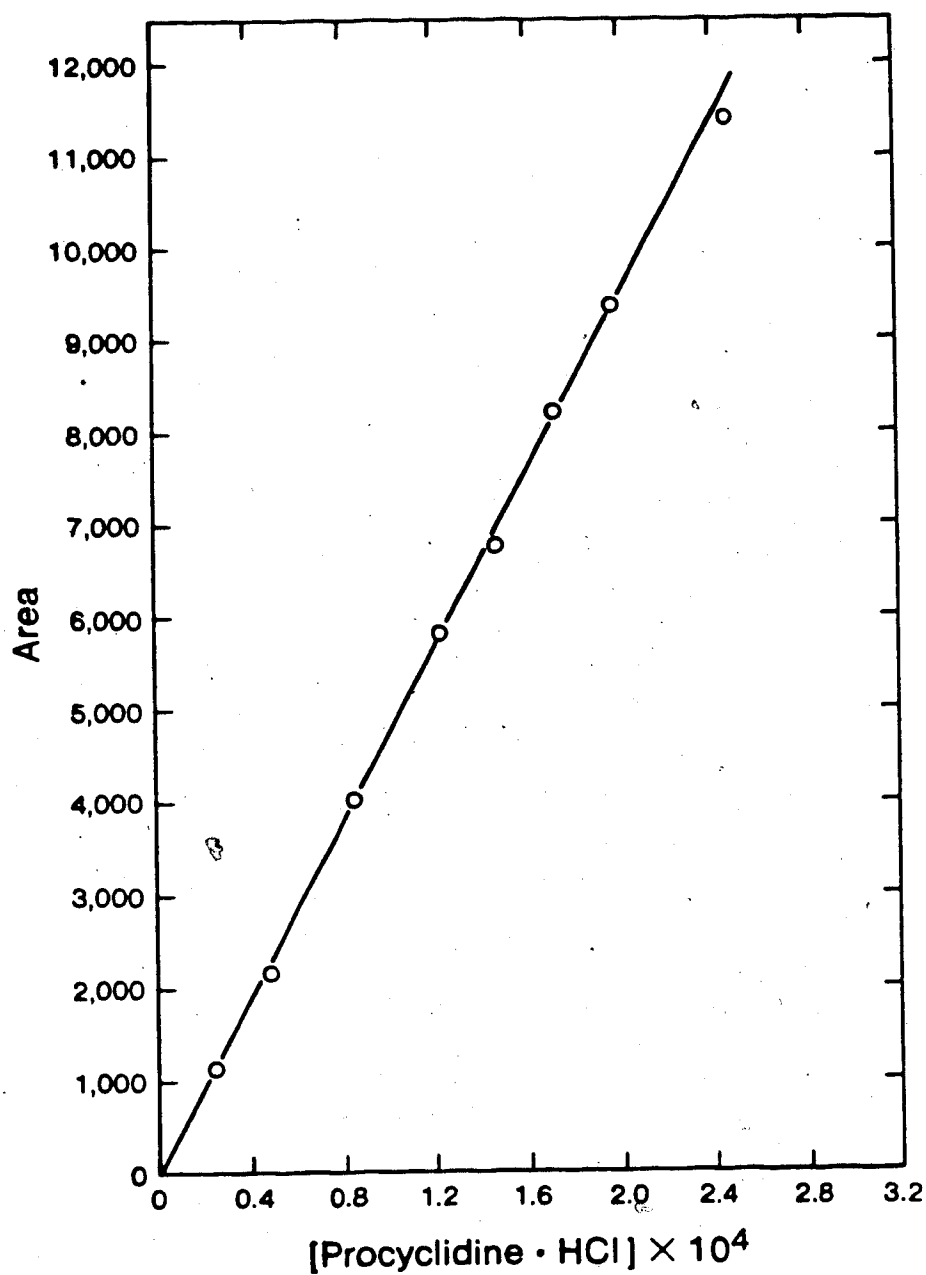


Figure 15. Calibration curve for procyclidine hydrochloride extracted as a picrate ion pair.

CHAPTER 4

ASSAY OF DRAMAMINE TABLETS BY SIMULTANEOUS MONITORING OF AQUEOUS AND ORGANIC PHASES

4.1 Introduction

The single-membrane phase separator, discussed in Chapter 2, proved to be an excellent device for removing a portion of the organic phase from the two-phase flow in a solvent extraction/FIA system. In some cases it is desirable to monitor both phases, to determine a compound that extracts into the organic phase as well as one that is left behind in the aqueous phase. Alternatively, one may want to monitor the concentration of a single component in both phases in order to determine its distribution coefficient and/or its acidity constant. A dual-membrane phase separator was therefore developed to allow simultaneous monitoring of both the aqueous and organic phases of an extraction/FIA system.

The phase separator incorporates a hydrophobic Teflon membrane and a hydrophilic paper membrane to allow passage of a portion of the organic phase, free from entrained aqueous phase, through to one detector and at the same time permits flow of a portion of the aqueous phase, free

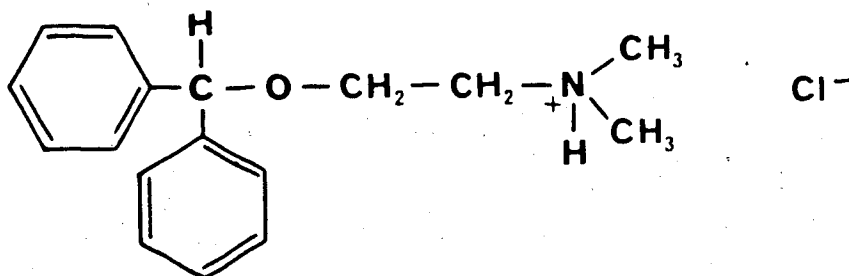
of entrained organic phase, through to another detector. The dual-membrane phase separator is compatible with high flow rates, and can be used for weeks to months before the membranes need to be replaced.

This chapter describes the use of the dual-membrane phase separator in the assay of diphenhydramine and 8-chlorotheophylline in Dramamine motion sickness tablets by the extraction/FIA technique [31]. At a suitable pH, which is readily ascertained by measuring the extraction-pH profiles of both drugs, the former drug is extracted quantitatively into cyclohexane and the latter remains quantitatively in the aqueous buffer.

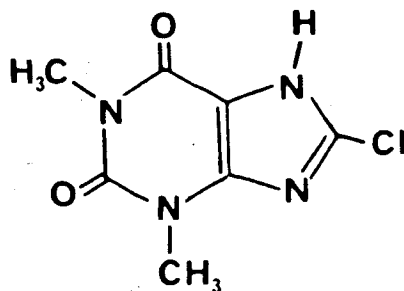
4.2 Experimental

4.2.1 Chemicals and Solvents

Diphenhydramine Hydrochloride was supplied by L. Chatten, Pharmacy Department, University of Alberta. It was previously assayed as $99.8 \pm 0.1\%$ [65]. Its structure is:



8-Chlorotheophylline was obtained from G.D. Searle and Co., Chicago, Illinois. The purity was 99.7% as reported by the manufacturer. Its structure is:



Dramamine Tablets (Dimenhydrinate, 50 mg) supplied by G.D. Searle and Co., Chicago, Illinois, were USP grade.

Other Chemicals including citric acid, sodium phosphate monobasic, sodium phosphate dibasic, concentrated aqueous ammonia and ammonium chloride were all reagent grade.

Double Distilled Water was described in Chapter 2.

Acetone and Cyclohexane were both analytical reagent grade and were filtered before use with a 25-50 μ pore size sintered glass funnel.

4.2.2 Standards and Samples

8-Chlorotheophylline Standard (1.25×10^{-3} M) and Diphenhydramine Hydrochloride Standard (1.25×10^{-3} M) for the tablet assay were prepared by placing the appropriate

weights of 8-chlorotheophylline and diphenhydramine hydrochloride into 200 mL volumetric flasks, which were then partially filled with warm pH = 7.0 phosphate buffer and shaken to effect dissolution. The solutions were cooled to room temperature and diluted to volume with room temperature pH = 7.0 buffer.

8-Chlorotheophylline Standard (7.51×10^{-4} M) and Diphenhydramine Hydrochloride Standard (7.49×10^{-4} M) for the tablet assay were prepared by placing the appropriate aliquots of the pH = 7.0, 1.25×10^{-3} M 8-chlorotheophylline and diphenhydramine standards into 100 mL volumetric flasks, which were then diluted to volume with pH = 7.0 phosphate buffer.

Dramamine Sample Solutions were prepared by first weighing then grinding to a fine powder, twenty Dramamine tablets using a mortar and pestle. One equivalent tablet weight of powder was transferred in duplicate into 100 mL volumetric flasks, shaken for 5 minutes with 75 mL of warm pH = 7.0 phosphate buffer, cooled and diluted to volume with room temperature pH = 7.0 buffer. The clear, light yellow supernatant obtained upon centrifuging constituted the sample solution.

8-Chlorotheophylline Stock Solution (2.50×10^{-3} M) was prepared by placing the appropriate weight of 8-chlorotheophylline into a 500 mL volumetric flask which

was then partially filled with pH = 7.6 phosphate buffer, shaken to effect dissolution and diluted to volume with more buffer.

8-Chlorotheophylline Calibration Solutions of concentrations 1.50×10^{-3} M, 1.25×10^{-3} M, 9.99×10^{-4} M, 7.49×10^{-4} M, 4.99×10^{-4} M and 2.50×10^{-4} M were prepared by placing the appropriate aliquots of the 2.5×10^{-3} M stock solution into 100 mL volumetric flasks and diluting to volume with pH = 7.6 phosphate buffer.

Diphenhydramine Hydrochloride Calibration Solutions of concentrations 2.00×10^{-3} M, 1.50×10^{-3} M, 1.25×10^{-3} M, 9.99×10^{-4} M, 7.50×10^{-4} M, 5.00×10^{-4} M and 2.50×10^{-4} M were prepared by pipetting the appropriate aliquots of an aqueous 2.50×10^{-3} M diphenhydramine hydrochloride stock solution into 100 mL volumetric flasks and diluting to volume with water.

4.2.3 Reagents

Citric Acid/ Na_2HPO_4 Buffers of pH values 3.01, 4.24, 5.24, 6.19 and 7.06 were prepared by combining the appropriate volumes of 0.2 M Na_2HPO_4 and 0.1 M citric acid to give a final volume of 500 mL.

pH = 10.10 and pH = 10.29 Ammonia Buffers for the extraction coil length study and reagent pH study respectively were prepared by combining NH_4Cl with

concentrated aqueous ammonia to give a final analytical ammonia concentration of 1.18 M.

• pH = 10.2 Ammonia Buffers for the calibration curve, tablet dissolution and tablet assay studies were prepared by combining NH_4Cl with concentrated aqueous ammonia to give a final analytical ammonia concentration of 0.66 M.

pH = 7.0 Phosphate Buffer used in dissolving standards and samples for the tablet assay were prepared by combining Na_2HPO_4 and NaH_2PO_4 to give a final analytical phosphate concentration of 0.025 M.

pH = 7.6 Phosphate Buffer used in preparing sample solutions for the 8-chlorotheophylline calibration curve study was made by combining Na_2HPO_4 and NaH_2PO_4 to give a final analytical phosphate concentration of 0.025 M. a

4.2.4 Apparatus

A diagram of the extraction/FIA system is presented in Figure 16. The components prior to the dual-membrane phase separator, M, have been discussed in Chapter 2. The organic extracting solvent, in this case, is cyclohexane and the rinse solvent is acetone. The latter was used only when the system was to be flushed out such as on the rare occasion when the conditions used caused a solvent to break through the wrong membrane.

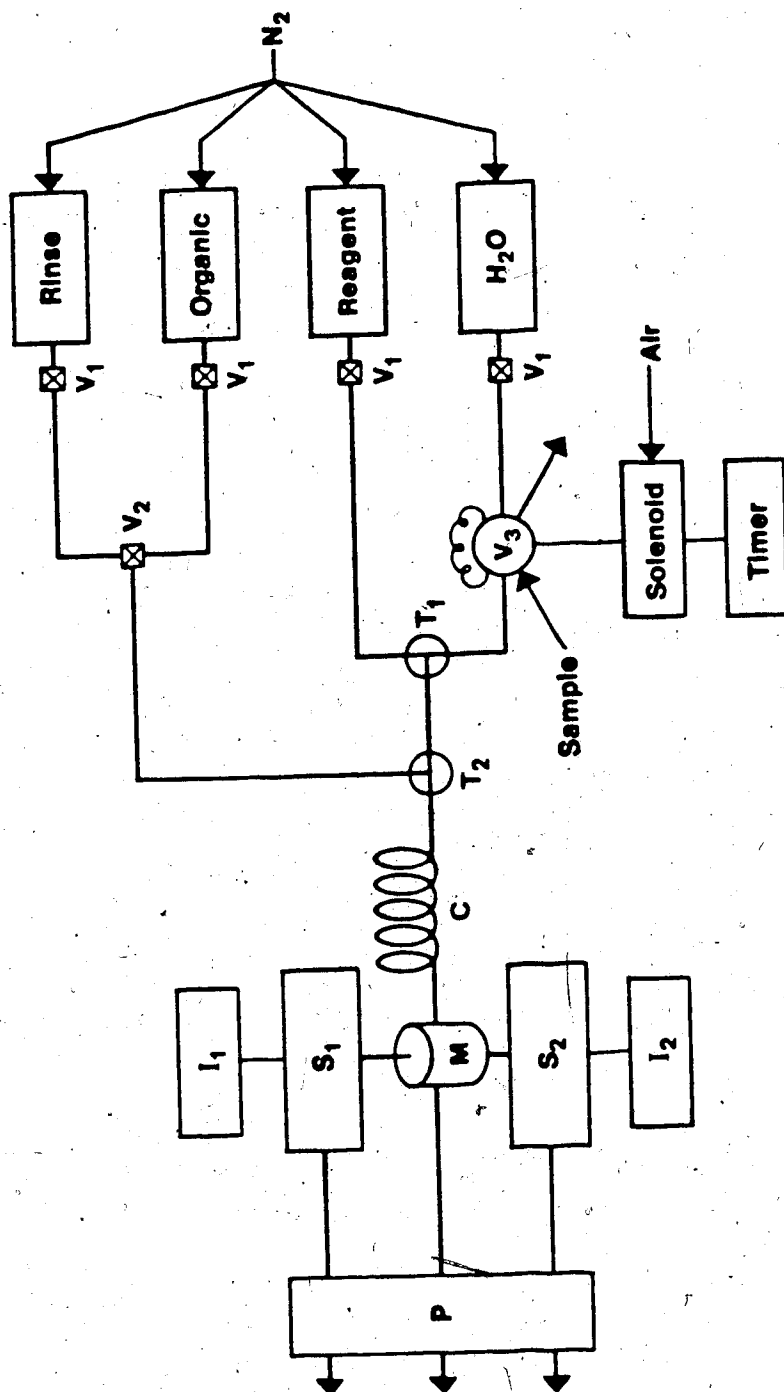


Figure 16. Solvent extraction/FIA system used with the dual-membrane phase separator for the Dramamine assay. H₂O, reagent, organic and rinse are in pressure cylinders; V₁ and V₂ are two-way and three-way valves; V₃ is an injection valve; T₁ and T₂ are tees; C is the extraction coil; M is the dual-membrane phase separator; S₁ and S₂ are spectrophotometers; I₁ and I₂ are integrators and P is a peristaltic pump. See text for details.

Figure 17 shows a cross section of the dual-membrane phase separator. The hydrophobic membrane, represented with short dashes, consists of two layers of 4 mil, 10-20 μm pore size Zitex Teflon membrane (No. E 249-122, Chemplast Inc., Wayne, NJ). The hydrophilic membrane, represented with long dashes, consists of two layers of Whatman No. 5 filter paper. The membranes are placed in each well of the Kel-F central body piece and are sandwiched in position by the two Kel-F outer body pieces. The surfaces of these outer pieces lying just behind the membranes are textured in a spokelike pattern to facilitate uniform flow through the membranes. All three Kel-F body pieces are pressed together by stainless steel end plates held with screws. The four threaded holes shown in Figure 17 accept standard Cheminert end pieces (No. TEF 107, Laboratory Data Control, Riviera Beach, FL) and flared Teflon tubing.

During operation of the system shown in Figure 16, the cyclohexane phase which has passed through the Teflon membrane flows through a 10 μL flow cell in spectrophotometer S_1 (VariChrom, photometric detector, Varian). Simultaneously, the aqueous phase which has passed through the paper membrane flows through the 10 μL flow cell in spectrophotometer S_2 (UV-50, photometric detector, Varian). The cyclohexane exiting S_1 , the

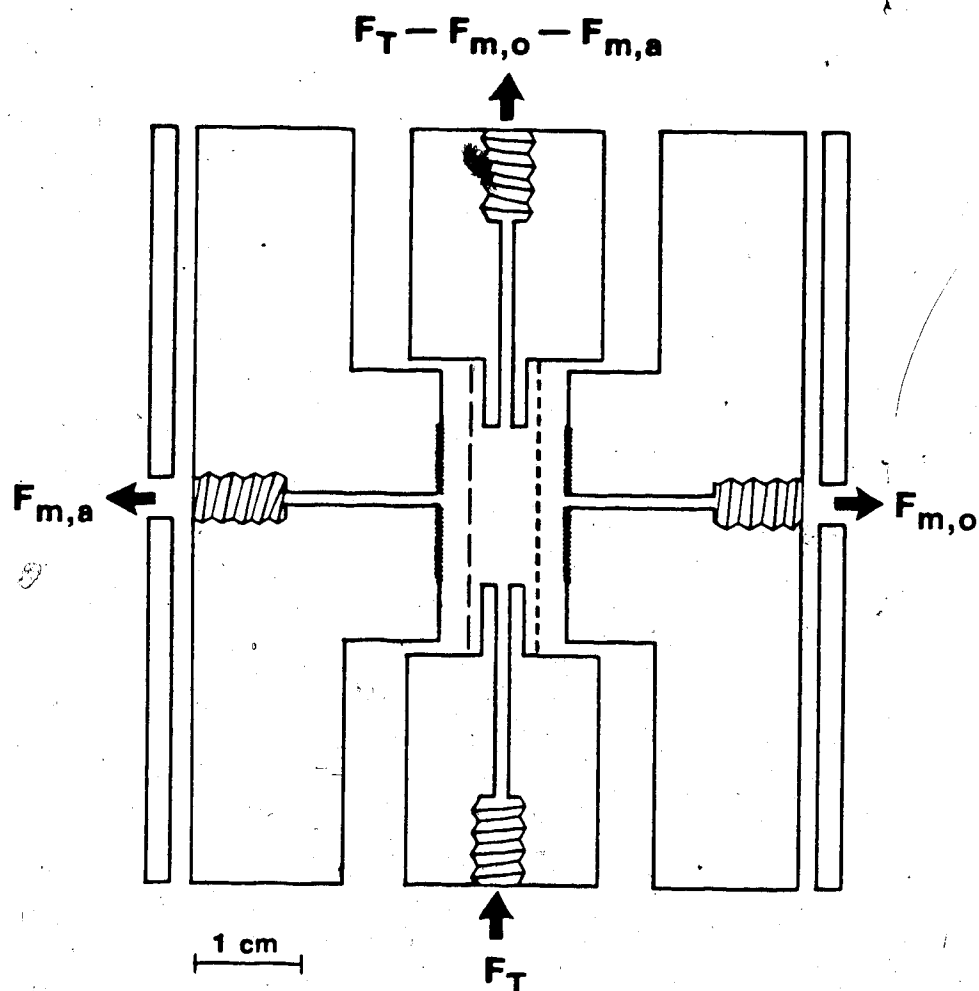


Figure 17. Cross section of the dual-membrane phase separator: Teflon membrane (---), paper membrane (— — —); F_T total flow rate is the sum of F_o and F_a (organic plus aqueous); $F_{m,o}$ and $F_{m,a}$ are flow rates through the Teflon and paper membranes respectively.

aqueous solution exiting S_2 , and the combined cyclohexane/aqueous solution exiting the top of the phase separator pass through Acidflex pump tubes (Technicon Corp.) in a Minipuls variable speed peristaltic pump, P (Gilson Instruments, Ville-le-Belle, France), to provide accurate flow control.

The signals from S_1 and S_2 are fed to the digital integrators, I_1 (Minigrator, Spectra Physics) and I_2 (Model 3390A, Hewlett Packard), respectively, to obtain peak areas. The signals were also monitored as peaks on recorders (not shown).

When pH was a variable, as in the measurement of the extraction-pH profile of diphenhydramine, the single-reagent pressure cylinder shown in Figure 16 was replaced by a multireagent pressure cylinder constructed as follows. An aluminum cylinder large enough to hold seven 400 mL glass bottles was fitted with seven exit ports. A combination of a six-port rotary valve (No. R6031V6, Laboratory Data Control) and a three-port slider valve (No. CAV 3031, LDC) allowed for convenient selection of any of the seven reagent solutions, six of which were buffer solutions and the seventh water.

Initial start-up of the dual-membrane system required a special technique because of the necessity of wetting each membrane with the appropriate solvent. Before the

phase separator was assembled, the Teflon membrane was soaked in cyclohexane and the paper membrane in water. Segmented flow was established in the system with the outlet end of the extraction coil disconnected from the phase separator. Flow was stopped by closing all V_1 valves simultaneously. The wetted membranes were put in place, the phase separator was assembled, and the outlet of the extraction coil was connected to the phase separator. V_1 valves were opened simultaneously. This procedure works well and was performed only once, at the time of initial set-up. Shutdown at the end of the day required only closing V_1 valves and releasing the pressure from all aluminum cylinders. The membranes remained wet overnight so that restarting was accomplished by merely pressurizing the cylinders and opening valves V_1 .

4.2.5 Calibration Curves

Calibration curves for 8-chlorotheophylline and diphenhydramine were measured using the apparatus shown in Figure 16. 8-Chlorotheophylline sample solutions were made up in pH = 7.6 phosphate buffer to aid in dissolution. The buffer capacity of this buffer was much less than that of the pH = 10.19 ammonia buffer used as the reagent stream. Diphenhydramine hydrochloride sample solutions were made up in water.

Peak areas were measured for diphenhydramine in the organic phase and 8-chlorotheophylline in aqueous phase upon replicate injections of diphenhydramine hydrochloride and 8-chlorotheophylline sample solutions ranging in concentration from 2.50×10^{-4} M to 2.50×10^{-3} M, with a pH = 10.19 ammonia buffer as the reagent.

Instrument parameters for the 8-chlorotheophylline calibration study were: wavelength, 300 nm; absorbance range, 0.5; extraction coil, 200 cm; injection volume, 44 μ L; sampling frequency, two injections per minute, N₂ pressure, total cyclohexane flow rate, F_O , 3.09 mL/min; total aqueous flow rate, F_a , 3.60 mL/min; cyclohexane flow through the membrane, $F_{m,O}$, 1.21 mL/min; aqueous flow through the membrane, $F_{m,a}$, 1.33 mL/min.

Instrument parameters for the diphenhydramine calibration study that differed from those given above were: wavelength, 254 nm; absorbance range, 0.2; F_O , 3.06 mL/min; F_a , 3.66 mL/min; $F_{m,O}$, 1.22 mL/min; $F_{m,a}$, 1.32 mL/min.

4.2.6 Tablet Assay

Standards and samples for the tablet assay (prepared as in Section 4.2.2) were injected into the solvent extraction/FIA system shown in Figure 16 with the organic and aqueous phase monitored simultaneously. Peak areas

were measured for six injections of each solution. A pH = 10.19 ammonia buffer was used as the reagent.

Important instrument parameters for the tablet assay were as follows: wavelength of S_1 , 254 nm; wavelength of S_2 , 300 nm; injection volume, 44 μ L; sampling frequency, two injections per minute; extraction coil length, 200 cm; N_2 pressure, 56 psig; total cyclohexane flow rate, 2.87 mL/min, total aqueous flow rate, 3.33 mL/min; cyclohexane flow through the membrane, 1.23 mL/min; aqueous flow through the membrane, 1.07 mL/min.

4.3 Results and Discussion

The extraction behavior of 8-chlorotheophylline and diphenhydramine was characterized as a function of pH and other system parameters in order to design the optimum conditions for the Dramamine tablet assay. Also studied were the conditions necessary for dissolving Dramamine from tablet formulations.

The following symbols are used in this chapter: flow rates: F_o is the total flow rate of the organic phase, F_a is the total flow rate of the aqueous phase, $F_{m,o}$ is the flow rate of the organic phase through the Teflon membrane and $F_{m,a}$ is the flow rate of the aqueous phase through the paper membrane. Each data point plotted

on every figure in this chapter is an average resulting from six replicate injections of sample.

4.3.1 Instrument Parameters

An injection volume of 44 μL was chosen on the basis of the study discussed in Chapter 2 concerning the effect of injection volume on peak areas and widths. The area of the peaks obtained in the cyclohexane phase upon injection of a 2×10^{-3} M aqueous solution of diphenhydramine hydrochloride was studied as a function of extraction coil length. The reagent was a pH = 10.10 ammonia buffer. As seen in the next section, at this pH the free-base species of diphenhydramine should be quantitatively extracted at equilibrium.

Instrument parameters for the study were as follows: wavelength, 254 nm; sampling frequency, one injection per minute; N_2 pressure, 40 psig; $F_0 \sim 1.7$ mL/min; $F_a \sim 2.5$ mL/min; $F_{m,o} \sim 0.87$ mL/min and $F_{m,a} \sim 0.74$ mL/min. Since flow rates varied somewhat with increasing length of the extraction coil, peak areas were corrected to $F_0 = 1.79$ mL/min via equation 2.6, as discussed for caffeine in Chapter 2.

The plot of peak area vs extraction coil length is shown in Figure 18 for lengths between 25 cm and 326 cm. The shape is similar to the corresponding plots for

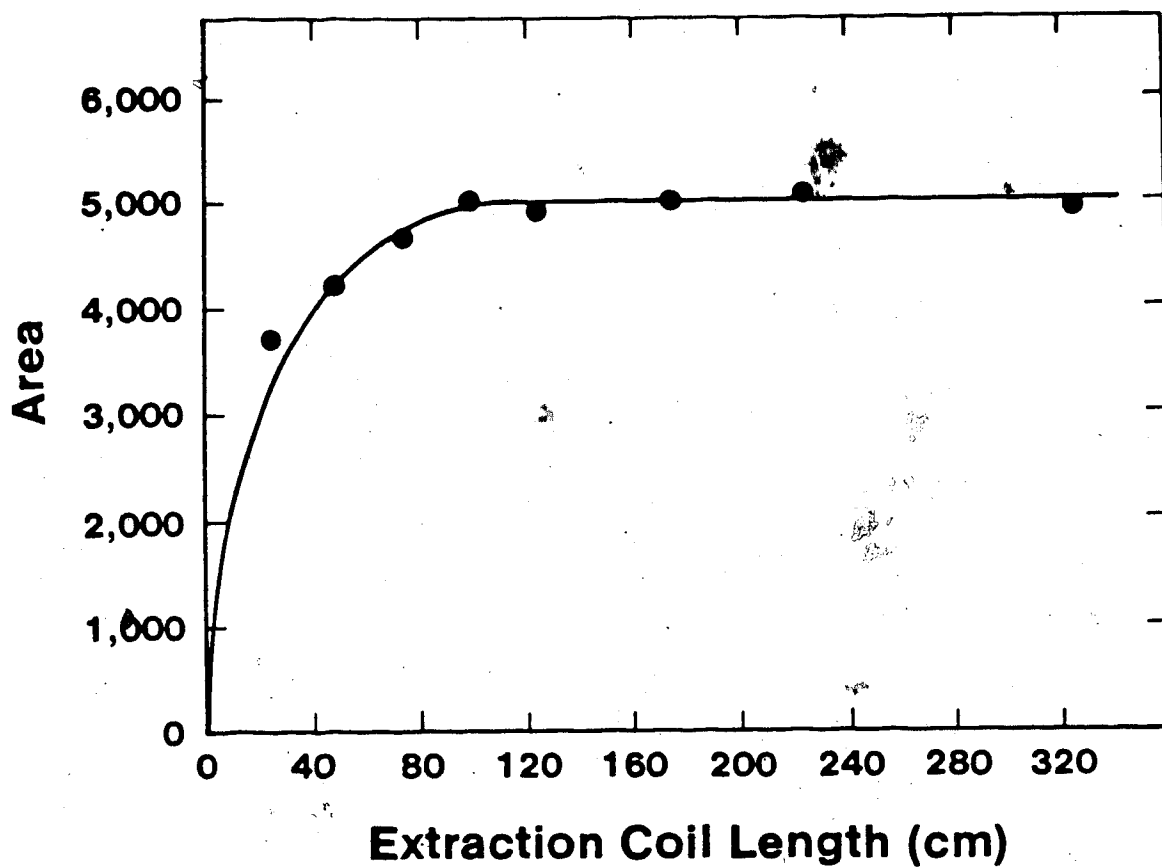


Figure 18. Peak area versus extraction coil length for diphenhydramine. The relative standard deviation in peak area, for each plotted point, falls within the range of 0.76% to 2.0%.

caffeine and procyclidinium-picrate given in Figures 4A and 13 respectively. Extraction equilibrium is obtained at a somewhat longer coil length (~100 cm) for the extraction of diphenhydramine into cyclohexane. A coil length of 200 cm was used for subsequent studies and for tablet assays. At high pH, 8-chlorotheophylline remains unextracted in the aqueous phase so that no equilibration time is required on its account.

4.3.2 Reagent pH

Since diphenhydramine is a weak base, the fraction of this compound extracted into cyclohexane depends on the pH of the aqueous phase as well as on the distribution coefficients of its two conjugate species BH^+ and B and on the flow rates of the cyclohexane and aqueous phases. Although the cationic conjugate acid, BH^+ , is extracted into more polar organic solvents such as chloroform as an ion pair with simple inorganic anions [61], it is not extracted significantly into cyclohexane. Only the neutral free-base species, B, is extracted with a distribution coefficient previously reported as 3×10^3 [66]. The pK_a of BH^+ at 25°C has been reported as 9.12 for the "mixed" constant at ionic strength of 0.06 [67]. A study of the dependence of peak area on reagent pH for the distribution of diphenhydramine between cyclohexane

and the buffered aqueous phase was performed with the dual-membrane extraction/FIA system using the multireagent pressure cylinder. Reagents used were citric acid/ Na_2HPO_4 buffers of pH values 3.01, 4.24, 5.24, 6.19 and 7.06, and an ammonia buffer of pH = 10.29. Replicate injections of a 2×10^{-3} M aqueous diphenhydramine hydrochloride solution resulted in peaks for both the organic and aqueous phases, which were integrated simultaneously to obtain peak areas A_o and A_a respectively. Since the sample is injected into a pure water flow stream, it can be assumed that when this stream joins the reagent buffer at T_1 , the resulting aqueous phase will have the same pH as the reagent. This was verified by measuring the pH of the aqueous effluent.

Instrument parameters for the study were the same as those used for the extraction coil length study with $F_o = 2.02$ mL/min, $F_a = 2.42$ mL/min, $F_{m,o} = 0.97$ mL/min, $F_{m,a} = 0.91$ mL/min and extraction coil length = 200 cm.

The resulting plots of A_a and A_o versus reagent pH are shown in Figure 19A and 19B respectively. It is evident from these plots that use of a reagent pH of 10 or greater results in quantitative extraction of diphenhydramine into cyclohexane.

The sigmoidal dependence of peak area in the organic phase, A_o , on pH is predicted from equation 5.26, derived in Chapter 5 and presented here for easy reference:

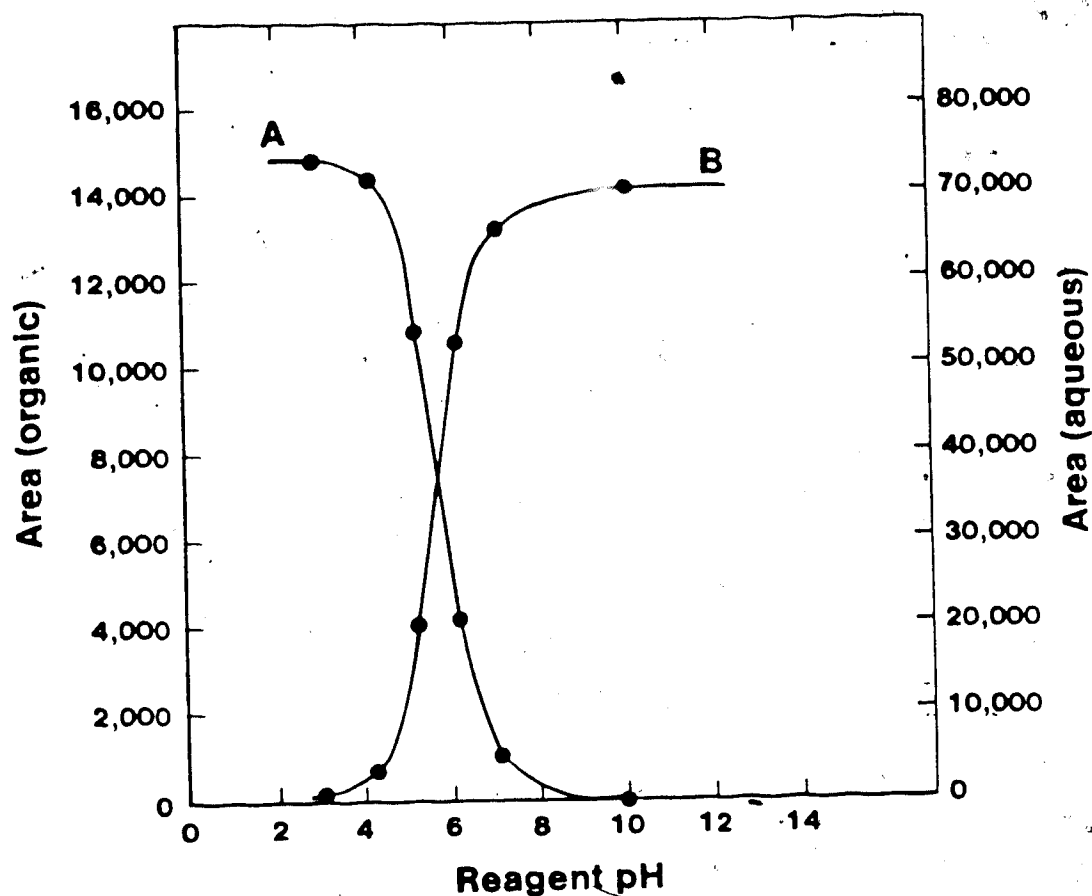


Figure 19. Peak area for the aqueous phase (A) and the organic phase (B) versus reagent pH for diphenhydramine. The relative standard deviation in peak area ranged from 0.74% to 3.4% for points plotted on graph B, and from 2.1% to 2.7% for points plotted on graph A (except for the value of 6.1% at pH = 7.06 which is high due to the high level of noise associated with the aqueous phase detector).

$$A_0 = \frac{f b n \epsilon_{B,O} K_B K_a}{F_a a_H + F_a K_a + F_O K_B K_a} \quad (4.1)$$

where f is a response factor which relates the absorbance from the detector to a count rate on the integrator, b is the pathlength of the spectrophotometer flowcell, $\epsilon_{B,O}$ is the molar absorptivity of the neutral form of the sample species in the organic phase, K_B is the distribution coefficient, K_a is the acidity constant, a_H is the hydrogen ion activity in the aqueous phase and F_O and F_a are the total flow rates of the organic and aqueous phases respectively.

If K_B is large, as it is for diphenhydramine, equation 4.1 predicts that A_0 will be zero at very low pH, will reach a plateau value of $fbn\epsilon_{B,O}/F_O$ at high pH, and will have a value of $fbn\epsilon_{B,O}/(F_O + F_a)$ on the rising part of the sigmoidal curve at $pH = pK_a - \log K_B$.

The relationship between peak areas for the aqueous phase, A_a , and hydrogen ion activity is derived in Chapter 5, and is expressed in equation 5.30 for a BH^+ charge type acid. If, however, K_B is large, the concentration of B can be neglected in the aqueous phase and the only absorbing species to consider is BH^+ . The appropriate equation for peak areas in the aqueous phase is then:

$$\Lambda_a = \frac{f'b'n \epsilon_{BH^+,a} (a_H + K_a)}{F_a a_H + F_a K_a + F_o K_B K_a} \quad (4.2)$$

where f' is the response factor for the aqueous phase detector and integrator, b' is the pathlength of the aqueous phase spectrophotometer flowcell and $\epsilon_{BH^+,a}$ is the molar absorptivity of the protonated sample species in the aqueous phase.

This equation predicts an inverted sigmoidal relationship between Λ_a and pH. At high pH the value of Λ_a is zero; at low pH it reaches a plateau value of $f'b'n \epsilon_{BH^+,a}/F_a$; and at $pH = pK_a - \log K_B$ it has a value of $f'b'n \epsilon_{BH^+,a}/(F_o + F_a)$.

A value for the product $K_a K_B$ can be determined from the plot of peak area versus reagent pH for either the organic or aqueous phase. Considering first the organic phase, the peak area at $pH = pK_a - \log K_B$ will be equal to the peak area on the plateau multiplied by the ratio $F_o/(F_o + F_a)$. For the diphenhydramine reagent pH study this ratio is 0.46. From Figure 19B, the peak area at $pH = pK_a - \log K_B$ is therefore 6,492 corresponding to a $pH = 5.7 \pm 0.1$.

Considering now the aqueous phase, the peak area at $pH = pK_a - \log K_B$ will be equal to the peak area on the

plateau multiplied by the ratio $F_a/(F_o + F_a)$. For the diphenhydramine reagent pH study this ratio is 0.54. From Figure 19A, the peak area at $pH = pK_a - \log K_B$ is therefore 40,093 corresponding also to a $pH = 5.7 \pm 0.1$.

The value of K_B is then calculated from $\log K_B = pK_a - 5.7$. Since ionic strength was not maintained constant in this study, the pK_a value of BH^+ is best estimated by the literature value of 9.12 for the "mixed" constant [67]. Using this value for the pK_a of diphenhydramine, the value of $\log K_B$ is estimated to be 3.4, which is in agreement with the reported value of 3.5 [66].

Equation 4.1 can be linearized by taking the reciprocal of both sides. The resulting equation predicts a linear relationship between the inverse of peak area in the organic phase and the hydrogen ion activity (see equation 5.33 in Chapter 5). A plot of $1/A_o$ vs a_{H^+} for the data points from Figure 19B in the pH range 4-8 yields a straight line as predicted, with a slope and standard deviation of 24.6 ± 0.4 and with an intercept and 95% confidence limits of $(8.6 \pm 4.6) \times 10^{-5}$.

A study of the effect of reagent pH on the extraction of 8-chlorotheophylline by cyclohexane was performed in a manner similar to that used for the diphenhydramine study. This compound was found to remain quantitatively unextracted by cyclohexane at all reagent pH values. The

pK_a of 8-chlorotheophylline, as determined in a separate experiment, is 5.35 ± 0.06 (see Appendix II). Thus neither its anionic conjugate base nor its neutral conjugate acid are perceptibly extracted from aqueous solution.

On the basis of the studies described in this section, a reagent pH of 10.2 was used in the Dramamine tablet assay. At this pH diphenhydramine is quantitatively extracted and 8-chlorotheophylline is quantitatively unextracted from the aqueous phase.

4.3.3 Calibration Curves

At a constant pH of 10.2 and with a constant injection volume, the peak area for diphenhydramine in the cyclohexane phase and the peak area for 8-chlorotheophylline in the aqueous phase should be proportional to the concentrations of these compounds in the injected solutions. Figure 20 shows the calibration plot for diphenhydramine. It is linear with a relative standard deviation of 1.4% for the slope. The y-intercept and 95% confidence limits are -114 ± 3114 integration units. The calibration plot for 8-chlorotheophylline is given in Figure 21. It too is linear with a relative standard deviation of 0.4% for the slope. The y-intercept and 95% confidence limits are 185 ± 193 integration units.

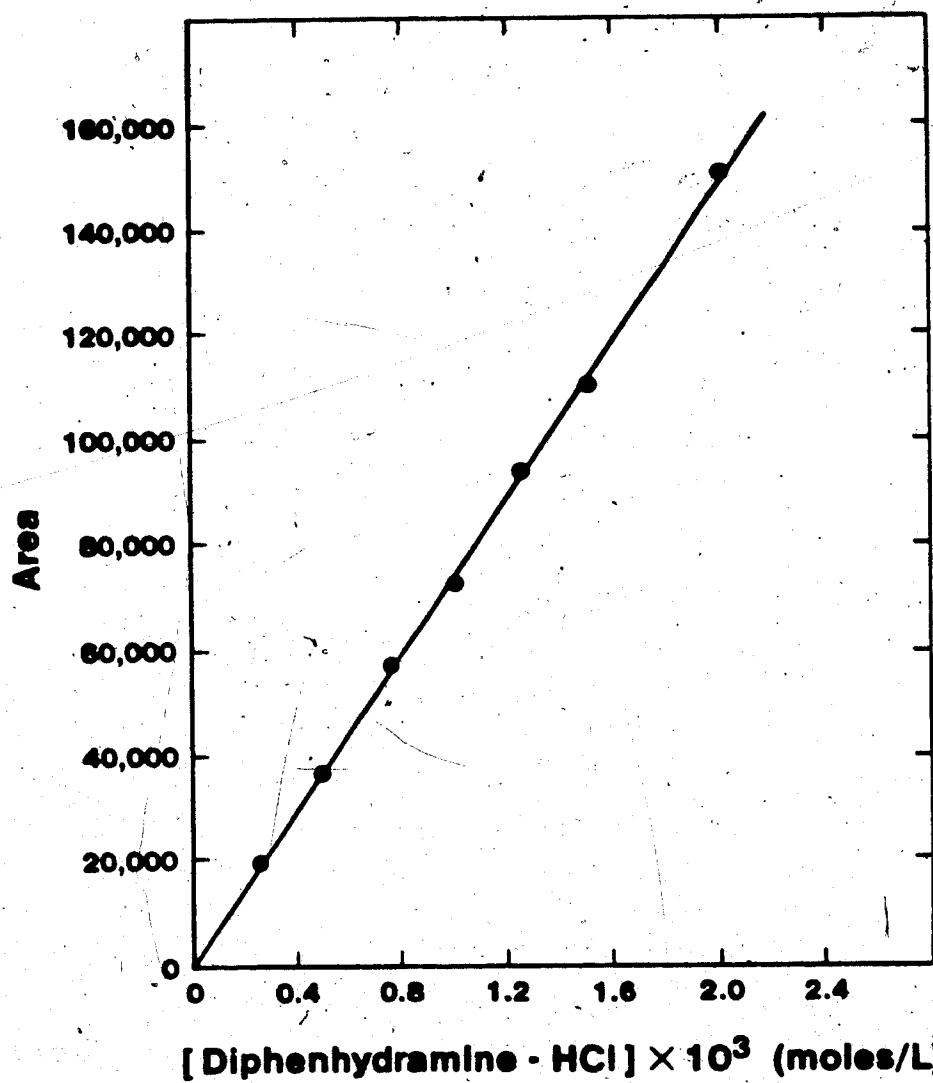


Figure 20. Calibration curve for diphenhydramine in the organic phase.

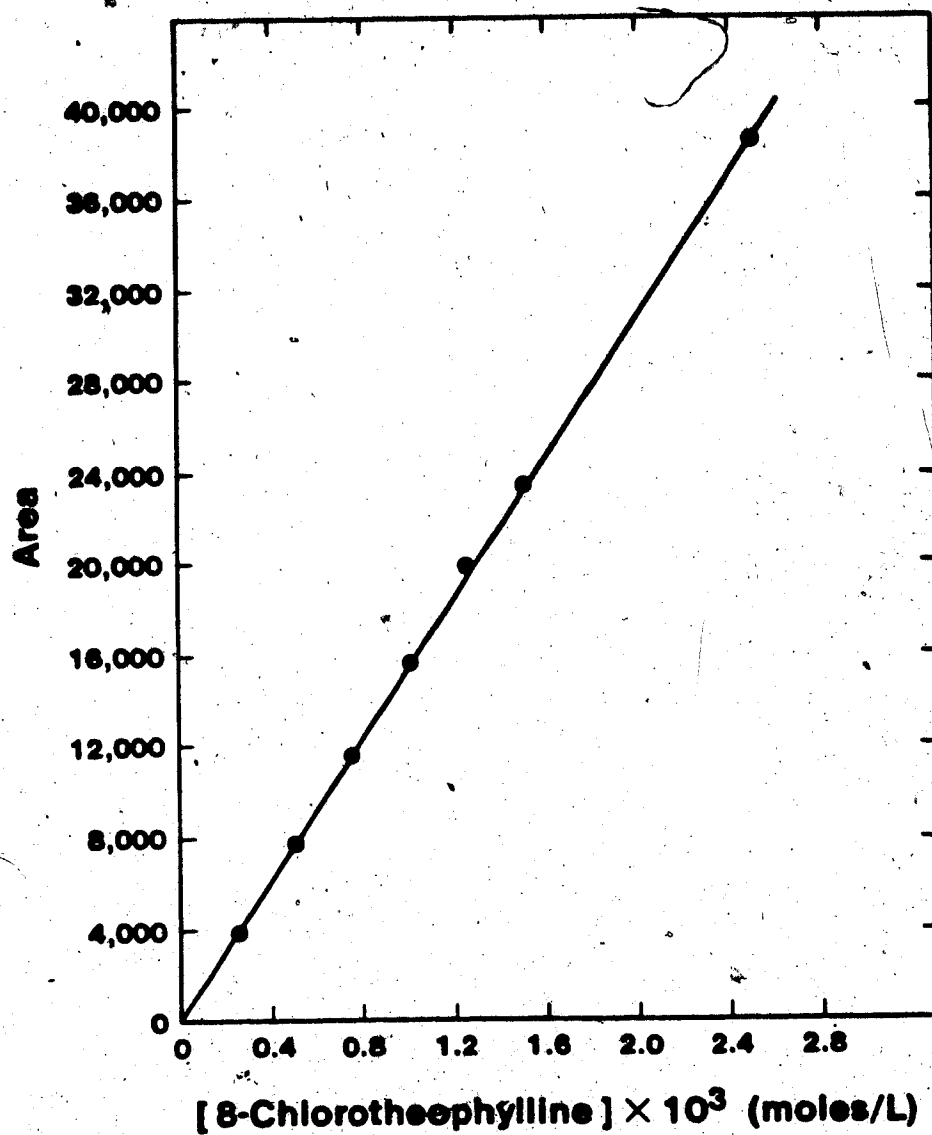


Figure 21. Calibration curve for 8-chlorotheophylline in the aqueous phase.

4.3.4 Tablet Assay

Dramamine (dimenhydrinate) is a 1:1 compound of diphenhydramine and 8-chlorotheophylline. Dramamine tablets are formulated with the yellow azosulfate dye tartrazine which is not extracted into cyclohexane. By use of a wavelength of 300 nm, which is near a minimum in the absorption spectrum of tartrazine, the quantity of dye in the tablet contributes an absorbance in the aqueous phase that is only 0.25% of the absorbance expected for the amount of 8-chlorotheophylline in the tablet. This was considered a negligible interference. The absorption spectra of 8-chlorotheophylline and of diphenhydramine have been published [68,69].

In order to ensure that both the drug components would be quantitatively dissolved from the powdered tablet in the assay procedure, the effects on drug recovery of both the volume of the aqueous dissolution medium and shaking time were investigated. Solvent pH was chosen to be above the pK_a of 8-chlorotheophylline and below the pK_a of diphenhydraminium ion (BH^+) so that both components would be ionized. A pH = 7.0 phosphate buffer was used. Its buffer capacity was far below that of the pH = 10.2 reagent buffer used in the subsequent extraction/FIA step so that the extraction by cyclohexane would occur at pH = 10.2. In one study, equivalent tablet weights of powder

were shaken for 5 min with volumes of phosphate buffer ranging from 25 to 200 mL and then centrifuged. Aliquots of the clear supernatant were diluted and the resulting solutions subjected to extraction/FIA analysis. For both diphenhydramine and 8-chlorotheophylline the amount recovered was independent of the volume of phosphate buffer used for dissolution, demonstrating that complete dissolution is achieved even for a volume of 25 mL.

The effect of shaking time on dissolution of the drug components was investigated by shaking equivalent tablet weights of powder with 100 mL portions of pH = 7.0 buffer for times varying from 1 to 15 min. Assay of the centrifuged supernatant again yielded a constant recovery of both drug components, indicating that shaking times as short as 1 minute are sufficient to quantitatively dissolve them. To be on the safe side, a dissolution volume of 100 mL and a shaking time of 5 min were used in the tablet assay procedure.

Assay of a batch of Dramamine tablets supplied by the manufacturer, using the procedure given in Section 4.2.6, gave 22.3 ± 0.2 (95% CL) mg/tablet of 8-chlorotheophylline and 26.4 ± 0.2 (95% CL) mg/tablet of diphenhydramine. Calculation of the amount of Dramamine per tablet based on the assay values of 8-chlorotheophylline and diphenhydramine respectively gave 48.9 ± 0.4 mg/tablet and

48.5 \pm 0.4 mg/tablet. The average value of 48.7 mg/tablet is in excellent agreement with the value of 49.0 mg/tablet obtained by the manufacturer using a modified compendial procedure that does not give values for the two individual components of Dramamine. These assay values are well within the tolerance limits of the 50 mg/tablet label claim [70,71] for Dramamine.

4.3.5 Comments

When the immiscible phases were cyclohexane and an aqueous buffer, and when the flow rates were those specified for the tablet assay, "breakthrough" of the wrong solvent was virtually never encountered with either the paper or the Teflon membranes. Although all studies reported in this Chapter were done with the dual-membrane device shown in Figure 17, it was found that two single-membrane phase separators, each designed as discussed in Chapter 2 and placed in series, worked as well.

CHAPTER 5

ACIDITY CONSTANT DETERMINATION BY SOLVENT EXTRACTION/FIA

5.1 Introduction

The use of solvent extraction for determining acidity constants is particularly attractive for compounds that have a low solubility in water and whose two conjugate species have similar absorption spectra. For such compounds, the solubility prevents accurate pK_a determinations by conventional potentiometric titrations in water, and the similarity of the spectra precludes the use of the spectrophotometric technique. Alternate methods include potentiometric titration in mixed aqueous-organic solvents, conductimetry and solubility measurements.

Albert and Serjeant [72] discourage the use of potentiometric pK_a determinations in mixed-aqueous solvent systems except when comparing closely related compounds. The pK_a determined in a mixed-aqueous solvent will not generally be the same as the pK_a determined in water. The organic solvent component contributes extra acidic and basic species to the medium, and the two solvent components may differ in their solvating power [73,74].

The activity coefficient for species "i" in a mixed-aqueous solvent system is the product of the salt activity coefficient (medium effect), which represents the effect of electrostatic ion-ion interactions, and the transfer activity coefficient, which represents the difference in ion-solvent interactions between the mixed-aqueous solvent and water [75]. Unfortunately, transfer activity coefficients are not rigorously measurable by thermodynamic methods.

By definition, the salt activity coefficient approaches unity at infinite dilution of the solute. The overall activity coefficient for mixed-aqueous solvents, referred to the standard state in water, however will approach the value of the transfer activity coefficient as the solute concentration is decreased and this limit may differ greatly from unity [76]. Therefore, direct comparison of acidities between mixed-aqueous solvents and water are not possible because different standard states are then necessarily involved [75].

pH measurements of a mixed-aqueous solvent system obtained using a pH meter, calibrated with aqueous buffers, include a residual liquid junction potential due to the difference in liquid junction potentials for the calibration and sample solutions. These potentials may be estimated, but not determined exactly. An additional

complication results from a possible shift in the asymmetry potential of the glass electrode on transfer from the aqueous buffers to the mixed solvent system [76].

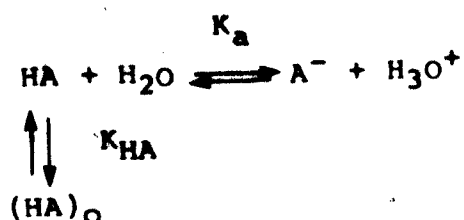
Often pK_a values are obtained in varying concentrations of alcohol and these values are then plotted versus % alcohol. The plot is extrapolated to zero % alcohol to find the aqueous pK_a . Unfortunately, these plots are rarely linear, and the pK_a value may be highly suspect when extrapolated from media with a % alcohol greater than 10 or 20% [73,77].

Conductimetry, in aqueous solution, may yield accurate pK_a values at low sample concentrations for acids with sufficiently low pK_a values [72]. However, both the measurements and calculations are time-consuming. Other disadvantages include the necessity of precise temperature control and high purity of both sample and solvent (the most common impurity being dissolved carbon dioxide). Conductometric titrations, a modification of the technique, have proven useful for pK_a determinations of very weak acids.

The solubility method [72] may be used to measure acidity constants at constant ionic strength. The technique, however, is laborious and not highly accurate.

The application of liquid-liquid extraction to determine acidity constants, unlike the spectrophotometric

method, does not require a difference in the absorption spectra of the two conjugate sample species in the aqueous phase. The equilibria involved for an HA charge type acid in a two-phase system can be represented as follows, in the case where only the neutral species, HA, extracts into the organic phase:



At pH values in the vicinity of the $\text{p}K_a$ of the sample, a mixture of the HA and A^- species will exist in the aqueous phase. The extent of the extraction of the HA species will depend upon the distribution coefficient for the sample, K_{HA} , the acidity constant, K_a , and the pH of the aqueous phase. An analogous situation exists for a BH^+ charge type acid. The analysis becomes more complicated if secondary equilibria, such as self-association or ion-pair extraction, occur.

The acidity constant can therefore be determined by measuring the pH dependence of the distribution of the sample between the organic and aqueous phases, with the sample initially dissolved in either phase [73,78-88].

The pH of the aqueous phase is changed either by addition of increasing amounts of acid or base, or by use of a series of aqueous buffers of various pH. The concentrations in one or both phases are usually measured by UV spectrophotometry, and the hydrogen ion activities in the aqueous phase are determined potentiometrically. Due to the low solubility of the organic solvent in the aqueous phase, the pH readings represent a true measure of a_H with respect to the usual standard state in water. Continuous extraction systems employing rapid phase separation make it possible to perform solvent extraction measurements much more rapidly and conveniently and therefore make pK_a determination by solvent extraction more attractive [13,46,85].

In the present study, acidity constants are determined by a solvent extraction/FIA technique employing a dual-membrane phase separators which allows simultaneous spectrophotometric monitoring of concentration in both the aqueous and organic phases. Equations are derived which relate peak areas in the aqueous and organic phases to hydrogen ion activities in the aqueous phase and which permit determination of acidity constants of both HA and BH^+ charge type acids. Validity of the equations is experimentally demonstrated using 3,5-dimethylphenol and p-toluidinium ion as test acids. The distribution

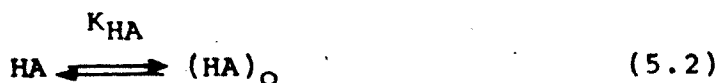
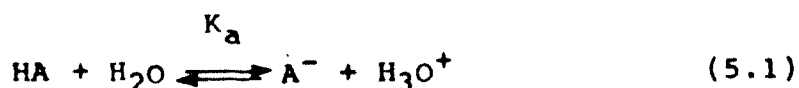
coefficient of the neutral conjugate species is also obtained during the experiment.

5.2 Theory

In this section equations are presented which allow determination of acidity constants from the dependence of the ratio of peak areas in the aqueous and organic phases on the hydrogen ion activity in the aqueous phase.

5.2.1 HA Charge Type Acid

The equilibria describing the dissociation of an HA charge type acid in water and the distribution of the neutral conjugate species between the aqueous and organic phases are:



Species without a subscript are in the aqueous phase while those with a subscript "o" are in the organic phase. The equilibrium constants of interest in this discussion,

pertaining to the equilibria above, are given in equations 5.3 and 5.4 where K_a is a mixed acidity constant (incorporating the activity of the hydrogen ion, a_H , and the concentrations of the HA and A^- species), and K_{HA} is the distribution coefficient.

$$K_a = \frac{[A^-] a_H}{[HA]} \quad (5.3)$$

$$K_{HA} = \frac{[HA]_O}{[HA]} \quad (5.4)$$

In considering the distribution of the sample between the organic and aqueous phases at different values of a_H , we are interested in the distribution of all sample species present. This is best described by the distribution ratio, D , which is the ratio of the formal concentrations of the sample in the organic and aqueous phases. For an HA charge type acid, D is defined as:

$$D_{HA} = \frac{[HA]_O}{[HA] + [A^-]} \quad (5.5)$$

assuming that neutral HA is the only extractable species.

We can obtain an expression relating the distribution ratio of the sample to the activity of the hydrogen ion in the aqueous phase by substituting into equation 5.5 the expression for $[HA]_O$ obtained from equation 5.4, and the expression for $[A^-]$ obtained from equation 5.3 to yield the following:

$$D_{HA} = \frac{a_H K_{HA}}{a_H + K_a} \quad (5.6)$$

In Chapter 2 an expression was derived for solvent extraction/FIA relating peak area in the organic phase, A_O , to the distribution ratio for the sample, D , the number of moles of sample injected, n , and the flow rates of the organic and aqueous phases, F_O and F_a respectively. Equation 2.4 of chapter 2 can be rearranged viz:

$$D = \frac{A_O F_a}{nK - A_O F_O} \quad (5.7)$$

The system constant, K , can be defined as:

$$K = f b \epsilon_{HA,O} \quad (5.8)$$

where f is a response factor which relates the absorbance from the detector to a count rate on the integrator, b is the pathlength of the spectrophotometer flowcell and $\epsilon_{HA,O}$ is the molar absorptivity of the HA species in the organic phase. Substitution of K from equation 5.8 into equation 5.7, subsequent substitution of that expression into equation 5.6, followed by rearrangement yields:

$$A_O = \frac{b f n \epsilon_{HA,O} K_{HA} a_H}{F_a a_H + F_a K_a + F_O K_{HA} a_H} \quad (5.9)$$

A similar type of expression can be derived relating peak area in the aqueous phase, A_a , to the hydrogen ion activity. The contribution to peak area from both the HA and A^- forms of the sample must be considered. For both species, the peak area contribution will be inversely proportional to the flow rate of aqueous phase through the detector, $F_{m,a}$, and will be proportional to the fraction of aqueous phase that goes through the membrane and thus through the detector, $F_{m,a}/F_a$. The peak area contributed by each species will also be proportional to the pathlength of the spectrophotometer flowcell, b' ; to the response factor for the aqueous phase detector and

integrator, f' (which converts the absorbance from the detector to a count rate on the integrator); to the number of moles of sample injected, n ; and to the fraction of the sample present in the aqueous phase at equilibrium, $1/(k'+1)$, where k' is the capacity factor for the sample as defined in Chapter 2. The peak area due to the HA species will also be proportional to the molar absorptivity of the HA species in the aqueous phase, $\epsilon_{HA,a}$, and to the fraction of the sample present in the HA form, α_{HA} . The peak area due to the A^- species will be proportional to the molar absorptivity of the A^- species in the aqueous phase, $\epsilon_{A^-,a}$, and to the fraction of the sample present in the A^- form, α_{A^-} .

Combining these relations, we obtain the following equation for peak area in the aqueous phase:

$$A_a = b' f' \frac{n}{F_{m,a}} \frac{F_{m,a}}{F_a} \frac{1}{k' + 1} (\epsilon_{HA,a} \alpha_{HA} + \epsilon_{A^-,a} \alpha_{A^-}) \quad (5.10)$$

As shown earlier in Chapter 2, the capacity factor can be expressed as:

$$k' = D F_0 / F_a \quad (5.11)$$

The fraction of sample present in the aqueous phase in the HA and A⁻ forms are given in equations 5.12 and 5.13 respectively [89].

$$\alpha_{HA} = \frac{a_H}{a_H + K_a} \quad (5.12)$$

$$\alpha_{A^-} = \frac{K_a}{a_H + K_a} \quad (5.13)$$

Replacement of k', α_{HA} and α_{A^-} in equation 5.10 with the appropriate quantities expressed in equations 5.11 - 5.13, followed by rearrangement and simplification yields:

$$A_a = \frac{b' f' n}{D F_0 + F_a} \left(\frac{\epsilon_{HA,a} a_H + \epsilon_{A^-,a} K_a}{a_H + K_a} \right) \quad (5.14)$$

Substituting for D from equation 5.6 into equation 5.14 gives the following expression relating peak areas in the aqueous phase to the hydrogen ion activity:

$$A_a = \frac{b' f' n (\epsilon_{HA,a} a_H + \epsilon_{A^-,a} K_a)}{F_a a_H + F_a K_a + F_0 K_{HA} a_H} \quad (5.15)$$

The denominators of equations 5.9 and 5.15 are the same so that dividing equation 5.15 by equation 5.9 yields the following expression:

$$\frac{A_a}{A_o} = \frac{b' f' \epsilon_{HA,a}}{b f \epsilon_{HA,o} K_{HA}} + \frac{1}{a_H} \cdot \frac{b' f' \epsilon_{A^-,a} K_a}{b f \epsilon_{HA,a} K_{HA}} \quad (5.16)$$

When a sample is injected into reagent buffers of various pH values, and peak areas are simultaneously measured in the organic and aqueous phases, a plot of A_a/A_o vs. $1/a_H$ should yield a straight line. The acidity constant for HA can be determined from the quotient of the slope, S_1 , and intercept, I_1 , of that plot multiplied by the molar absorptivity ratio of the protonated and deprotonated sample species in the aqueous phase:

$$K_a = \frac{S_1}{I_1} \cdot \frac{\epsilon_{HA,a}}{\epsilon_{A^-,a}} \quad (5.17)$$

The distribution coefficient of HA can also be calculated using K_a and the data collected from the organic phase. Equation 5.9 can be linearized by taking the reciprocal of both sides viz:

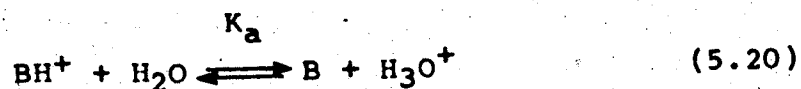
$$\frac{1}{A_o} = \frac{F_a + F_o K_{HA}}{b f n \epsilon_{HA,o} K_{HA}} + \frac{1}{a_H} \cdot \frac{F_a K_a}{b f n \epsilon_{HA,o} K_{HA}} \quad (5.18)$$

A plot of $1/A_0$ vs $1/a_H$ should yield a straight line with slope S_2 and y-intercept I_2 , from which the distribution coefficient can be calculated using the expression:

$$K_{HA} = \frac{I_2 F_a K_a - S_2 F_a}{S_2 F_o} \quad (5.19)$$

5.2.2 BH⁺ Charge Type Acid

Equations can also be derived for a BH⁺ charge type acid which relate peak areas in the organic and aqueous phases to hydrogen ion activities. The equilibria describing the dissociation and distribution processes are:



Again, the dissociation constant of interest is a mixed acidity constant, incorporating the activity of the hydrogen ion, a_H , and the concentration of the BH⁺ and B species.

$$K_a = \frac{[B] a_H}{[BH^+]} \quad (5.22)$$

The distribution coefficient, K_B , is the ratio of the concentrations of the B species between the organic and aqueous phases, while the distribution ratio, D_B , is the ratio of the formal concentrations of the sample in the two phases.

$$K_B = \frac{[B]_O}{[B]} \quad (5.23)$$

$$D_B = \frac{[B]_O}{[BH^+] + [B]} \quad (5.24)$$

It is again assumed here that neutral B is the only extractable species. Substituting into equation 5.24 the expressions for $[B]_O$, obtained from equation 5.23, and $[BH^+]$, obtained from equation 5.22 yields:

$$D_B = \frac{K_a K_B}{K_a + a_H} \quad (5.25)$$

Substitution of $K = f b \epsilon_{B,O}$ into equation 5.7, followed by substitution of that expression into equation 5.25 and rearranging gives:

$$A_o = \frac{f b n \epsilon_{B,o} K_B K_a}{F_a a_H + F_a K_a + F_o K_B K_a} \quad (5.26)$$

where $\epsilon_{B,o}$ is the molar absorptivity for the neutral form of the sample species in the organic phase.

Analogous to the case of an HA acid, an expression can be derived for a BH^+ type acid that relates peak areas in the aqueous phase to the hydrogen ion activity. Equating A_a to the variables which affect it yields:

$$A_a = b' f' \frac{n}{F_{m,a}} \frac{F_{m,a}}{F_a} \frac{1}{K_a + 1} (\epsilon_{BH^+,a} \alpha_{BH^+} + \epsilon_{B,a} \alpha_B) \quad (5.27)$$

where $\epsilon_{BH^+,a}$ and $\epsilon_{B,a}$ are the molar absorptivities for the protonated and neutral sample species respectively in the aqueous phase and α_{BH^+} and α_B are the fractions of the sample, in the aqueous phase, present respectively in the BH^+ and B forms.

$$\alpha_{BH^+} = \frac{a_H}{a_H + K_a} \quad (5.28)$$

$$\alpha_B = \frac{K_a}{a_H + K_a} \quad (5.29)$$

The expression for D given in equation 5.25 can be substituted into equation 5.11, and the resulting expression for the capacity factor can replace k' in equation 5.27. Further substitution of α_{BH^+} and α_B from equations 5.28 and 5.29 into equation 5.27, followed by rearrangement and simplification yields:

$$A_a = b' f' n \frac{(\epsilon_{BH^+,a} a_H + \epsilon_{B,a} K_a)}{a_H + \frac{K_a}{K_B} + \frac{\epsilon_{B,a} K_a}{\epsilon_{B,o} K_B}} \quad (5.30)$$

If peak areas are measured simultaneously in both the aqueous and organic phases, a simple expression can be obtained by dividing equation 5.30 by equation 5.26.

$$\frac{A_a}{A_o} = \frac{b' f' \epsilon_{B,a}}{b f \epsilon_{B,o} K_B} + a_H \cdot \frac{b' f' \epsilon_{BH^+,a}}{b f \epsilon_{B,o} K_a K_B} \quad (5.31)$$

Equation 5.31 indicates that a plot of A_a/A_o vs a_H should yield a straight line with slope S_3 and y-intercept I_3 , from which one can calculate the acidity constant for BH^+ via the following relation:

$$K_a = \frac{I_3}{S_3} \cdot \frac{\epsilon_{BH^+,a}}{\epsilon_{B,a}} \quad (5.32)$$

A linear relationship between the inverse of peak area in the organic phase and the hydrogen ion activity

can be obtained by taking the reciprocal of both sides of equation 5.26 viz:

$$\frac{1}{A_0} = \frac{F_0 K_a K_B + F_a K_a}{b f n \epsilon_{B,0} K_B K_a} + a_H \cdot \frac{F_a}{b f n \epsilon_{B,0} K_B K_a} \quad (5.33)$$

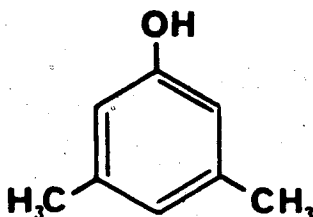
Having calculated the acidity constant from equation 5.32, a value for the distribution coefficient of the neutral conjugate species, B, can be determined from a plot of $1/A_0$ vs a_H . Such a plot should yield a straight line of slope S_4 and y-intercept I_4 allowing the distribution coefficient to be calculated from:

$$K_B = \frac{I_4 F_a - S_4 F_a K_a}{S_4 F_0 K_a} \quad (5.34)$$

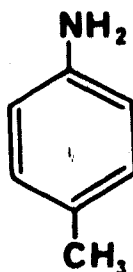
5.3 Experimental

5.3.1 Chemicals

3,5-Dimethylphenol was 99+% pure and was used as received from Aldrich Chemical Co., Milwaukee, Wisconsin. Its structure is:



p-Toluidine (4-methylaniline) was 99+ $\frac{1}{2}$ pure and was used as received from B.D.H. Laboratories, Poole, England. Its structure is:



Other chemicals used were all reagent grade.

5.3.2 Solvents and Reagents

Double Distilled Water has been described in, Chapter 2.

Cyclohexane (reagent grade) was purified by passage through a gravity flow silica gel column containing a sintered glass frit at the outlet. The silica gel was activated by heating in air for 8-16 hours at a temperature of 125-150°C, and then was allowed to cool in a stoppered glass bottle.

pH = 2 HCl, pH = 12 and 12.6 NaOH were prepared by appropriate dilution of a solution of concentrated HCl or NaOH with doubly distilled water until the desired pH was reached.

Ionic Strength 0.10 Ammonium Chloride/Ammonia Buffers of pH 9.6, 9.7, 9.8, 9.9, 10.0 and 10.1 were prepared by adding enough NH_4Cl to yield a final concentration of 0.10

M and enough aqueous ammonia to yield the desired pH in a final volume of 1000 mL.

Ionic Strength 0.10 Acetic Acid/Sodium Acetate

Buffers of pH 4.6, 4.8, 5.0, 5.1, 5.2 and 5.6 were prepared by adding enough sodium acetate to yield a final concentration of 0.10 M and enough glacial acetic acid to yield the desired pH in a final volume of either 500 or 1000 mL.

pH = 6.865 Phosphate Buffer, used for calibration of the pH meter at 25°C was prepared to be 0.025 M in KH_2PO_4 and 0.025 M in Na_2HPO_4 , using dried phosphate salts and freshly boiled and cooled water.

pH = 9.180 Borax Buffer, used for calibration of the pH meter at 25°C, was prepared to be 0.01 M in $\text{Na}_2\text{B}_4\text{O}_7 \cdot 10\text{H}_2\text{O}$, using freshly boiled and cooled water.

pH = 4.005 Potassium Hydrogen Phthalate Buffer, used for calibration of the pH meter at 25°C, was prepared to be 0.05 M in potassium hydrogen phthalate (KHP), using dried KHP and freshly boiled and cooled water.

Commercial Buffers (Fisher Scientific Co.) of pH = 7.00 ± 0.01 , pH = 10.00 ± 0.01 and pH = 4.00 ± 0.01 were used in some instances for calibration of the pH meter.

5.3.3 Sample Solutions

3,5-Dimethylphenol and p-Toluidine solutions were prepared at the following pH values and concentrations by mixing the appropriate volume of an aqueous stock solution of the sample with enough concentrated HCl or NaOH to yield the desired concentration and pH upon dilution to the final volume (100 or 200 mL):

- | | |
|------------------------------------|--------------------|
| 1. pH = 2.0, 3×10^{-4} M | 3,5-Dimethylphenol |
| 2. pH = 2.0, 6×10^{-4} M | 3,5-Dimethylphenol |
| 3. pH = 12.6, 3×10^{-4} M | 3,5-Dimethylphenol |
| 4. pH = 12.5, 6×10^{-4} M | 3,5-Dimethylphenol |
| 5. pH = 2.0, 5×10^{-4} M | p-Toluidine |
| 6. pH = 12.0, 5×10^{-4} M | p-Toluidine |

pH = 2.0, 1×10^{-3} M p-Toluidine (0.10 M in NaCl) and pH = 12.6, 4×10^{-4} M 3,5-Dimethylphenol (0.10 M in NaCl), for the ion-pair extraction test, were prepared by mixing the appropriate weight of sample and NaCl with water and enough HCl or NaOH to yield the desired sample concentration, pH and ionic strength upon dilution to a final volume of 1000 mL.

Ionic Strength 0.10 3,5-Dimethylphenol and Ionic Strength 0.10 p-Toluidine sample solutions all contained 0.10 M NaCl.

5.3.4 Apparatus

A diagram of the solvent extraction/FIA system used in the pK_a determinations is shown in Figure 22. Its design is similar to that shown in Figure 16 of Chapter 4, with the major difference being that there is only one flow stream of aqueous solvent. Solvent flows are maintained via constant N_2 pressure pumping. The organic phase is cyclohexane which is contained in a glass bottle inside an aluminum pressure cylinder. The six reagent buffers and water are held in seven glass containers inside a multireagent aluminum pressure cylinder described previously in Chapter 4.

Valve V_4 is a six-port rotary valve (part no. R6031V6, Laboratory Data Control) used to select any one of six reagent buffers. Valve V_2 is a three-port slider valve (part no. CAV 3031, LDC) which allows selection of either buffer or a water wash. All tubing is Teflon, with 0.3 mm i.d. tubing used whenever it is desirable to minimize sample band broadening or to provide increased resistance to flow, and 0.8 mm i.d. tubing used in the rest of the system.

The sample is injected via an automatic sample injection valve V_3 (part no. SVA-8031, LDC) into the reagent stream which is a buffer of known pH. This injection valve contains a "dummy" loop of equal size to

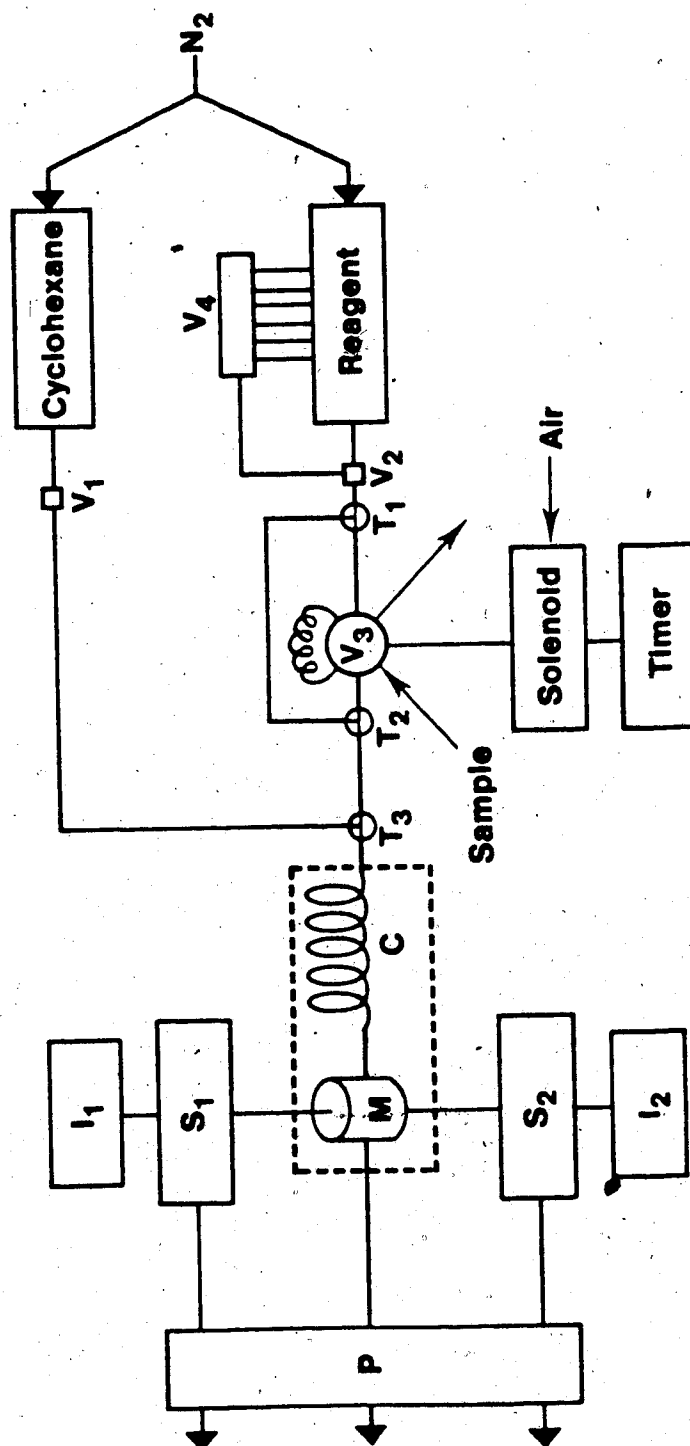


Figure 22. Solvent extraction/FIA system used to determine acidity constants. V_1 and V_2 are two-way and three-way valves; V_3 is an injection valve; V_4 is a six-port rotary valve; T_1 , T_2 and T_3 are tees; C is the extraction coil; M is the dual-membrane phase separator; S_1 and S_2 are spectrophotometers; I_1 and I_2 are integrators and P is a peristaltic pump. See text for details.

the injection loop, so that the flow rate of aqueous reagent is the same in both the load and inject positions. The reagent stream is split at T_1 (part no. CJ-3031, LDC) into two parallel branches which are reunited at T_2 to facilitate mixing between the sample and the buffer and to reduce refractive index effects (see Results and Discussion). The aqueous phase joins the cyclohexane stream at T_3 , and the resulting two phase flow passes through the extraction coil, C.

The aqueous phase is separated from the organic phase via a dual-membrane phase separator as described previously in Chapter 4. The extraction coil and phase separator are immersed in a constant temperature bath, shown as dashed lines in Figure 22. The absorbance of the aqueous phase is monitored with spectrophotometer S_1 (Spectroflow, 757, Kratos Analytical Instruments) while the absorbance of the organic phase is monitored with spectrophotometer S_2 (Varichrom photometric detector, Varian). The signals from S_1 and S_2 are fed to two channels of a digital integrator, I_1 and I_2 (VISTA CDS 401, Varian), to obtain peak areas. The signals are also monitored as peaks on recorders (not shown). Peristaltic pump P (Minipuls 2, Gilson Instruments) is used on the outlet lines to insure accurate flow control.

Figure 23 shows the apparatus used for the determination of molar absorptivity ratios of the protonated and deprotonated sample species in the aqueous phase. It was made by modification of the instrument shown in Figure 22 through disconnection of T_2 from T_3 ; disconnection of the membrane phase separator, M, from the aqueous phase detector, S_2 ; followed by direct connection of T_2 to S_2 .

All pH measurements were made with a glass and calomel electrode pair using an Accumet Model 525 pH meter (Fisher Scientific Co.). Flow rates were measured by collecting the effluents in burets or graduated cylinders and timing with a stopwatch. They are reported, in this chapter, rounded off to one or two significant figures unless they are used in the calculations, where a more accurate value is given along with an error estimate.

3.3.5 Calibration Curves

Calibration curves for 3,5-dimethylphenol and p-toluidine were measured using the apparatus shown in Figure 22. Samples were all 0.10 M in NaCl to reduce refractive index effects (see Results and Discussion). Calibration curves for 3,5-dimethylphenol were obtained by injecting samples ranging in concentration from 8.0×10^{-5} M to 8.0×10^{-4} M into an ionic strength 0.10, pH = 9.80

$\text{NH}_3/\text{NH}_4\text{Cl}$ buffer. Calibration curves for p-toluidine were obtained by injecting samples ranging in concentration from $4.0 \times 10^{-4} \text{ M}$ to $1.4 \times 10^{-3} \text{ M}$ into an ionic strength, 0.10, pH = 5.11 acetic acid/sodium acetate buffer. The organic and aqueous phases were monitored simultaneously and peak areas were measured for six replicate injections of each sample.

Important instrument parameters for the measurement of the calibration curves for 3,5-dimethylphenol were as follows: total cyclohexane flow rate, 2.4 mL/min; total aqueous flow rate, 2.1 mL/min; cyclohexane flow through the membrane, 0.9 mL/min; aqueous flow through the membrane, 1.0 mL/min; extraction coil length 200.4 cm; sample volume injected, 44 μL ; injection rate, one sample per min; wavelength for both detectors, 281 nm; nitrogen pressure, 42 psig; temperature of water bath, 25.0°C

Instrument parameters for the measurement of the calibration curves for p-toluidine, that differed from those listed above for 3,5-dimethylphenol were: total cyclohexane flow rate, 2.6 mL/min; total aqueous flow rate, 2.3 mL/min; aqueous flow through the membrane, 1.1 mL/min; wavelength for both detectors, 260 nm; temperature of water bath, 20.5°C.

5.3.6 Molar Absorptivity Ratios

Molar absorptivity ratios of the protonated and deprotonated sample species in the aqueous phase were measured for 3,5-dimethylphenol and p-toluidine using the apparatus shown in Figure 23. The same aqueous phase detector and wavelength setting were used as in the acidity constant determination.

The molar absorptivity ratio, $\epsilon_{HA,a}/\epsilon_{A^-,a}$, for 3,5-dimethylphenol was determined using two sample solutions, both 3.0×10^{-4} M in 3,5-dimethylphenol but one adjusted to pH = 2.0 with HCl and the other adjusted to pH = 12.6 with NaOH. These samples were injected into an HCl or NaOH reagent of the same pH and peak areas were measured for six replicate injections. Important instrument parameters were as follows: flow rate for pH = 2.0 reagent, 0.688 ± 0.004 mL/min; flow rate for pH = 12.6 reagent, 0.677 ± 0.004 mL/min; wavelength, 281 nm; sample volume injected, 44 μ L; injection rate, one sample per min; nitrogen pressure, 20 psig. Since the flow rates differed slightly for the two reagents, peak areas were corrected to a constant flow rate of 0.688 mL/min.

The molar absorptivity ratio, $\epsilon_{BH^+,a}/\epsilon_{B,a}$, for p-toluidine was determined similarly using sample solutions both 5.0×10^{-4} M in p-toluidine with one adjusted to pH 2.0 with HCl and the other adjusted to pH = 12.0 with

NaOH. Instrument parameters that differed from those listed above for 3,5-dimethylphenol were: flow rate for pH = 2.0 reagent, 0.473 ± 0.003 mL/min; flow rate for pH = 12.0 reagent, 0.490 ± 0.003 mL/min; wavelength, 260 nm. Peak areas were corrected to a constant flow rate of 0.473 mL/min.

5.3.7 Acidity Constant Determination

The acidity constants ^{for} 3,5-dimethylphenol and the p-toluidinium ion were determined using two phase analysis with the extraction/FIA apparatus shown in Figure 22. In the case of 3,5-dimethylphenol, a sample solution that was 4.0×10^{-4} M in 3,5-dimethylphenol and 0.10 M in NaCl was injected into reagent buffers of various pH. The reagents were ionic strength 0.10 $\text{NH}_3/\text{NH}_4\text{Cl}$ buffers that ranged in 0.1 increments of pH from pH = 9.6 to pH = 10.1. Additionally, a solution that was just 0.10 M in NaCl was injected into each reagent buffer to serve as a blank.

The extraction coil was made long enough to insure that extraction equilibrium was attained, and the extraction coil and phase separator were thermostatted to $25.0 \pm 0.1^\circ\text{C}$. Both the organic and aqueous phases were monitored simultaneously, and peak areas were measured for six replicate injections of each sample. The pH of the aqueous effluent was measured for each buffer used to

insure that no change in pH occurred during the extraction/FIA procedure. The pH meter (Fisher Scientific Co.) was standardized with freshly prepared pH = 6.865 phosphate buffer and either freshly prepared pH = 4.005 potassium hydrogen phthalate or pH = 9.180 borax buffer.

Important instrument parameters for the acidity constant determination of 3,5-dimethylphenol were as follows: wavelength for both detectors, 281 nm; extraction coil length, 200.4 cm; sample volume injected, 44 μ L; injection rate, one sample per min; nitrogen pressure, 42 psig. Flow rates for trial #1: $F_O = 2.50 \pm 0.02$ mL/min; $F_A = 2.18 \pm 0.02$ mL/min; $F_{m,O} = 0.86$ mL/min; $F_{m,A} = 1.06$ mL/min. Flow rates for trial #2: $F_O = 2.49 \pm 0.04$ mL/min; $F_A = 2.22 \pm 0.03$ mL/min; $F_{m,O} = 0.88$ mL/min; $F_{m,A} = 1.04$ mL/min.

The acidity constant of the p-toluidinium ion was determined in a similar manner using a sample solution that was 1.0×10^{-3} M in p-toluidine and 0.10 M in NaCl. The reagents were ionic strength 0.10 acetic acid/sodium acetate buffers that ranged in 0.2 pH increments from pH = 4.6 to pH = 5.6. The phase separator and extraction coil were thermostatted at $20.0 \pm 0.1^\circ\text{C}$. Instrument parameters that differed from those listed above for 3,5-dimethylphenol were: wavelength for both detectors, 260 nm. Flow rates for trial #1: $F_O = 2.50 \pm 0.04$ mL/min; F_A

= 2.12 ± 0.04 mL/min; $F_{m,O} = 0.86$ mL/min; $F_{m,a} = 0.99$ mL/min. Flow rates for trial #2: $F_O = 2.60 \pm 0.02$ mL/min; $F_a = 2.12 \pm 0.04$ mL/min; $F_{m,O} = 0.86$ mL/min; $F_{m,a} = 1.03$ mL/min.

5.4 Results and Discussion

Acidity constants were determined for 3,5-dimethylphenol and the p-toluidinium ion to test the validity of the equations derived for HA and BH^+ charge type acids. The distribution coefficient of the neutral conjugate species was also calculated.

5.4.1 Choice of Experimental Conditions

In designing the experiment for the determination of the acidity constant of a particular compound, several factors should be taken into account. The first is the choice of the organic solvent. In order to accurately measure peak areas in both the organic and aqueous phases, for reagent pH values in the vicinity of the expected pK_a of the sample, it is necessary that the distribution coefficient for the sample be neither too large nor too small. The value of K_{HA} or K_B should be between approximately 1 and 10, although this will depend on the molar absorptivities of the sample species in the two phases.

The likelihood of dimerization of the sample in the organic phase or possible ion-pair extraction of the sample with components present in the buffer must also be considered. The derivation presented in the theory section assumes that these effects are negligible. If they are not, the equations must be modified to take them into account. Dimerization of the sample in the organic phase is more likely to be encountered at higher concentrations and when the sample is polar and the organic phase non-polar. This problem may be avoided by keeping the sample concentration low.

When mutual solubility of the aqueous and organic solvents is significant the phases should be pre-equilibrated before they are used in the solvent extraction/FIA system. Pre-equilibration of the phases will not affect the value of the acidity constant but may affect the value of the measured distribution coefficient [63]. In using cyclohexane as the organic phase we did not worry about pre-equilibration of the phases since the solubility of cyclohexane in water is only 0.006% at 25°C and the solubility of water in cyclohexane is 0.01% at 20°C [90].

Unlike a spectrophotometric determination of acidity constants, it is not necessary that the molar absorptivities of the protonated and deprotonated sample

species in the aqueous phase be different at the wavelength chosen. It is, of course, also not necessary to have both spectrophotometers set to the same wavelength.

Salt was added to the sample solutions injected for two reasons. Most importantly, an inert electrolyte is added to insure constant ionic strength throughout the concentration profile of the sample zone and to match the ionic strength of the sample zone to the surrounding buffer. It additionally served to reduce refractive index effects, as discussed in Section 5.4.2. One must be careful, however, to check that the sample does not form an ion pair with components of the electrolyte that may extract into the organic phase.

Buffers should be avoided that absorb appreciably at the wavelength of analysis, or that have components that may extract as ion pairs with the sample. The buffers should be of sufficient concentration to maintain constant pH when a sample is injected. It is desirable to choose the pH values of the buffers to be in the vicinity of the inflection point of the plot of peak area vs reagent pH for the sample (see Figure 19 for diphenhydramine). For distribution coefficients in the suggested range of 1 to 10, this inflection point will occur within about one pH unit of the sample pK_a . Optimum choice of the extraction

coil length, sample injection volume and flow rates has previously been discussed in Chapter 2.

5.4.2 Refractive Index Peaks

Peaks can occur in flow injection analysis as a consequence of a difference in refractive index between the sample plug injected and the surrounding reagent stream. The effect is characterized by adjacent positive and negative peaks as the sample passes through the flow cell. The refractive index peak is superimposed upon the absorbance peak for the sample and may affect peak heights and shapes, especially for samples of low absorbance. Various authors have noted this effect [91-93] and Betteridge et al. [93] have given a detailed analysis of the phenomenon as it pertains to flow injection analysis.

When a sample of low salt content and hence low refractive index is injected into a stream of high salt content, a refractive index gradient will form in the unsegmented regions of the FIA system. Lines of equal salt concentration, referred to as isohalines, will be roughly parabolic in shape owing to wall drag and laminar flow. Each isohaline will have a refractive index different from that of an adjacent one resulting in a series of liquid lenses which will either focus or diverge the light [93].

(

When a leading isohaline passes through the flowcell, light passes from a medium of low refractive index to that of a higher refractive index. The light is refracted towards the normal to the isohalines, decreasing the amount of light reaching the detector. This shows up as an increase in absorbance and manifests itself as a positive slope. There will be a region in the middle of the sample zone where there is no change in refractive index over the cell length. The light is unrefracted and the trace passes through the baseline. As a trailing isohaline passes through the flowcell, light travels from a medium of high refractive index to a medium of lower refractive index and is refracted away from the normal to the isohalines. The light is therefore focused onto the detector, increasing the amount of light hitting the detector. This shows up as a decrease in absorbance and the trace moves in a negative direction with respect to the baseline.

The net result is a refractive index "peak" which is superimposed upon the sample absorbance peak. The shape of these peaks will be similar to those given in Figure 24. The height of the positive portion will always be greater than that of the negative portion for fast flow rates because the leading interface has the steeper gradient. Since refractive index is temperature

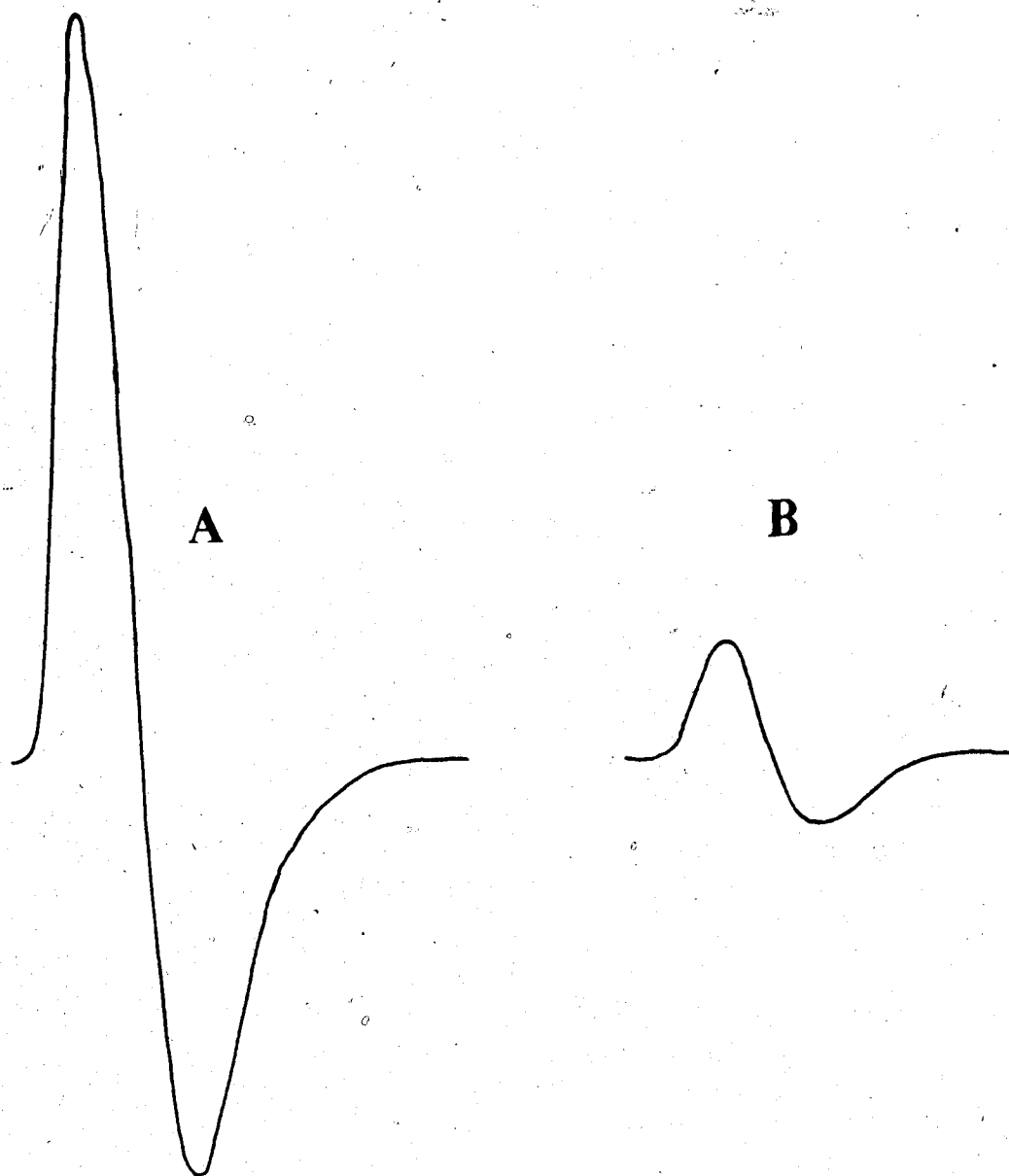


Figure 24. Recorder tracings for the aqueous phase injecting H_2O (A) and 0.1 M NaCl (B) into ionic strength 0.1, $\text{pH} = 9.8 \text{ NH}_3/\text{NH}_4\text{Cl}$ buffer. See text for details.

dependent, the size of the refractive index peaks may vary considerably if the system is not well thermostatted.

There are various ways to minimize refractive index effects. One alternative is through appropriate design of the detector flowcell. Ham [91] found that the use of longer flowcells reduced the significance of the refractive index phenomenon. Little and Fallick [94] describe a tapered bore cell in connection with a solvent gradient liquid chromatography system which reduces the amount of light that hits the cell walls, thus improving baseline stability.

Another way to diminish refractive index effects is to inject the sample into a carrier stream of similar refractive index, and then merge this stream with a reagent stream [91]. This configuration was tried but was found to produce refractive index peaks of a different nature due to the sample injection process. When the sample injection valve switches from the load position to the inject position and visa versa, the flow of carrier stream is cut off for an instant, momentarily increasing the reagent concentration in the aqueous stream. This results in a small refractive index peak each time the injection valve throws from one position to another. The negative portion of that peak falls directly in front of the sample absorbance peak, thus interfering with proper integration of the sample peak.

An alternative solution to the problem is to match the refractive index of the sample and reagent stream. In the present case, where acidity constants were to be determined at a certain constant ionic strength, we instead matched the ionic strength of the sample solution to that of the reagent stream by adding salt (NaCl) to the sample. While this did not completely match the refractive indices, it brought them much closer together and greatly reduced the size of the refractive index peaks.

This is illustrated in Figure 24 where water (A) and 0.1 M NaCl (B) were injected into an ionic strength 0.1, pH = 9.80 $\text{NH}_3/\text{NH}_4\text{Cl}$ buffer using the extraction/FIA system shown in Figure 22. Important instrument parameters were: wavelength, 281 nm; absorbance, 0.1; chart speed, 20 cm/min; F_0 , 2.4 mL/min; F_A , 2.1 mL/min, $F_{m,0}$, 0.9 mL/min; $F_{m,a}$, 1.0 mL/min. As can be seen from Figure 24, matching the ionic strength of the sample to that of the stream considerably reduced (about 85%) the size of the refractive index peaks. Duplicate injections of water and 0.1 M NaCl were made and peak areas were measured with a planimeter. In both cases, the area of the positive portion of the refractive index peak equalled the area of the negative portion within the measuring error of the planimeter. A refractive index peak that is superimposed

on the sample absorbance peak should not therefore affect the net peak area.

If, however, the sample absorbance peak is small compared to the refractive index peak, the observed peak shape will be distorted, preventing proper integration by an electronic integrator. This effect is illustrated in Figure 25A where 2×10^{-4} M 3,5-dimethylphenol (no added NaCl) was injected into ionic strength 0.1, pH = 9.8 $\text{NH}_3/\text{NH}_4\text{Cl}$ buffer. Figure 25B, on the other hand, shows the resulting peak from a 2×10^{-4} M 3,5-dimethylphenol sample that has been adjusted to ionic strength 0.1 with NaCl before injection into the extraction/FIA system. Measurement of peak areas with a planimeter indicated that the net areas for peaks A and B were the same. Peak A, however, cannot be properly integrated by most electronic integrators. All samples were therefore adjusted to the ionic strength of the reagent stream using NaCl before they were injected into the solvent extraction/FIA system. The size and shape of the refractive index peaks were routinely monitored by injection of 0.1 M NaCl into each reagent in place of the sample. No refractive index peaks were observed in monitoring the organic phase.

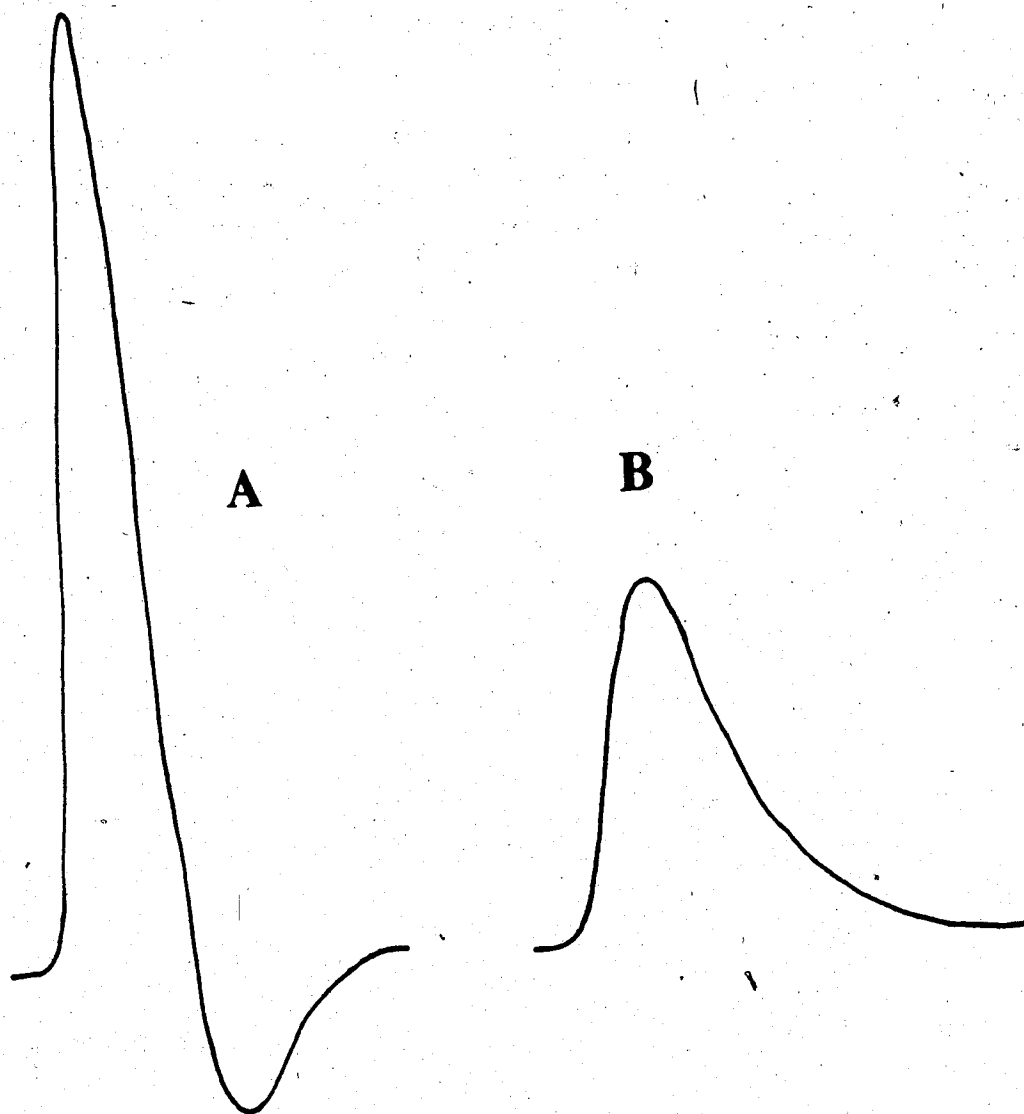


Figure 25. Recorder tracings for the aqueous phase injecting 2×10^{-4} M 3,5-dimethylphenol (A) and ionic strength 0.1, 2×10^{-4} M 3,5-dimethylphenol (B) into ionic strength 0.1, pH = 9.8 $\text{NH}_3/\text{NH}_4\text{Cl}$ buffer. See text for details.

5.4.3 Ultraviolet Absorption Spectra

Absorption spectra for 3,5-dimethylphenol in cyclohexane, in pH = 2.0 HCl and in pH = 12.5 NaOH, measured on a Cary 118 spectrophotometer, are given in Figure 26. The wavelength chosen for analysis of both the organic and aqueous phases in the pK_a determination was 281 nm. The molar absorptivities of the HA species in the aqueous phase, the A^- species in the aqueous phase and the HA species in cyclohexane were respectively in units of L moles⁻¹cm⁻¹: 984, 1957, 1691.

Absorption spectra for p-toluidine in cyclohexane, in pH = 2.0 HCl and in pH = 12.0 NaOH appear in Figure 27. The wavelength of analysis chosen was 260 nm. The molar absorptivities of the BH^+ and B species in the aqueous phase, and the B species in the organic phase were respectively in units of L moles⁻¹cm⁻¹: 265, 576, 876.

5.4.4 Dimerization and Ion-Pair Extraction

A preliminary check for dimerization was made via Beer's law plots for 3,5-dimethylphenol and p-toluidine in cyclohexane using the Cary 118 spectrophotometer over the concentration ranges of interest. For the former compound, the plot of absorbance at 281 nm vs concentrations from 4×10^{-5} M to 8×10^{-4} M is given in Figure 28. It was linear with a relative standard

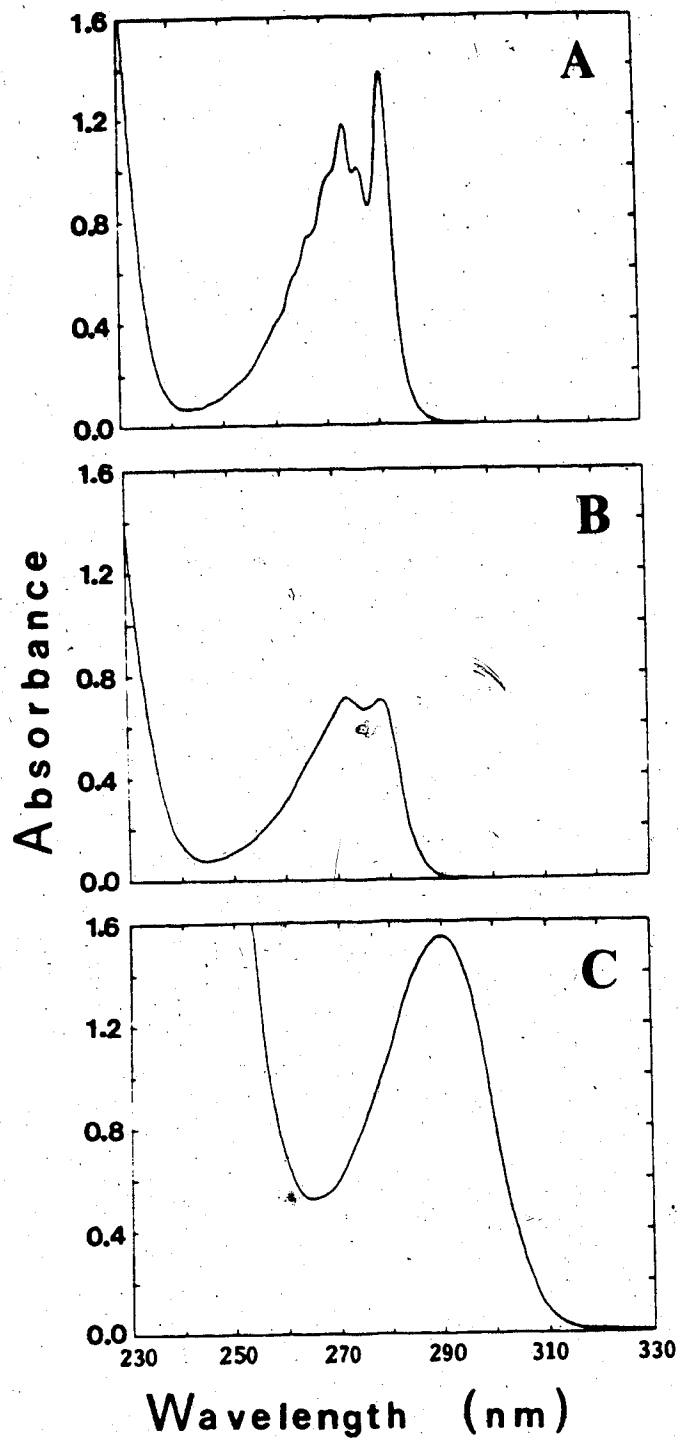


Figure 26. U.V. absorption spectra of: (A) 8.0×10^{-4} M 3,5-dimethylphenol in cyclohexane; (B) pH = 2.0, 6.0×10^{-4} M aqueous 3,5-dimethylphenol; (C) pH = 12.5, 6.0×10^{-4} M aqueous 3,5-dimethylphenol.

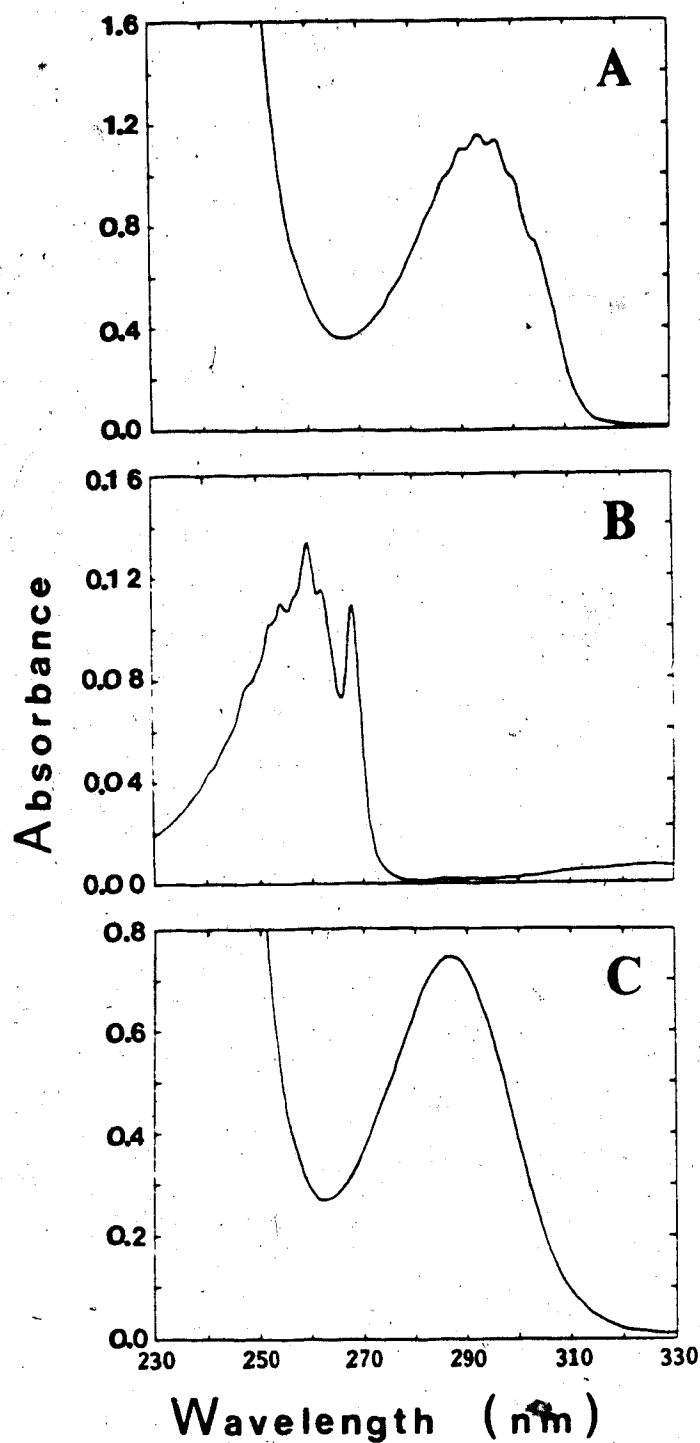


Figure 27. U.V. absorption spectra of: (A) $6.0 \times 10^{-4} \text{ M}$ p-toluidine in cyclohexane; (B) pH = 2.0, $5.0 \times 10^{-4} \text{ M}$ aqueous p-toluidine; (C) pH = 12.0, $5.0 \times 10^{-4} \text{ M}$ aqueous p-toluidine.

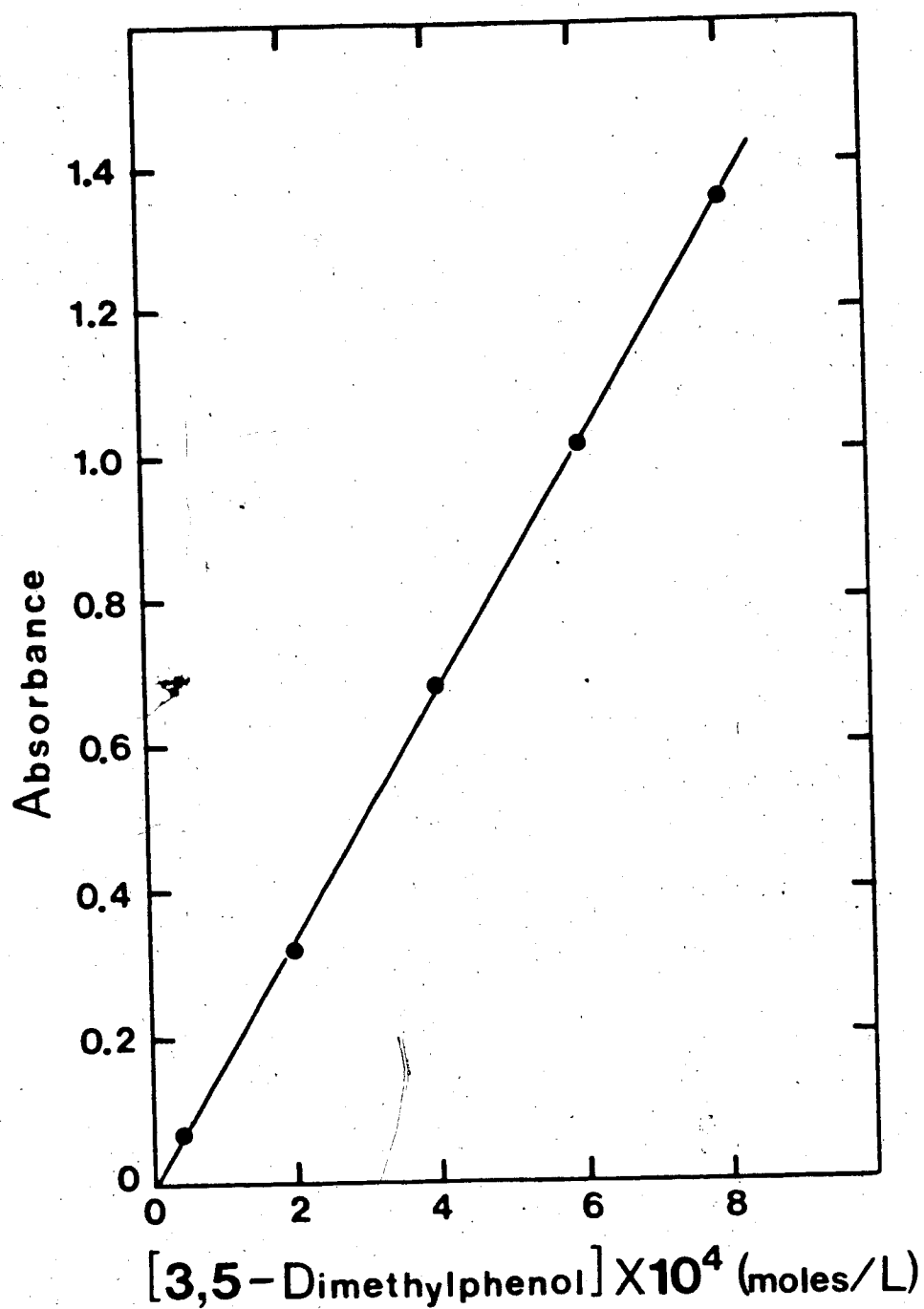


Figure 28. Beer's law plot for 3,5-dimethylphenol in cyclohexane at 281 nm.

deviation (RSD) for the slope of 0.19%. The y-intercept and its 95% confidence limits were $1.3 \times 10^{-3} \pm 4.9 \times 10^{-3}$. For the latter compound, the Beer's law plot over the concentration range $4 \times 10^{-5} \text{ M}$ to $1 \times 10^{-3} \text{ M}$, made at 287 nm, appears in Figure 29. It too was linear with a RSD for the slope of 0.23%. The y-intercept and its 95% confidence limits were $-5.3 \times 10^{-3} \pm 5.5 \times 10^{-3}$. The linearity and zero y-intercepts of these plots suggest that no dimerization of the samples occurred in cyclohexane over the concentrations studied.

The absence of ion-pair extraction of 3,5-dimethylphenolate (A^-) and of p-toluidinium (BH^+) was checked by seeing if detectable concentrations of these species were extracted into cyclohexane from 0.10 M NaCl solutions adjusted to pH's where either A^- or BH^+ were the only species present in significant amounts. In batch extractions, with absorbances of the cyclohexane phases measured on the Cary 118 spectrophotometer, no detectable 3,5-dimethylphenol was extracted from a pH = 12.6 aqueous phase that was $4 \times 10^{-4} \text{ M}$ in 3,5-dimethylphenol and 0.10 M in NaCl. Similarly, no detectable p-toluidine was extracted from a pH = 2.0 aqueous phase that was $1 \times 10^{-3} \text{ M}$ in p-toluidine and 0.10 M in NaCl.

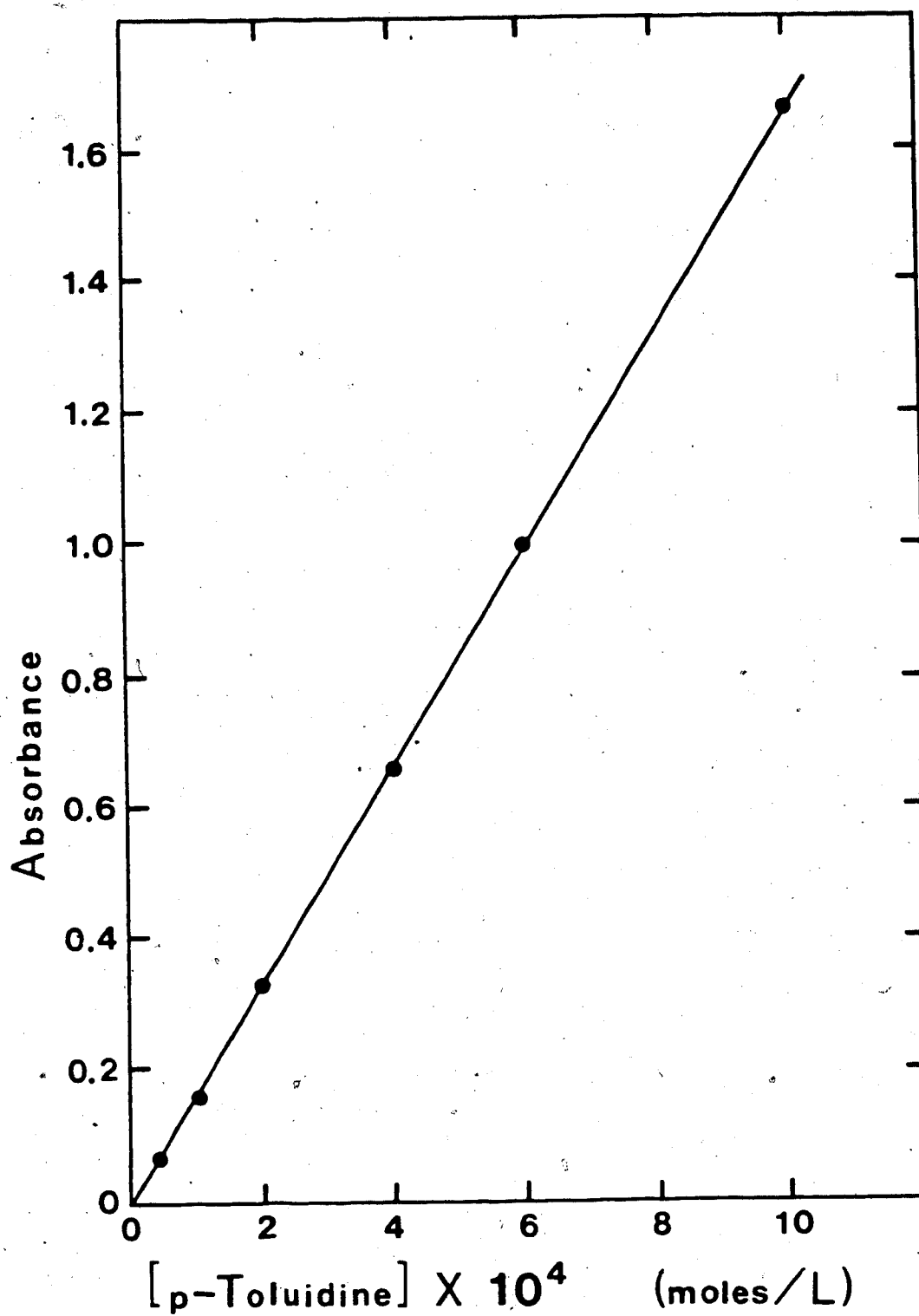


Figure 29. Beer's law plot for p-toluidine in cyclohexane at 287 nm.

5.4.5 Calibration Curves

The equations presented in the theory section for determination of acidity constants and distribution coefficients assume a linear relationship between integrator signal and concentration. This was checked for 3,5-dimethylphenol and p-toluidine for both the organic and aqueous phases using the solvent extraction/FIA system. Plots of peak area vs concentration were linear for both compounds in both phases. The slopes, y-intercepts and associated errors for these plots are listed in Table 2. The zero y-intercepts for the aqueous phase plots show that the underlying refractive index peaks do not have a net effect on sample peak areas.

5.4.6 Molar Absorptivity Ratios

Accurate ratios for the molar absorptivities of the two conjugate acid-base species in the aqueous phase are required in equations 5.17 and 5.32. These were measured by a flow injection technique without solvent extraction, as described in Section 5.36, in which the ratio of peak areas obtained at low and high pH is equal to the ratio of molar absorptivities. Flow rates for the two reagent streams differed slightly, so peak areas were corrected to a constant flow rate using the relation $A = nK/F$; where A is the peak area, n is the number of moles of sample injected, K is the system constant and F is the flow rate.

Table 2. Calibration Curve Data for 3,5-Dimethylphenol and p-Toluidine.

Compound	Organic Phase		Aqueous Phase	
	Slope (\pm % RSD) ^a	y-Intercept ^b	Slope (\pm % RSD) ^a	y-Intercept ^b
3,5-Dimethylphenol	5.16×10^7 ($\pm 0.28\%$)	64.0 ± 64.8	5.88×10^8 ($\pm 0.46\%$)	-3038 ± 4219
p-Toluidine	4.43×10^7 ($\pm 0.74\%$)	9.4 ± 881	2.08×10^8 ($\pm 1.2\%$)	1557 ± 6632

a) Percent relative standard deviation.

b) Uncertainties are 95% confidence limits.

The molar absorptivity ratio for 3,5-dimethylphenol, $\epsilon_{HA,a}/\epsilon_{A^-,a}$, determined at 281 nm was 0.500 ± 0.005 , and for p-toluidine $\epsilon_{BH^+,a}/\epsilon_{B,a}$ at 260 nm was 0.353 ± 0.006 . In principle the molar absorptivity ratio could be calculated from literature values or from absorbance measurements made on another spectrophotometer, but this can lead to appreciable error in the acidity constant if the spectrophotometer wavelength is not accurately calibrated. Even a 1 nm difference between the wavelength of analysis for the aqueous phase and the wavelength at which the molar absorptivity ratio was determined can lead to significant error in the pK_a if the wavelength of analysis lies on a sharp slope of the absorption spectrum for one of the sample species.

5.4.7 Acidity Constants

The acidity constant for 3,5-dimethylphenol was determined by applying equation 5.17 to a plot of A_a/A_o vs $1/a_H$. The experiment was run twice and peak areas obtained were based on an average of six replicate injections of sample into each buffer. The data for trials 1 and 2 are given in Appendix I, and plots are given in Figures 30 and 31. The lines are linear least squares fits to the data points. The linearity of the plots is evidence for the validity of the equations for an HA charge type acid.

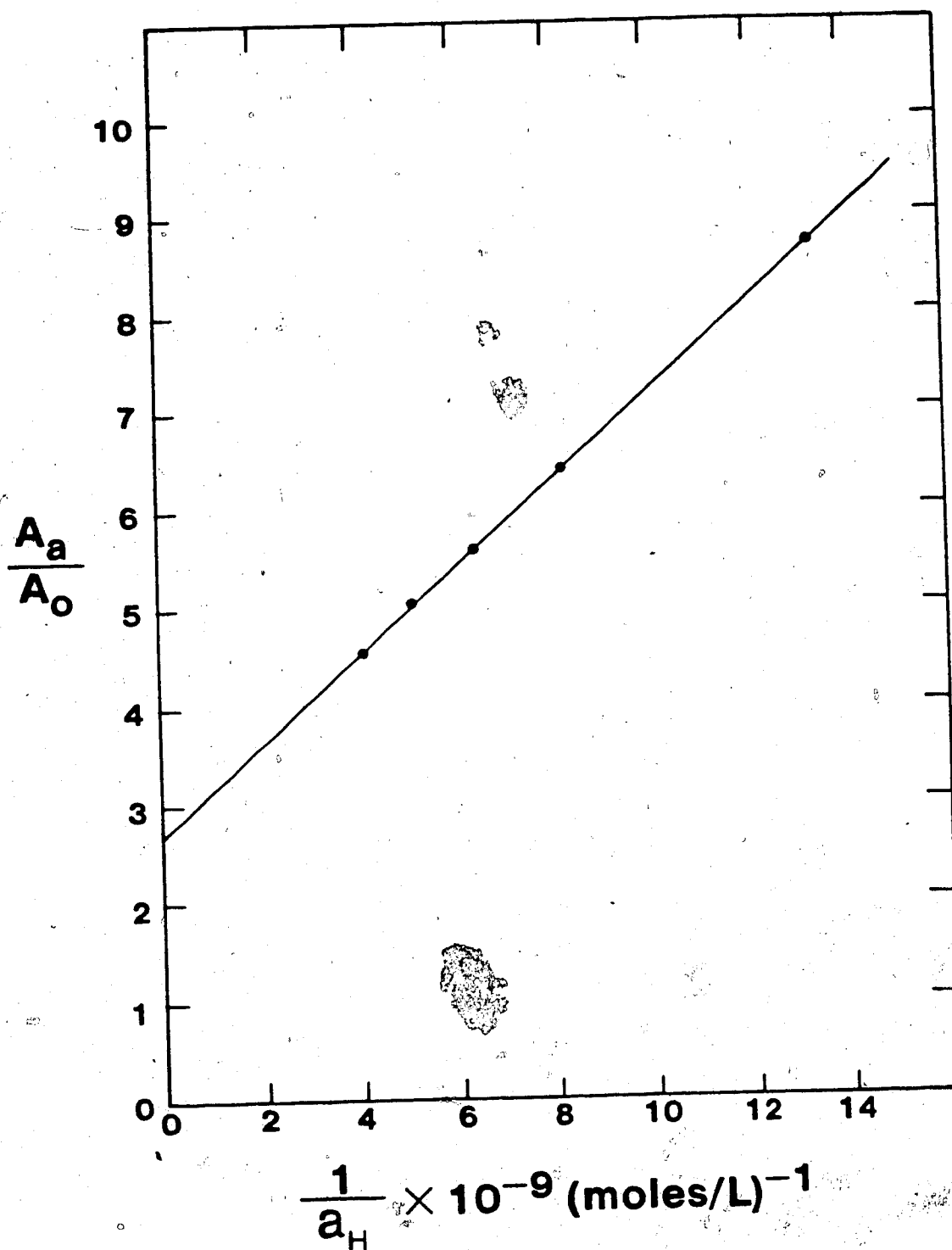


Figure 30. Plot of A_a/A_o versus $1/a_H$ for trial #1 of the K_a determination of 3,5-dimethylphenol at 25.0°C with ionic strength = 0.10.

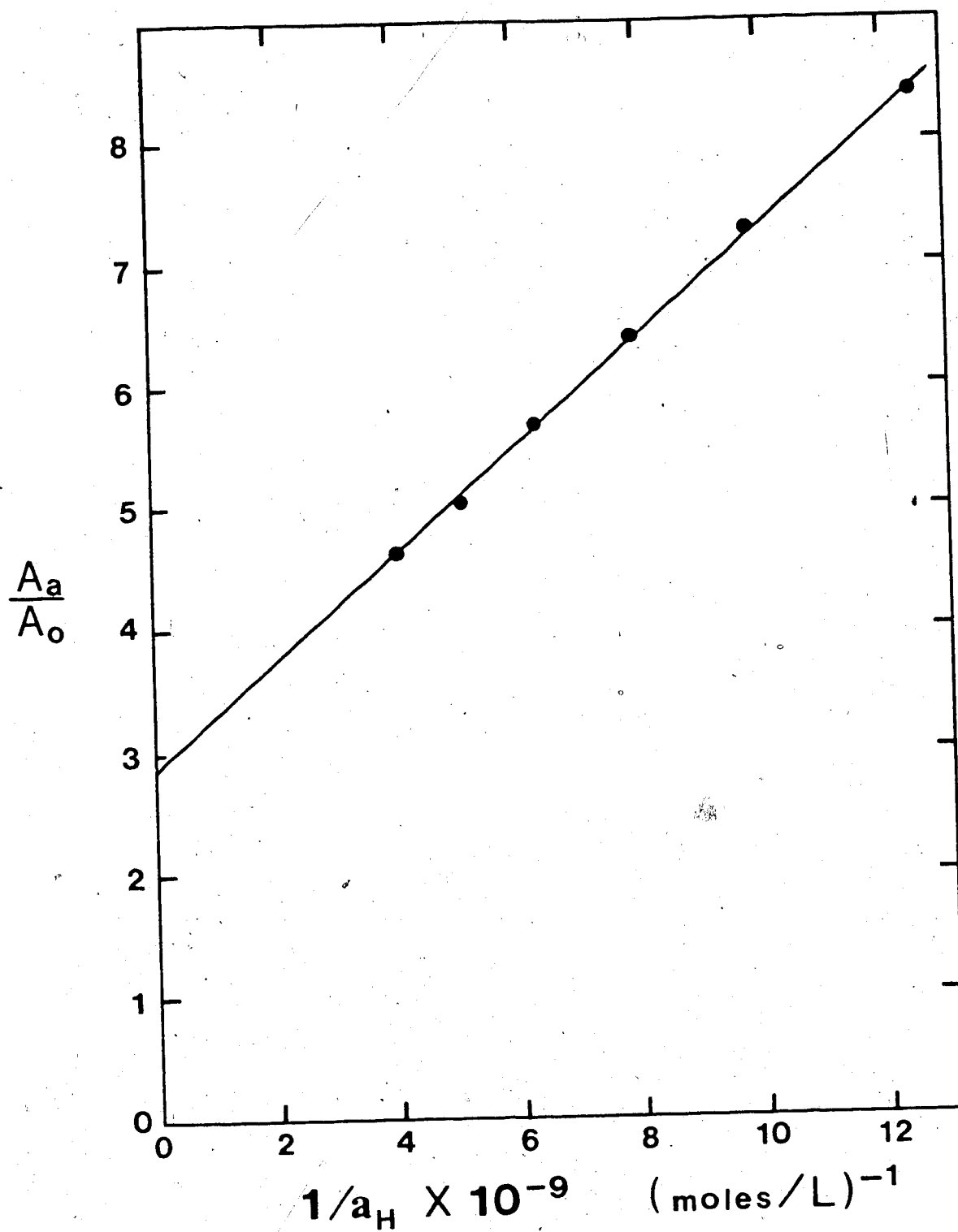


Figure 31. Plot of A_a/A_o versus $1/a_H$ for trial #2 of the K_a determination of 3,5-dimethylphenol, at 25.0°C with ionic strength = 0.10.

The slope and y-intercept values of the plots along with the calculated pK_a 's and computed errors are reported in Table 3. The uncertainties associated with the pK_a values are one standard deviation and include the computed error in determining the slope, y-intercept and molar absorptivity ratio as well as an estimated error (0.01) due to calibration of the pH meter used to measure the pH's of the reagent buffer solutions. The computed error is obtained through propagation of the relative standard deviations of the slope, y-intercept and molar absorptivity ratio [95]. The computed and estimated errors are combined as the square root of the sum of the squares [96].

The average value of the pK_a for 3,5-dimethylphenol at an ionic strength of 0.10 and temperature of 25°C was $10.09 \pm 0.01_4$. Literature values for the pK_a of 3,5-dimethylphenol at 25°C determined spectrophotometrically and corrected for activity coefficient effects to zero ionic strength are 10.20 [97] and 10.19 [98]. For comparison purposes, if we correct our pK_a value to zero ionic strength by calculating the activity coefficient via the Davies equation [99] we obtain a pK_a° value of 10.20.

The acidity constant for the p-toluidinium ion was determined by applying equation 5.32 to duplicate plots of

Table 3. Acidity Constant Determination by Solvent Extraction/FIA.

Compound	Trial #	Slope (\pm RSD) ^a	y-Intercept ^b	pK _a ^c
3,5-Dimethylphenol	1	4.49×10^{-10} ($\pm 1.3\%$)	2.71 ± 0.10	$10.08 \pm 0.01_4^d$
	2	4.49×10^{-10} ($\pm 1.1\%$)	2.84 ± 0.08	$10.10 \pm 0.01_3^d$
p-Toluidinium	1	4.31×10^5 ($\pm 0.73\%$)	6.17 ± 0.08	$5.30 \pm 0.01_3^e$
	2	4.10×10^5 ($\pm 0.77\%$)	6.16 ± 0.09	$5.27 \pm 0.01_3^e$

a) Percent relative standard deviation.

b) Uncertainties are 95% confidence limits.

c) Uncertainties are one standard deviation.

d) Temperature = $25.0 \pm 0.1^\circ\text{C}$ and ionic strength = 0.10.e) Temperature = $20.0 \pm 0.1^\circ\text{C}$ and ionic strength = 0.10.

A_a/A_o vs a_H . The data for trials 1 and 2 are given in Appendix I, and plots are given in Figures 32 and 33. The results are reported in Table 3, and the linearity of the plots is proof of the validity of the equations for a BH^+ charge type acid. The average value of the pK_a for the p-toluidinium ion at an ionic strength of 0.10 and a temperature of 20.0°C was $5.28 \pm 0.01_3$. Literature values determined at 20°C and an ionic strength of 0.1 are 5.44 [100], 5.21 [101] and 5.159 [102]. Since the literature values show considerable variation we can only say that our value is well within the range of reported values.

5.4.8 Distribution Coefficients

The distribution coefficients for HA and B between cyclohexane and aqueous buffers can be calculated from equations 5.19 and 5.35 respectively. However, since the experiment was optimized for determination of acidity constants, the pH region examined is not the best for accurate measurement of K_B and K_{HA} . Data for plots of $1/A_o$ vs $1/a_H$ for trials 1, 2 and 3 of the K_{HA} determination of 3,5-dimethylphenol are given in Appendix I, and the plots are given in Figures 34, 35 and 36. Data for plots of $1/A_o$ vs a_H for trials 1 and 2 of the K_B determination of p-toluidine are given in Appendix I, and the plots are given in Figures 37 and 38.

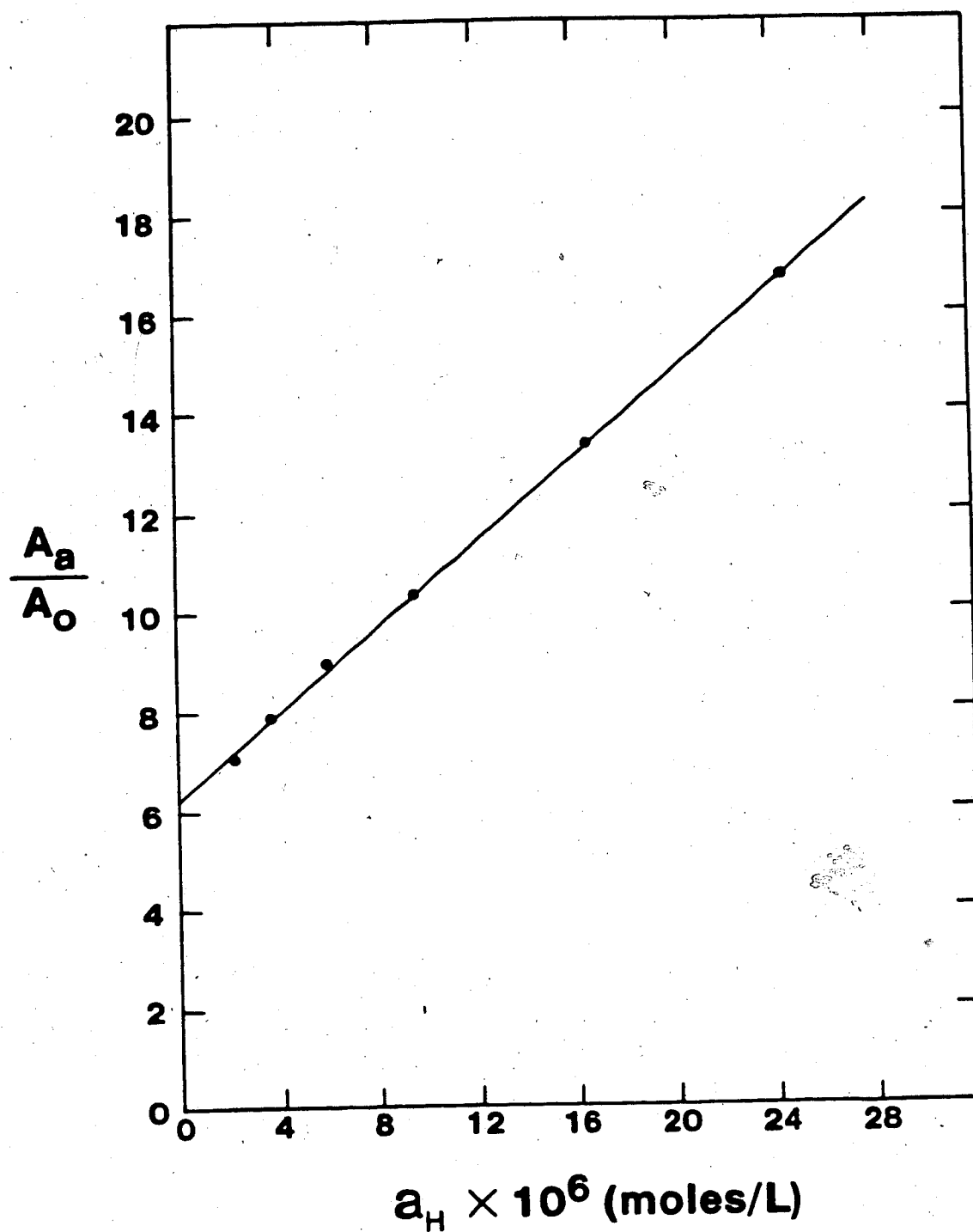


Figure 32. Plot of A_a/A_o versus a_H for trial #1 of the K_a determination of p-toluidinium at 20.0°C with ionic strength = 0.10.

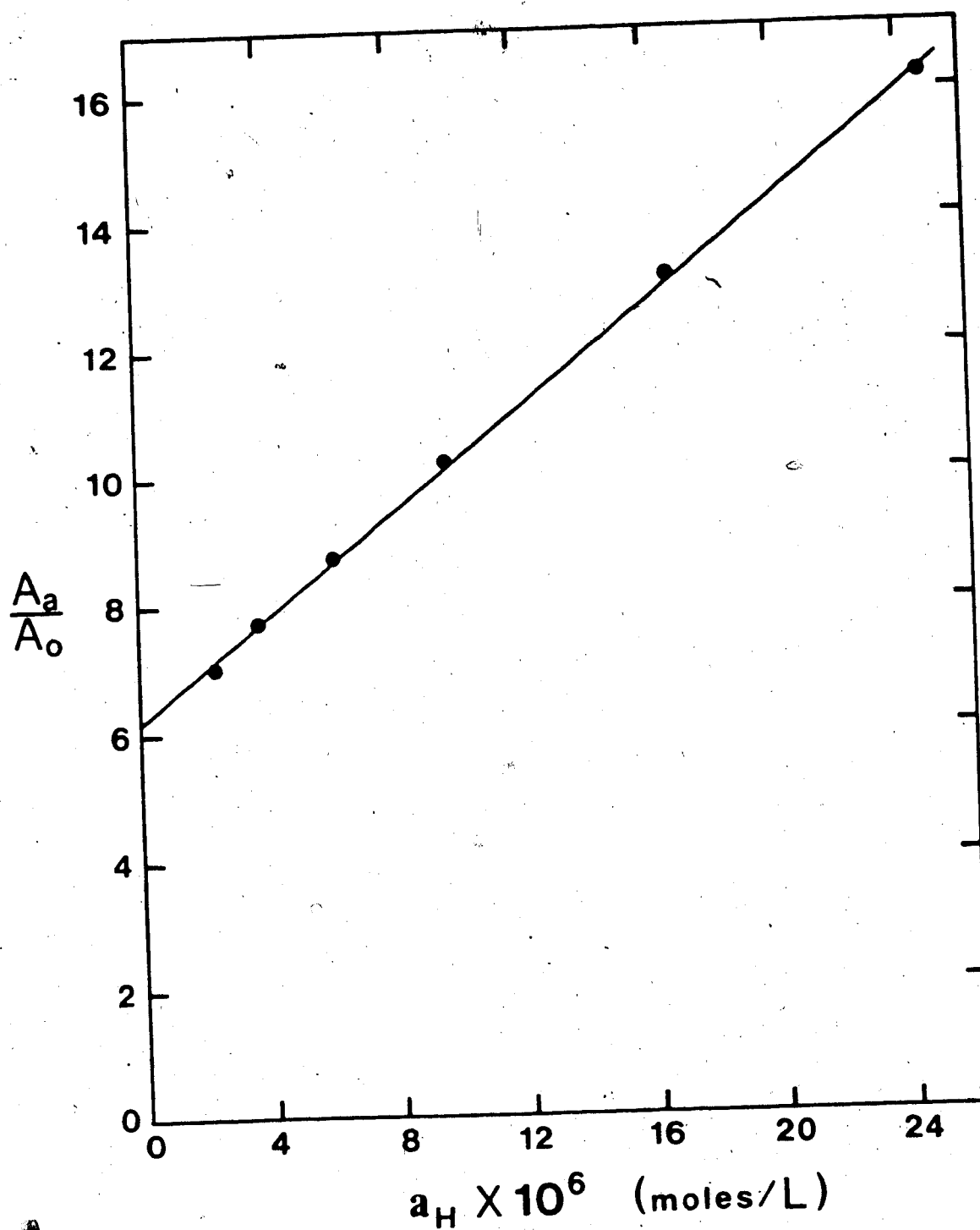


Figure 33. Plot of A_a/A_o versus a_H for trial #2 of the K_a determination of p-toluidinium at 20.0°C with ionic strength = 0.10.

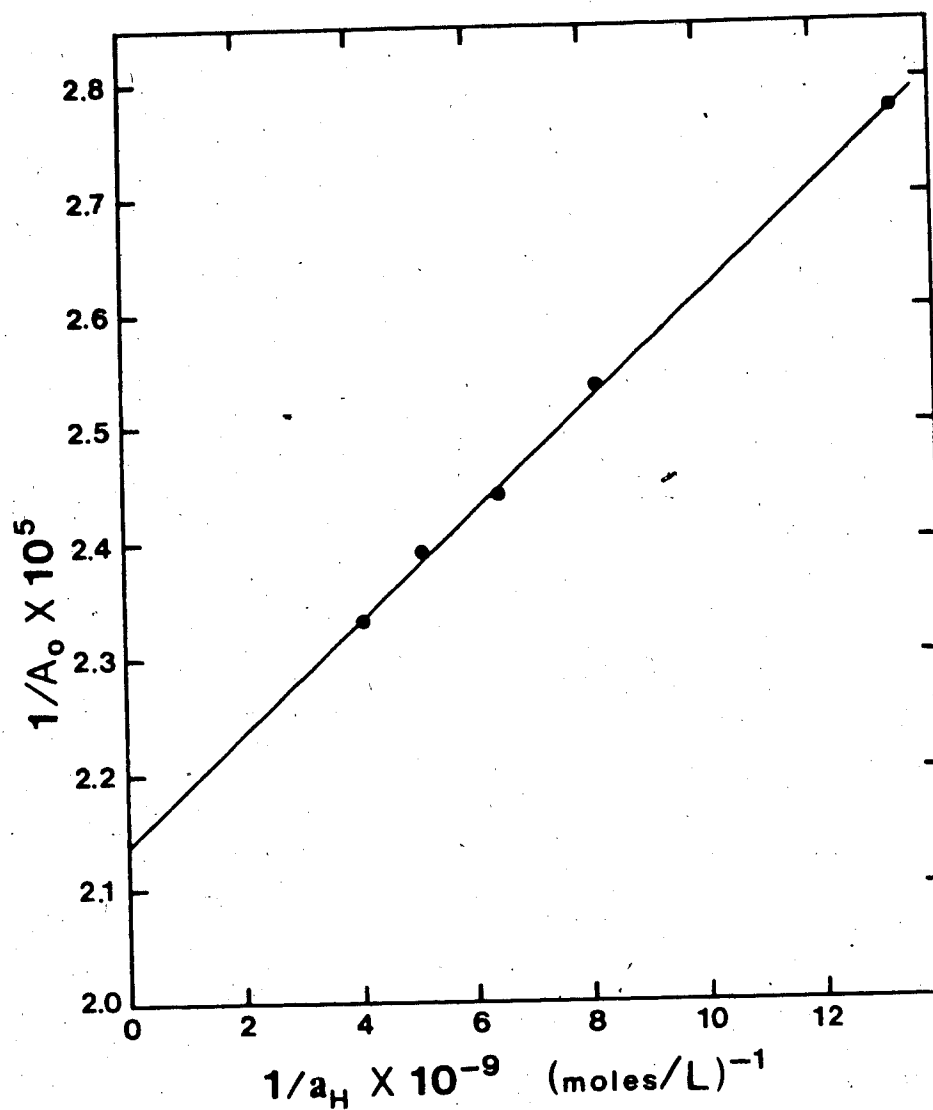


Figure 34. Plot of $1/A_0$ versus $1/a_H$ for trial #1 of the K_{HA} determination of 3,5-dimethylphenol between cyclohexane and ionic strength 0.10 ammonia buffer at 25.0°C.

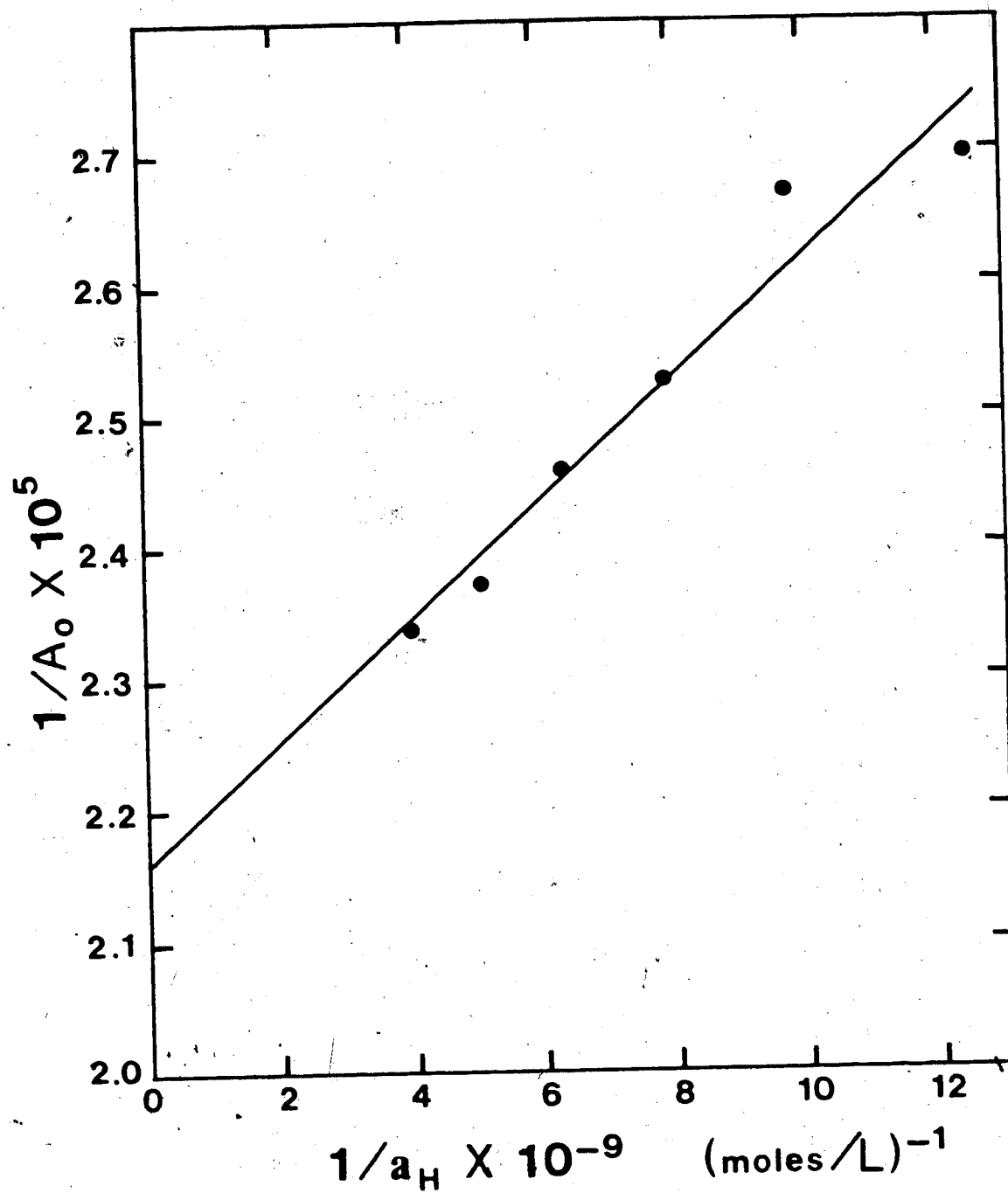


Figure 35. Plot of $1/A_0$ versus $1/a_H$ for trial #2 of the K_{HA} determination of 3,5-dimethylphenol between cyclohexane and ionic strength 0.10 ammonia buffer at 25.0°C.

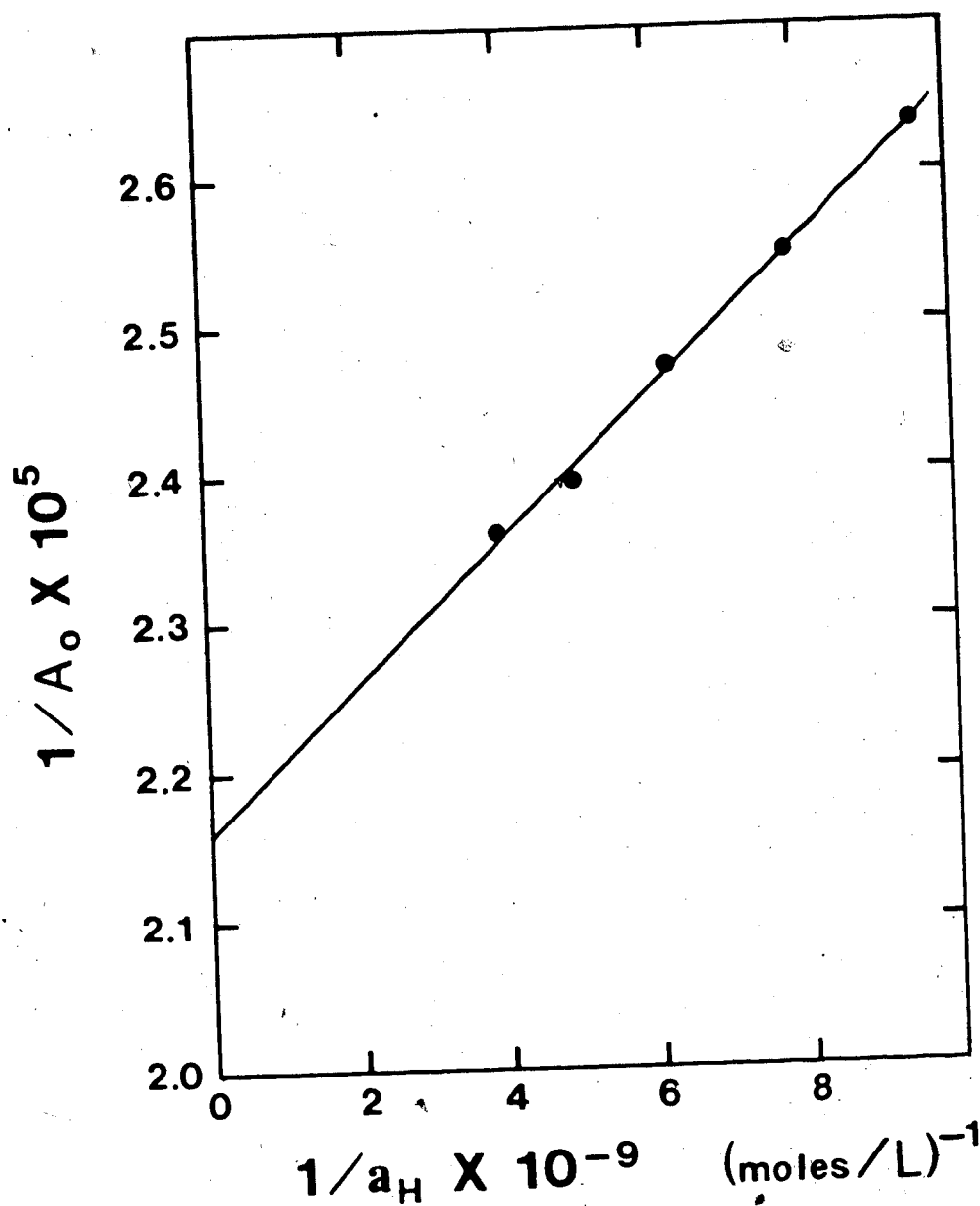


Figure 36. Plot of $1/A_0$ versus $1/a_H$ for trial #3 of the K_{HA} determination of 3,5-dimethylphenol between cyclohexane and ionic strength 0.10 ammonia buffer at 25.0°C.

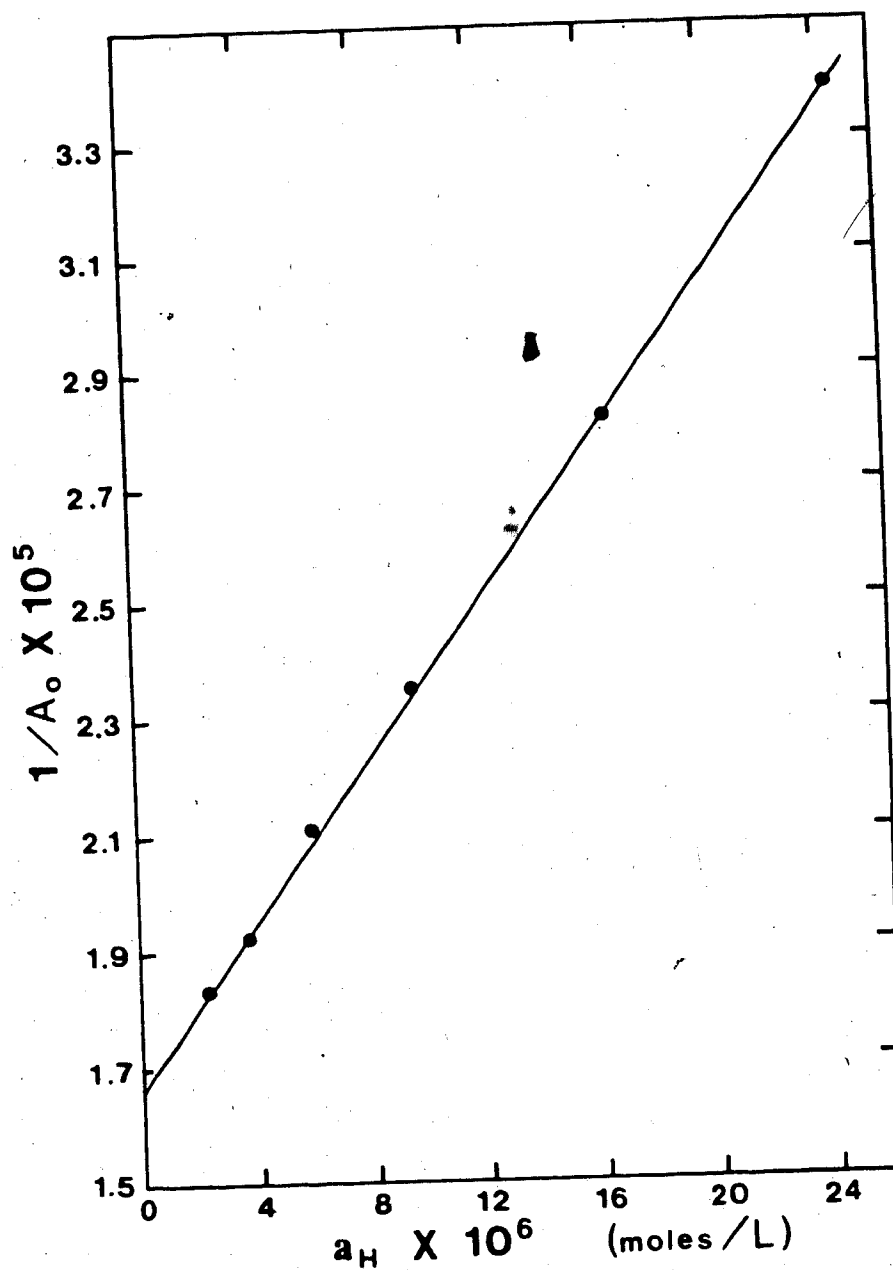


Figure 37. Plot of $1/A_0$ versus a_H for trial #1 of the K_B determination of p-toluidine between cyclohexane and ionic strength 0.10 acetate buffer at 20.0°C.

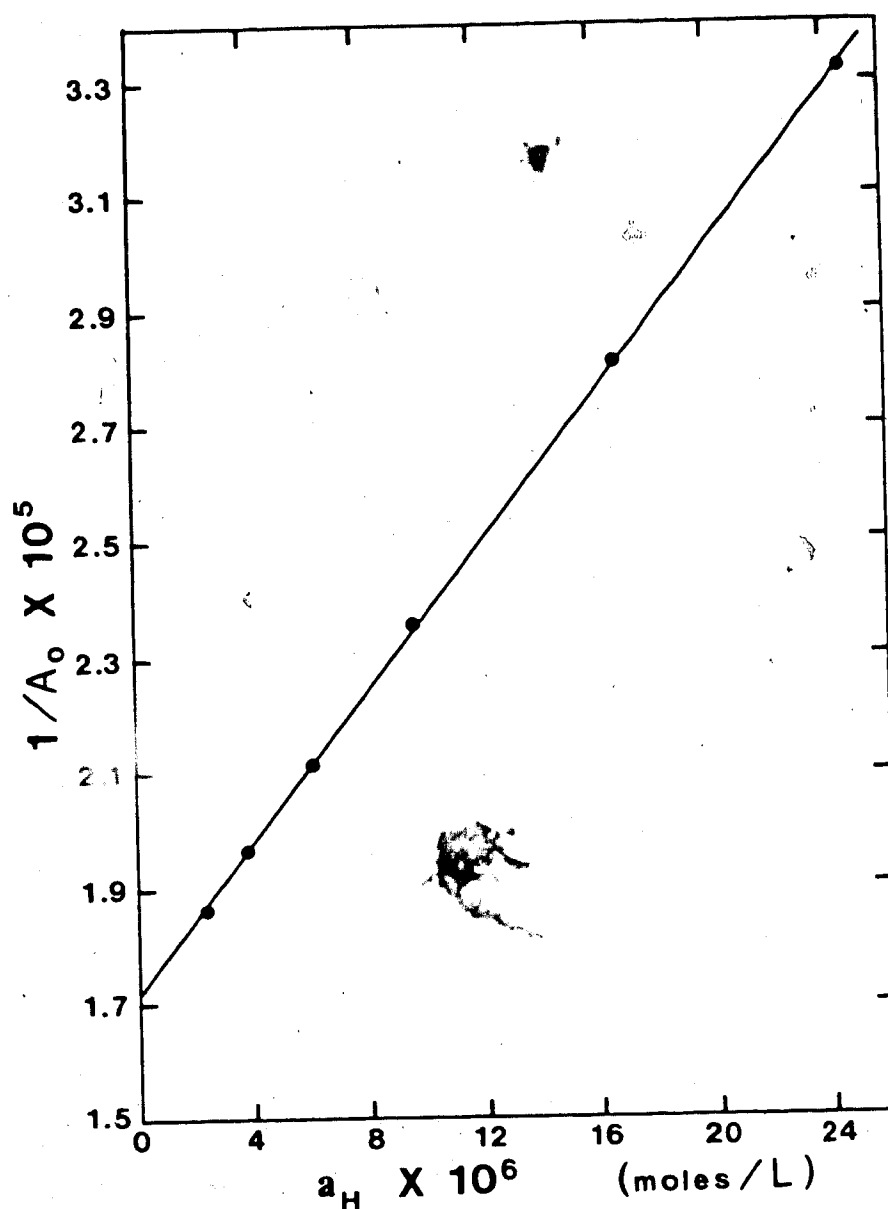


Figure 38. Plot of $1/A_0$ versus a_H for trial #2 of the K_B determination of p-toluidine between cyclohexane and ionic strength 0.10 acetate buffer at 20.0°C.

The slopes and y-intercepts of these plots, the total flow rates of the aqueous and organic phases (F_a and F_o) and the calculated distribution coefficients and computed errors are reported in Table 4. The uncertainties are one standard deviation and include the computed error in determining the slope, y-intercept, acidity constant, F_a and F_o as well as an estimated error (0.1) due to calibration of the pH meter. The errors were combined as discussed in the previous section.

5.4.9 Comments

Although this discussion has dealt with the determination of acidity constants using data collected from both the organic and aqueous phases, it is possible to determine them by monitoring peak areas in only the organic phase. This approach is described in Appendix II and is utilized in the measurement of the acidity constant of 8-chlorotheophylline. While the disadvantage of the two-membrane method described in this chapter, compared to the one-membrane method, is that two spectrophotometric detectors are necessary in the former, there are some distinct advantages to measuring peak areas in both phases. It is not necessary to know the flow rates, the number of moles of sample injected, the extraction constant or the system constant. It is also not necessary

Table 4. Distribution Coefficient Determination by Solvent Extraction/FIA.

Compound	Trial #	Slope (\pm RSD) ^a	y-Intercept ^b	F _O mL/min	F _a mL/min	Distribution Coefficient ^c
3,5-Dimethylphenol	1	4.75×10^{-16} ($\pm 2.1\%$)	$(2.14 \pm 0.02) \times 10^{-5}$	2.50	2.18	2.4 ± 0.2^d
	2	4.60×10^{-16} ($\pm 4.3\%$)	$(2.16 \pm 0.03) \times 10^{-5}$	2.49	2.22	2.4 ± 0.2^d
	3	4.94×10^{-16} ($\pm 2.2\%$)	$(2.16 \pm 0.02) \times 10^{-5}$	2.57	2.26	2.2 ± 0.2^d
p-Toluidine	1	0.700 ($\pm 0.47\%$)	$(1.669 \pm 0.009) \times 10^{-5}$	2.50	2.12	3.2 ± 0.2^e
	2	0.648 ($\pm 0.63\%$)	$(1.72 \pm 0.01) \times 10^{-5}$	2.60	2.12	3.3 ± 0.2^e

a) Percent relative standard deviation.

b) Uncertainties are 95% confidence limits.

c) Uncertainties are one standard deviation.

d) Temperature = $25.0 \pm 0.1^\circ\text{C}$ and ionic strength = 0.10.e) Temperature = $20.0 \pm 0.1^\circ\text{C}$ and ionic strength = 0.10.

that the phases be pre-equilibrated or that the flow rates be constant from one injection to the next. These conclusions become evident upon examination of equations 5.16, 5.17, 5.31 and 5.32 in which none of the above parameters appear either explicitly or implicitly. The net effect is that very accurate values for the acidity constants can be obtained.

BIBLIOGRAPHY

1. C. Ranger, Anal. Chem. 53, 20A (1981).
2. Betteridge, Anal. Chem. 50, 832A (1978).
3. J. Ruzicka and E.H. Hansen, Chemtech Dec., 756 (1979).
4. C. Ranger, Am. Lab. 14, 56 (1982).
5. B. Rocks and C. Riley, Clin. Chem. 28, 409 (1982).
6. J. Ruzicka and E.H. Hansen, Anal. Chim. Acta 145, 1 (1983).
7. B.I. Karlberg, Am. Lab. 15, 73 (1983).
8. J. Ruzicka and E.H. Hansen, "Flow Injection Analysis", John Wiley and Sons, New York (1981).
9. R. Tijssen, Anal. Chim. Acta 114, 71 (1980).
10. L. Snyder, J. Levine, R. Stoy and A. Conetta, Anal. Chem. 48, 942A (1976).
11. B. Karlberg and S. Thelander, Anal. Chim. Acta 98, 1 (1978).
12. H. Bergamin F^o., J.X. Medeiros, B.F. Reis and E.A.G. Zagatto, Anal. Chim. Acta 101, 9 (1978).
13. J.F.M. Kinkel and E. Tomlinson, Int. J. Pharmaceutics 6, 261 (1980).
14. D.C. Shelly, T.M. Rossi and I.M. Warner, Anal. Chem. 54, 87 (1982).

15. T.M. Rossi, D.C. Shelly and I.M. Warner, Anal. Chem. 54, 2056 (1982).
16. M. Bengtsson and G. Johansson, Anal. Chim. Acta 158, 147 (1984).
17. L.R. Snyder and H.J. Adler, Anal. Chem. 48, 1022 (1976).
18. B. Karlberg, P.A. Johansson and S. Thelander, Anal. Chim. Acta 104, 21 (1979).
19. K. Backstrom, L.G. Danielsson and L. Nord, Analyst 109, 323 (1984).
20. T. Imasaka, T. Harada and N. Ishibashi, Anal. Chim. Acta 129, 195 (1981).
21. J.F. Lawrence, U.A.Th. Brinkman and R.W. Frei, J. Chromatogr. 185, 473 (1979).
22. P.A. Johansson, B. Karlberg and S. Thelander, Anal. Chim. Acta 114, 215 (1980).
23. A.H.M.T. Scholten, U.A.Th. Brinkman and R.W. Frei, J. Chromatogr. 205, 229 (1981).
24. A. Sodergren, Analyst 91, 113 (1966).
25. K. Kina, K. Shiraishi and N. Ishibashi, Talanta 25, 295 (1978).
26. J. Kawase, A. Nakae, M. Yamanaka, Anal. Chem. 51, 1640 (1979).
27. L. Nord and B. Karlberg, Anal. Chim. Acta 118, 285 (1980).

28. J. Kawase, Anal. Chem. 52, 2124 (1980).
29. L. Fossey and F.F. Cantwell, Anal. Chem. 54, 1693 (1982).
30. K. Ogata, K. Taguchi and T. Imanari, Anal. Chem. 54, 2127 (1982).
31. L. Fossey and F.F. Cantwell, Anal. Chem. 55, 1882 (1983).
32. O. Klinghoffer, J. Ruzicka and E.H. Hansen, Talanta 27, 169 (1980).
33. L. Nord and B. Karlberg, 125, 199 (1981).
34. L. Nord and B. Karlberg, 145, 151 (1983).
35. K. Ogata, S. Tanabe and T. Imanari, Chem. Pharm. Bull. 31, 1419 (1983).
36. J.A. Sweileh and F.F. Cantwell, Anal. Chem., in press.
37. J.F. Lawrence, U.A.Th. Brinkman and R.W. Frei, J. Chromatogr. 171, 73 (1979).
38. C. van Buuren, J.F. Lawrence, U.A.Th. Brinkman, I.L. Honigberg and R.W. Frei, Anal. Chem. 52, 700 (1980).
39. R.J. Reddingius, G.J. de Jong, U.A.Th. Brinkman and R.W. Frei, J. Chromatogr. 205, 77 (1981).
40. C.P. Terweij-Groen, J.C. Kraak, W.M.A. Niessen, J.F. Lawrence, C.E. Werkhoven-Goewie, U.A.Th. Brinkman and R.W. Frei, Intern. J. Environ. Anal. Chem. 9, 45 (1981).

41. F. Smedes, J.C. Kraak, C.E. Werkhoven-Goewie, U.A.Th. Brinkman and R.W. Frei, J. Chromatogr. 247, 123 (1982).
42. A.H.M.T. Scholten, U.A.Th. Brinkman and R.W. Frei, Anal. Chem. 54, 1932 (1982).
43. K. Tsuji, J. Chromatogr. 158, 337 (1978).
44. C.E. Werkhoven-Goewie, U.A.Th. Brinkman and R.W. Frei, Anal. Chim. Acta 114, 147 (1980).
45. D.P. Kirby, P. Vouros, B.L. Karger, B. Hidy and B. Petersen, J. Chromatogr. 203, 139 (1981).
46. L. Fossey and F.F. Cantwell, Anal. Chem., in press.
47. J.A. Sweileh and F.F. Cantwell, Can. J. Chem., submitted for publication.
48. J. Ruzicka and E.H. Hansen, Anal. Chim. Acta 99, 37 (1978).
49. J.C. Sternberg "Advances in Chromatography", ed. J.C. Giddings and R.A. Keller, Marcel Dekker, New York, Chapter 6 (1966).
50. B.L. Karger, L.R. Snyder and C. Horvath, "An Introduction to Separation Science", Wiley-Interscience, New York, Chapter 2 (1973).
51. A. Leo, C. Hansch and D. Elkins, Chem. Rev. 71, 525 (1971).
52. "National Formulary", 14th Rev., Mack Printing Co., Easton, PA (1975).

53. G. Schill, K.O. Borg, R. Modin and B.A. Persson, "Ion-Pair Extraction in the Analysis of Drugs and Related Compounds" in "Essays on Analytical Chemistry", ed. E. Wanninen, Pergamon Press, Oxford, England, p. 379 (1977).
54. T. Higuchi, A. Michaelis, T. Tan and A. Hurwitz, Anal. Chem. 39, 974 (1967).
55. G. Schill, "Isolation of Drugs and Related Compounds by Ion-Pair Extraction", Vol. 6 in "Ion Exchange and Solvent Extraction", ed. J.A. Marinsky and Y. Marcus, Marcel Dekker, New York, Chapter 1 (1974).
56. K. Gustavii and G. Schill, Acta Pharm. Suecica 3, 241 (1966).
57. K. Gustavii and G. Schill, Acta Pharm. Suecica 3, 259 (1966).
58. K. Gustavii, Acta Pharm. Suecica 4, 233 (1967).
59. H.Y. Mohammed and F.F. Cantwell, Anal. Chem. 51, 1006 (1979).
60. H.Y. Mohammed and F.F. Cantwell, Anal. Chem. 52, 553 (1980).
61. F.F. Cantwell and M. Carmichael, Anal. Chem. 54, 697 (1982).
62. T. Sekine and Y. Hasegawa, "Solvent Extraction Chemistry, Fundamentals and Applications", Marcel Dekker, New York (1977).

63. M. Carmichael and F.F. Cantwell, Can. J. Chem. 60, 1286 (1982).
64. Burroughs-Wellcome Co., La Salle, Quebec, personal communication.
65. F.F. Cantwell and H.Y. Mohammed, Anal. Chem. 51, 218 (1979).
66. G.L. Starobinets, V.V. Egorov, Zh. Anal. Khim. 33, 1395 (1978).
67. A.C. Andrews, T.D. Lyons, and T.D. O'Brien, J. Chem. Soc., 1776 (1962).
68. T.J. Siek, R.J. Osiewicz, and R.J. Bath, J. Forensic Sci. 21, 525 (1976).
69. T.J. Siek, J. Forensic Sci. 19, 193 (1974).
70. British Pharmacopeia, Vol. II, London, England (1980).
71. U.S. Pharmacopeia, National Formulary, 20th revision; Rockville, MD (1979).
72. A. Albert and E.P. Serjeant, "The Determination of Ionization Constants", Chapman and Hall, London (1971).
73. E.J. King, "Acid-Base Equilibria", Vol. 4 in "Equilibrium Properties of Electrolyte Solutions", ed. R.A. Robinson, Macmillan, New York (1965).
74. R.F. Cookson, Chem. Rev. 74, 5 (1974).
75. H.A. Laitinen and W.E. Harris, "Chemical Analysis",

2nd edition, McGraw-Hill, New York, Chapter 4
(1975).

76. R.G. Bates, "Determination of pH, Theory and Practice", 2nd edition, John Wiley and Sons, New York (1973).
77. L.Z. Benet and J.E. Goyan, J. Pharm. Sci. 56, 665 (1967).
78. K. Ezumi and T. Kubota, Chem. Pharm. Bull. 28, 85 (1980).
79. T. Kubota and K. Ezumi, Chem. Pharm. Bull. 28, 3673 (1980).
80. J. Hanamura, K. Kobayashi, K. Kano and T. Kubota, Chem. Pharm. Bull. 31, 1357 (1983).
81. C. Golumbic, M. Orchin and S. Weller, J. Am. Chem. Soc. 71, 2624 (1949).
82. C. Golumbic and M. Orchin, J. Am. Chem. Soc. 72, 4145 (1950).
83. C. Golumbic and G. Goldbach, J. Am. Chem. Soc. 73, 3966 (1951).
84. T.M. Xie and D. Dyrssen, Anal. Chim. Acta 160, 21 (1984).
85. A. Khan and F.F. Cantwell, unpublished results.
86. T. Sekine and Y. Hasegawa, "Solvent Extraction Chemistry, Fundamentals and Applications", Marcel Dekker, New York, p. 320 (1977).

87. D. Dyrssen, *Acta Chem. Scand.* 11, 1771 (1957).
88. T. Sekine, Y. Hasegawa and N. Ihara, *J. Inorg. Nucl. Chem.* 35, 3968 (1973).
89. H.A. Laitinen and W.E. Harris, "Chemical Analysis", 2nd edition, McGraw-Hill, New York, p. 42 (1975).
90. "High-Purity Solvent Guide", Burdick and Jackson Laboratories, Muskegon, MI (1980).
91. G. Ham, *Anal. Proc.* 18, 69 (1981).
92. L. Anderson, *Anal. Chim. Acta* 110, 123 (1979).
93. D. Betteridge, E.L. Dagless, B. Fields, N.F. Graves, *Analyst* 103, 897 (1978).
94. J.N. Little, G.J. Fallick, *J. Chromatogr.* 112, 389 (1975).
95. D.A. Skoog and P.M. West, "Fundamentals of Analytical Chemistry", 3rd edition, Holt, Rinehart and Winston, New York, Chapter 4 (1976).
96. L.A. Currie, "Treatise on Analytical Chemistry", Part I, Volume 1, 2nd edition, ed. I.M. Kolthoff and P.J. Elving, John Wiley and Sons, New York, Chapter 4 (1978).
97. D.T.Y. Chen and K.J. Laidler, *Trans Faraday Soc.* 58, 480 (1962).
98. E.F.G. Herington, W. Kynaston, *Trans Faraday Soc.* 53, 138 (1957).
99. C.W. Davies, *J. Chem. Soc.* 2093 (1938).

100. P.D. Bolton and F.M. Hall, Aust. J. Chem. 20, 1797 (1967).
101. A.V. Willi and H. Meir, Helv. Chim. Acta 39, 318 (1956).
102. C. Bernasconi, W. Koch, Hch. Zollinger, Helv. Chim. Acta 46, 1184 (1963).

APPENDIX I

Table A1. Data for Trial #1 of the Determination of the Acidity Constant and Distribution Coefficient for 3,5-Dimethylphenol (Figures 30 and 34).

$1/a_H$ (moles/L) ⁻¹	A_a/A_o	$1/A_o \times 10^5$
4.102×10^9	4.555	2.326
	4.498	2.331
	4.614	2.371
	4.606	2.316
	4.492	2.318
5.140×10^9	5.009	2.392
	5.066	2.413
	5.130	2.394
	5.135	2.387
	5.043	2.373
	4.889	2.393
6.457×10^9	5.803	2.466
	5.584	2.450
	5.345	2.433
	5.551	2.422
	5.526	2.424
	5.672	2.428
8.204×10^9	6.321	2.526
	6.484	2.537
	6.412	2.533
	6.360	2.524
	6.421	2.561
	6.426	2.524
1.334×10^{10}	8.631	2.744
	8.720	2.787
	8.555	2.784
	8.620	2.761
	8.815	2.784
	8.878	2.778

Table A2. Data for Trial #2 of the Determination of the Acidity Constant and Distribution Coefficient for 3,5-Dimethylphenol (Figures 31 and 35).

$1/a_H$ (moles/L) ⁻¹	A_a/A_o	$1/A_o \times 10^5$
3.990×10^9	4.556	2.349
	4.633	2.334
	4.569	2.328
	4.661	2.345
	4.610	2.326
	4.829	2.339
5.035×10^9	5.068	2.363
	4.999	2.356
	5.072	2.399
	5.104	2.366
	4.975	2.377
	5.001	2.364
6.295×10^9	5.827	2.467
	5.617	2.465
	5.592	2.447
	5.679	2.466
	5.667	2.455
	5.717	2.445
7.852×10^9	6.366	2.509
	6.322	2.544
	6.519	2.553
	6.442	2.522
	6.391	2.519
	6.396	2.512

Continued

Table A2 (Continued)

$1/a_H$ (moles/L) ⁻¹	A_a/A_o	$1/A_o \times 10^5$
9.772×10^9	7.326	2.676
	7.399	2.668
	7.173	2.654
	7.128	2.688
	7.254	2.659
	7.333	2.664
1.247×10^{10}	8.309	2.688
	8.356	2.684
	8.447	2.696
	8.353	2.684
	8.438	2.680
	8.477	2.733

Table A3. Data for Trial #3 for the Determination of the Distribution Coefficient for 3,5-Dimethylphenol (Figure 36).

$1/a_H$ (moles/L) ⁻¹	$1/A_O \times 10^5$
3.908×10^9	2.364
	2.371
	2.361
	2.361
	2.350
	2.350
4.943×10^9	2.378
	2.404
	2.396
	2.389
	2.398
	2.391
6.194×10^9	2.473
	2.469
	2.463
	2.481
	2.480
	2.459
7.834×10^9	2.540
	2.574
	2.553
	2.536
	2.543
	2.537
9.572×10^9	2.634
	2.638
	2.627
	2.632
	2.651
	2.618

Table A4. Data for Trial #1 of the Determination of the Acidity Constant and Distribution Coefficient for p-Toluidine (Figures 32 and 37).

a_H (moles/L)	A_a/A_o	$1/A_o \times 10^5$
2.371×10^{-6}	7.046	1.829
	6.880	1.827
	6.967	1.831
	7.027	1.835
	6.992	1.838
	7.055	1.825
	7.064	1.833
3.767×10^{-6}	7.800	1.921
	7.868	1.922
	7.712	1.913
	7.893	1.919
	7.895	1.912
	7.924	1.917
6.026×10^{-6}	8.922	2.115
	8.872	2.093
	9.035	2.122
	8.791	2.112
	9.028	2.112
	8.846	2.112
9.594×10^{-6}	10.299	2.366
	10.411	2.359
	10.200	2.326
	10.358	2.363
	10.255	2.336
	10.474	2.337

Continued

Table A4 (Continued)

a_H (moles/L)	A_a/A_o	$1/A_o \times 10^5$
1.652×10^{-5}	13.374	2.804
	13.444	2.840
	13.068	2.804
	13.262	2.816
	13.187	2.808
	13.439	2.819
2.449×10^{-5}	16.584	3.385
	16.529	3.391
	16.750	3.375
	16.592	3.374
	16.886	3.399
	16.649	3.393

Table A5. Data for Trial #2 of the Determination of the Acidity Constant and Distribution Coefficient for p-Toluidine (Figures 33 and 38).

a_H (moles/L)	A_a/A_o	$1/A_o \times 10^5$
2.366×10^{-6}	6.954	1.855
	6.973	1.892
	7.093	1.870
	6.971	1.857
	6.984	1.857
	7.123	1.864
3.793×10^{-6}	7.815	1.967
	7.615	1.960
	7.673	1.961
	7.698	1.966
	7.805	1.982
	7.767	1.977
6.095×10^{-6}	8.697	2.113
	8.730	2.119
	8.789	2.119
	8.735	2.112
	8.579	2.107
	8.837	2.121
9.638×10^{-6}	10.139	2.359
	10.103	2.360
	10.257	2.386
	10.315	2.379
	10.205	2.349
	10.141	2.370

Continued

Table A5 (Continued)

a_H (moles/L)	A_a/A_o	$1/A_o \times 10^5$
1.667×10^{-5}	12.903	2.782
	13.277	2.834
	13.036	2.814
	13.206	2.820
	13.013	2.768
	13.029	2.820
2.472×10^{-5}	16.254	3.308
	16.054	3.301
	15.991	3.313
	15.995	3.291
	16.317	3.334
	16.570	3.365

APPENDIX II

APPENDIX II

ACIDITY CONSTANT DETERMINATION BY SOLVENT EXTRACTION/FIA FROM SINGLE PHASE ANALYSIS. pK_a OF 8-CHLOROTHEOPHYLLINE

A. Theory

Acidity constants can be determined by analysis of the organic phase alone, as opposed to simultaneous analysis of both the organic and aqueous phases. Considering first the case of an HA charge type acid, equation 5.18 from Chapter 5 indicates that a plot of $1/A_0$ vs $1/a_H$ should yield a straight line with slope S_2 and y-intercept I_2 . If the system constant, $K = f b \epsilon_{HA,0}$ is measured in a separate experiment and accurate values are obtained for F_0 and n , a value for K_{HA} can be calculated from the intercept:

$$K_{HA} = \frac{F_a}{I_2 n K - F_0} \quad (A.1)$$

and then K_a can be obtained from the slope:

$$K_a = \frac{S_2 n K K_{HA}}{F_a} \quad (A.2)$$

The acidity constant for a BH^+ charge type acid can be determined from a plot of $1/A_O$ vs a_H , as illustrated in equation 5.34 of Chapter 5, if the system constant, $K = f b \epsilon_{B,O}$, is measured in a separate experiment and accurate values are obtained for F_a , F_O and n . A value for K_B is obtained from the intercept, I_4 , of the plot of $1/A_O$ vs a_H :

$$K_B = \frac{F_O}{I_4 n K - F_O} \quad (A.3)$$

and then the acidity constant can be calculated from the slope:

$$K_a = \frac{F_a}{S_4 n K K_B} \quad (A.4)$$

B. Samples and Reagents

2.00×10^{-4} M 8-Chlorotheophylline was prepared by placing the appropriate weight of 8-chlorotheophylline into a large beaker. Water was then added and enough of a saturated solution of NaOH to effect dissolution. The solution was then neutralized with HCl and transferred quantitatively to a 1 litre volumetric flask.

pH = 5.114 Citric Acid/ Na_2HPO_4 Buffer was prepared by mixing 257.5 mL of 0.2 M Na_2HPO_4 with 242.5 mL of 0.1 M citric acid.

pH = 6.082 Citric Acid/ Na_2HPO_4 Buffer was prepared by mixing 315.75 mL of 0.2 M Na_2HPO_4 with 184.25 mL of 0.1 M citric acid.

pH = 7.012 Citric Acid/ Na_2HPO_4 Buffer was prepared by mixing 411.75 mL of 0.2 M Na_2HPO_4 with 88.25 mL of 0.1 M citric acid.

C. Apparatus

The diagram of the solvent extraction/FIA system used in the 8-chlorotheophylline pK_a determination with single-phase analysis is shown in Figure A1. Its design is similar to that used for system characterization, as described in Chapter 2, with the main difference being that the single-reagent pressure cylinder is replaced by a multi-reagent pressure cylinder that has previously been discussed in Chapter 4. Chloroform is used as the organic phase. Valve V_4 is a six-port rotary valve (part no. R60 31V6, Laboratory Data Control) used to select any one of six reagent buffers. A three-port slider valve, V_2 , (part no. CAV 3031, LDC) is used in combination with valve V_4 to

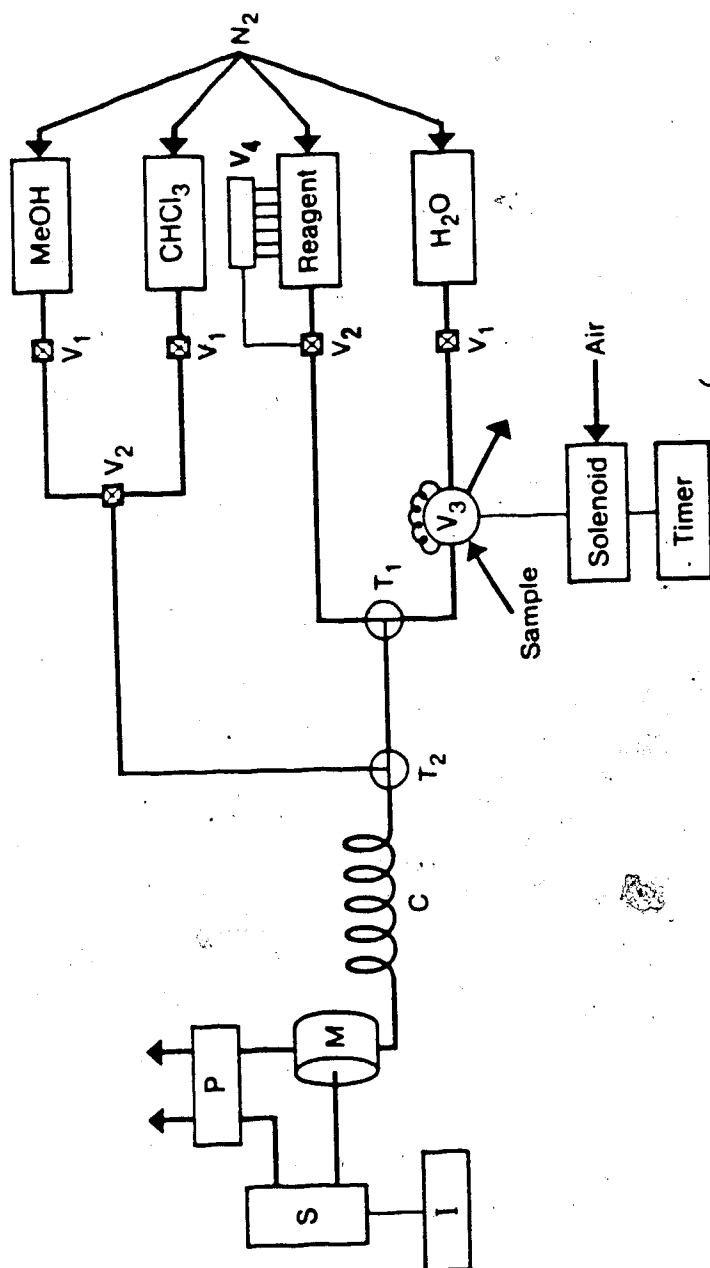


Figure A1. Apparatus used to determine the acidity constant of 8-chlorotheophylline. H₂O, reagent, chloroform and methanol are in pressure cylinders; V₁ and V₂ are two-way and three-way valves; V₃ is an injection valve; V₄ is a six-port rotary valve; T₁ and T₂ are tees; C is the extraction coil; M is the membrane phase separator; S is the spectrophotometer; I is the integrator and P is a peristaltic pump. See text for details.

allow selection of either buffer or a water wash. The organic phase which passes through the Teflon membrane of the phase separator is monitored by a spectrophotometer, S (Varichrom photometric detector, Varian), and the signal from S is fed to a digital recording integrator, I (Model 3390A, Hewlett-Packard Co.), to obtain peak areas.

The apparatus used in the system constant, K, determination for 8-chlorotheophylline is shown in Figure A2. The solvents are contained in glass bottles inside aluminum cylinders which are pressurized by nitrogen. All tubing is 0.3 mm i.d. Teflon. Valves V_1 are two-way Teflon valves (part no. CAV 2031, LDC) that allow shut-off of either solvent flow. Valve V_2 is a three-way Teflon valve (part no. CAV 3031, LDC) which allows selection of either chloroform or methanol. The latter is used to wash out the system at the end of the experiment. The sample, dissolved in chloroform, is injected into the chloroform stream via automatic injection valve V_3 (part no. SVA-8031, LDC). This injection valve is activated by an air solenoid valve (part no. SOL-3-24-VDC, LDC) controlled by an electrical timer which allows variation of load time and injection time. As before, V_3 contains a "dummy" loop of equal size to the injector loop so that the flow rate of aqueous reagent is the same in both the load and inject positions. The sample is loaded into the injection valve

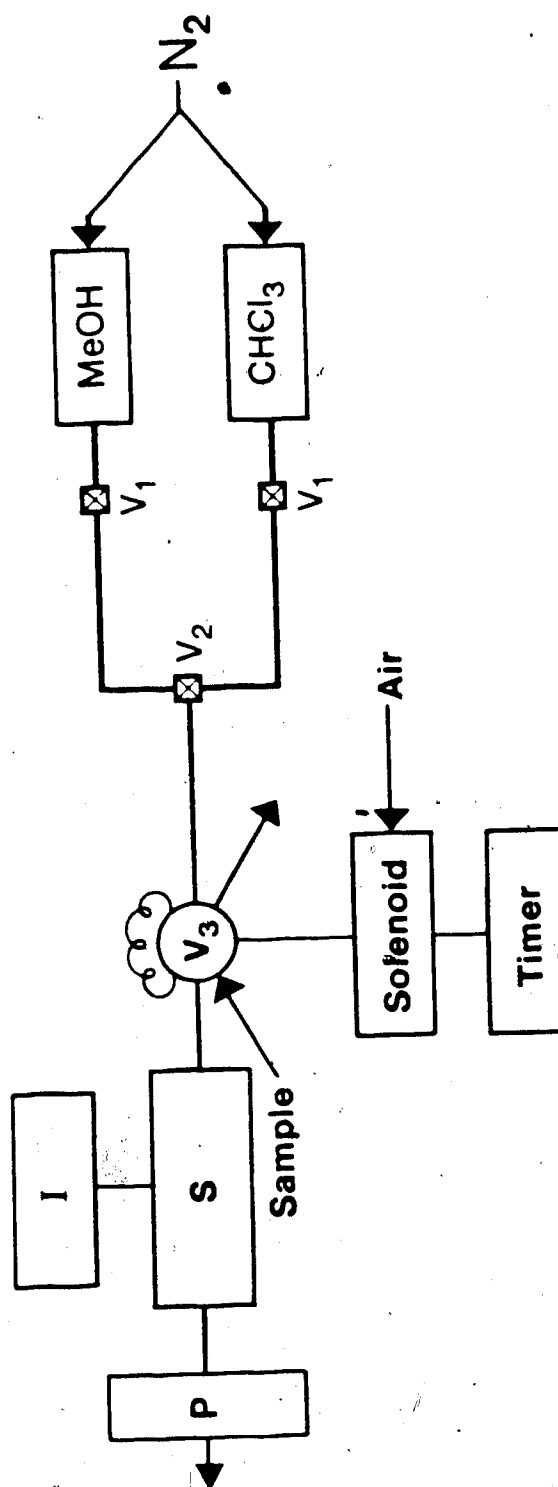


Figure A2. Apparatus used to measure the system constant for 8-chlorotheophylline. Chloroform and methanol are in pressure cylinders; V_1 and V_2 are two-way and three-way valves; V_3 is an injection valve; S is the spectrophotometer; I is the integrator and P is a peristaltic pump. See text for details.

using a peristaltic pump (not shown). Spectrophotometer, S, and integrator, I, are of course the same as those used for the pK_a determination. A peristaltic pump, P, (Minipuls 2, Gilson Instruments) is used on the outlet line to insure accurate flow control.

D. Acidity Constant Determination of 8-Chlorotheophylline

A sample solution that was 2×10^{-4} M in 8-chlorotheophylline was injected into citric acid/ Na_2HPO_4 reagent buffers of pH 5.114, 6.082 and 7.012. No attempt was made to control ionic strength as only an approximate pK_a value was desired. The buffer concentrations were sufficiently high to insure that no change in pH occurred during the extraction/FIA procedure. The desired reagent was selected via the six-port rotary valve, V_4 , and the resistances in each line were matched to provide equal flow rates for each reagent stream. The absorbance of the organic phase was monitored and peak areas were measured for six replicate injections of each sample.

Important instrument parameters for the acidity constant determination of 8-chlorotheophylline were as follows: total chloroform flow rate, 3.33 ± 0.04 mL/min; total aqueous flow rate, 2.07 ± 0.06 mL/min; chloroform flow rate through the membrane, 1.15 ± 0.02 mL/min;

extraction coil length, 200.4 cm; sample volume injected, 44 μ L; injection rate, two samples per min; wavelength, 275 nm; absorbance setting, 0.2; nitrogen pressure, 40 psig.

E. System Constant Determination for 8-Chlorotheophylline

The system constant, K, required for calculation of the acidity constant of 8-chlorotheophylline, was determined using the apparatus shown in Figure A2. This system constant pertains exclusively to the detection system shown in Figure A1. A sample of 2×10^{-4} M 8-chlorotheophylline in chloroform was injected six times into a chloroform stream and peak areas were measured. It is important that the same detector and integrator settings are used as in the experiment for the determination of the acidity constant for the sample. If, in order to bring peaks on scale, a different detector and/or integrator setting is required then the measured system constant must be corrected to that which would be applicable under the conditions used in the pK_a experiment.

Important instrument parameters for the system constant determination for 8-chlorotheophylline were as follows: flow rate, 1.51 ± 0.03 mL/min; sample volume

injected, 44 μ L; injection rate, two samples per min; wavelength, 275 nm; absorbance setting, 1.0; nitrogen pressure, 40[~]psig.

F. Results and Discussion

The primary purpose in determining the acidity constant for 8-chlorotheophylline was to facilitate the choice of the pH of the sample solution used in the Dramamine tablet assay, as discussed in Chapter 4. There was, at that time, no literature value available. Solvent extraction is a particularly appropriate approach to the acidity constant determination of 8-chlorotheophylline owing to the low solubility of this compound in water, which inhibits an accurate determination by normal potentiometric methods, and to the similarity of the absorption spectra of the protonated and deprotonated sample forms which prevents an accurate spectrophotometric determination [68].

The system constant for 8-chlorotheophylline was determined first, using single-phase analysis, from the relation:

$$K = \frac{A F}{n} \quad (A.5)$$

where A is the average peak area, F is the flow rate and n is the number of moles of sample injected. When the detector was set for an absorbance range of 1.0, the measured value of K was $(5.4 \pm 0.1) \times 10^{14}$ mL/min⁻¹mole⁻¹. The acidity constant of 8-chlorotheophylline was then determined from a plot of $1/A_0$ vs $1/a_H$, shown in Figure A3. The data for this figure are given in Table A6. The plot was linear with a slope and y-intercept of 2.72×10^{-13} and 2.00×10^{-7} respectively. The relative standard deviation for the slope was 0.39% and the 95% confidence limits for the y-intercept were $\pm 1.4 \times 10^{-8}$. The experiment quantifying the pH dependency of peak areas in the organic phase was run with a detector absorbance range setting of 0.2. The appropriate system constant for 8-chlorotheophylline to allow calculation of K_{HA} and K_a is therefore $(2.72 \pm 0.06) \times 10^{15}$ mL/min⁻¹mole⁻¹.

The distribution coefficient for 8-chlorotheophylline between chloroform and the aqueous citric acid/ Na_2PO_4 buffers was calculated from equation A.1 to be 1.4 ± 0.2 , the stated uncertainty being one standard deviation. The acidity constant was then calculated via equation A.2 yielding a $\text{p}K_a$ for 8-chlorotheophylline of 5.35 ± 0.06 . The uncertainty is one standard deviation and includes the computed error in calculating the K_a from equation A.2, as

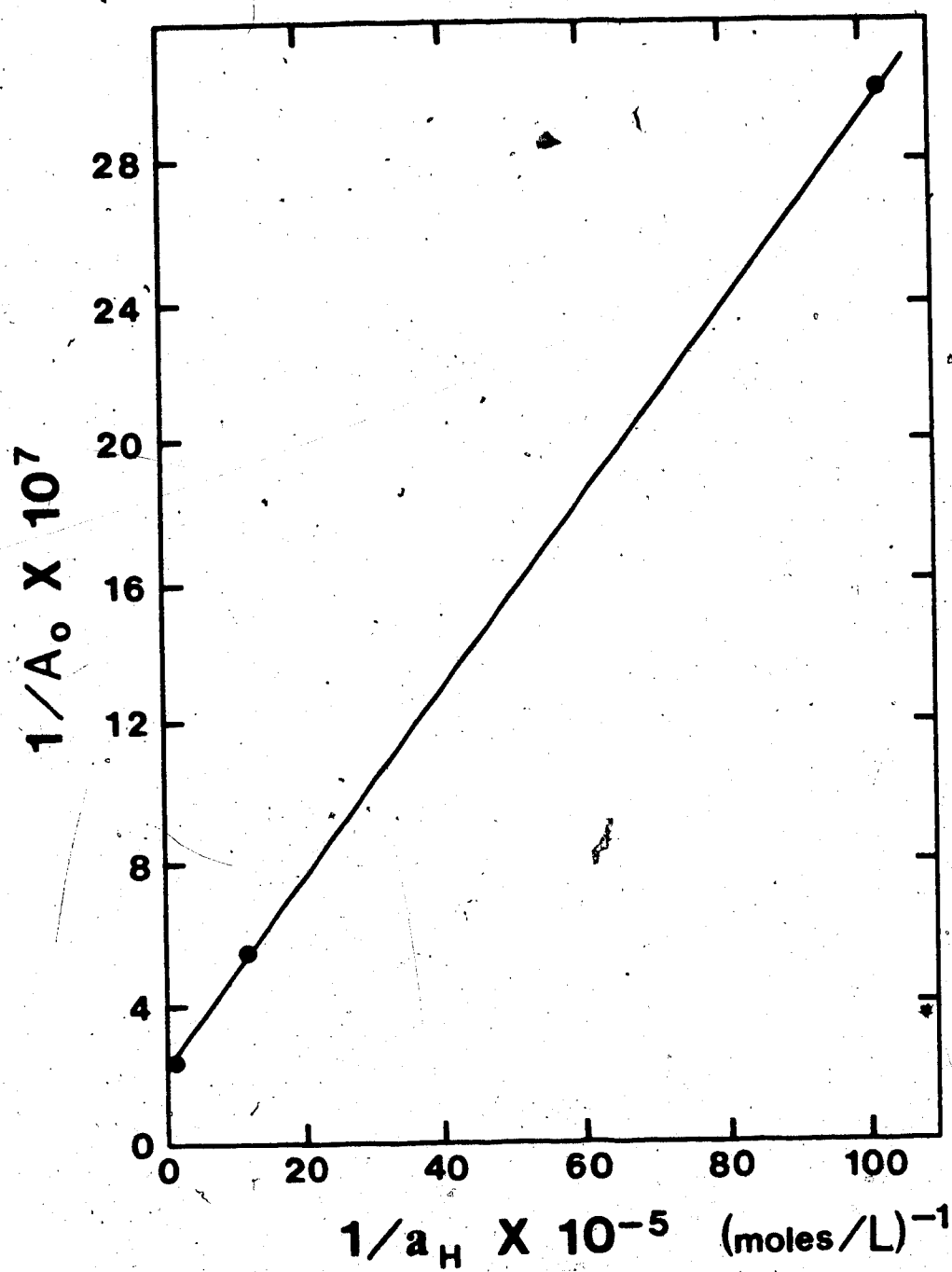


Figure A3. Plot of $1/A_0$ versus $1/a_H$ for the acidity constant determination of 8-chlorotheophylline.

Table A6. Data for the Acidity Constant Determination of 8-Chlorotheophylline (Figure A3).

$1/a_H$	F_a (mL/min)	F_o (mL/min)	$1/A_o \times 10^7$
1.300×10^5	2.00	3.28	2.243
			2.224
			2.229
			2.244
			2.259
			2.255
1.208×10^6	2.11	3.35	5.417
			5.467
			5.458
			5.417
			5.433
1.028×10^7	2.11	3.35	30.188
			30.029
			29.408
			30.127
			30.175
			29.901

well as an estimated error (0.01) due to calibration of the pH meter used to measure the pH values of the reagent buffer solutions. The ionic strength of the combined aqueous phase varied in this determination from 0.12 to 0.21. (Note that the reagent buffers were diluted 1:1 with the reagent stream.) Our pK_a for 8-chlorotheophylline agrees well with the value of 5.43 ± 0.03 determined at an ionic strength of 0.01 in our laboratory by a solvent extraction method using a filter-probe assembly [85].

If a more accurate pK_a value is desired, the ionic strength of the reagent buffers should of course be kept constant. As well, the extraction coil and phase separator should be thermostatted to the desired temperature and peak areas should be measured at additional pH values in the vicinity of the pK_a of the sample. As discussed in Chapter 5, simultaneous measurement of peak areas in both the organic and aqueous phases will lend a higher degree of accuracy to the pK_a determination.